UCSF
UC San Francisco Electronic Theses and Dissertations

Title
Molecular basis of fatty acid synthesis in the endoplasmic reticulum (ER) membrane and targeting of misfolded glycoproteins for ER-associated degradation

Permalink
https://escholarship.org/uc/item/41c18503

Author
Denic, Vladimir

Publication Date
2006

Peer reviewed|Thesis/dissertation

eScholarship.org Powered by the California Digital Library
University of California

Molecular Basis of Fatty Acid Synthesis in the Endoplasmic Reticulum (ER) Membrane and Targeting of Misfolded Glycoproteins for ER-Associated Degradation

by

Vladimir Denic

DISSERTATION

Submitted in partial satisfaction of the requirements for the degree of

DOCTOR OF PHILOSOPHY

in

BIOCHEMISTRY

in the

GRADUATE DIVISION

of the

UNIVERSITY OF CALIFORNIA, SAN FRANCISCO

[redacted]

LIBRARY

USF LIBRARY

Copyright (2006)
by
Vladimir Denic

for my mother

USC LIBRARY

ACKNOWLEDGMENTS

What should I say about Jonathan Weissman. I have interacted longer with him scientifically than with anyone else I know. In the beginning, this interaction was a double-edged sword that would tear at the nitty-gritty of our mentor-mentee relationship. On the one hand, he would be much faster at interpreting a result and suggesting follow-up experiments. To follow his advice, most of the times at least, would be to do your project a favor. However, what I saw as being good for the project I also saw as being detrimental from a pedagogical standpoint. Thus in the hope of losing a battle (or few, as it turned out) in order to win my war on getting an education, I focused my attention on opaque topics just outside of his interest or areas of expertise. It is there that I hoped to forge my scientific skills by working largely in isolation that at times was bordering on obscurity. Several years would pass before, for reasons to painful to recount in this margin, I came to the now obvious realization that a better strategy was to first think carefully about a problem and then try to engage him at a higher level. Needless to say, this exercise was often accompanied by a quick illustration of an oversight or some major flaw in my reasoning, but over time it got better. I would like to thank him for sticking by me through all the times I came up empty-handed and encouraging my pursuit of certain problems even if, as I secretly suspect, it was against his better judgment. Why he never tapped me on the shoulder and told me to stop the fight, I will never know. One possible explanation is that he fundamentally didn't care. Another is that he always believed I would in the end find my own way. I favor the latter.

UCSF LIBRARY

The problem with having been in the Weissman lab for a long time is that so
y people have come and gone that for the sake of brevity in this format I am forced to
s only on influences from recent memory. One person, in particular, I've been
nate enough to overlap with in the lab is Sean Collins. He is that rare confluence of
intellect, a sense of humor for the absurd and the satirical, and a personality that is
ole and unassuming almost to a fault. I cannot imagine my time in the lab without

Arunashree Bhamidipati has remained a good friend even after leaving the lab.
thing about coffee and cigarettes and a pretty Indian woman who laughs at most of
jokes, I guess. I think that she always felt bad that her external circumstance lead to
urden of finishing up the first ERAD paper falling on my shoulders and I think she
realized that she was actually doing me a favor.

Erin Quan is the closest I ever got to mentoring anyone in the lab. While the
ant proddings of most other people I find annoying, Erin has this quality of making
tually worry about her worrying about some of her problems. This unplanned
nood of sorts became increasingly a two-way streak over time as she would ask or
nething at group meeting and you would be all like (this is how they talk where
om) "My baby girl's all grown up. I can go now." An unexpectedly rewarding
nce even for a cynic like myself, I must admit.

UCSF LIBRARY

The arrival of Maya Schuldiner to the lab has elevated the level of discussion in the lab. In particular, her encyclopedic knowledge of variations in risqué sexual behavior will be hard to match for years to come. As an inside joke I will say this: here's to more girls getting on the Schuldiner diet. On a more serious note, Maya's keen eye for an obscure interaction in the ER E-MAP initiated my own efforts in the study of fatty acid synthesis in the ER and ultimately become the main portion of my thesis. If you are the type of person who believes in fate, you would say that my early years in the lab were nothing more than a waiting period for her to join the lab.

In the early days, the state of affairs in the Weissman lab could be compared to that in "Lord of the Flies": kids recklessly pipetting with no adult supervision. This all changed when John Newman came aboard. Here's a guy who has uttered derogatory comments at group meetings that made some of my best work in that area sound like compliments by comparison. All of a sudden, it wasn't cool anymore to get up in front of the whole lab and waste everybody's time by presenting some poorly thought out experiments in the form of an incoherent chalk-talk. As prickly as he was sometimes, John forced me to step back more often than I dared to from what I was doing and ask the question of whether what I was doing, even if it was working, was actually worth doing. He once told me that in order to become a truly great scientist you have to learn how to lie. You have to motivate yourself to get up in the morning and go into lab when nothing is working. You have to shatter and then you have to anneal. I told him that I could do the first part in my sleep. He replied this meant I was one step closer.

UCSF LIBRARY

id Breslow has been a very recent addition to the lab. Love at first
y soon, however, it became clear that for someone scarred by the
uate experience he has managed nonetheless to retain a delightfully
of humor and a sardonic wit. He might also be the only person I will
us honor of having gotten hooked on coffee. Being witness to its
ns over the years makes me reluctant to speculate about the type of
lab will be in the future. However, hints of Dave's scientific abilities
the best years are yet to come.

like to thank Peter Walter who in addition to being a member of my
also largely responsible for my acceptance into UCSF. It is amusing
than favorable view these days of the journal Cell because two
my scientific career centered around Peter and Cell. First, during a
llege in New Zealand I visited San Francisco and spent a fair bit of
n Parnassus reading biology textbooks for next year's classes. Yes, I
point while taking a study break I strolled around the area where all
magazines are on display. This I thought was the perfect time to
reading in the textbooks and see if the rubber can actually meet the
nost articles proved to be impenetrable to my mind so much so that
ion my intellectual abilities. Then I came across a paper that was so
at it sounded like something out of a textbook. Moreover, the results
sibly cool. A transmembrane kinase in the endoplasmic reticulum
folded proteins and that results in the splicing of an mRNA that

UCSF LIBRARY

a transcription factor *et cetera, et cetera.* It took two visits to the library and
:s of my head hurting to get to the end of the article. At that point all I wanted
s who is doing this and where are they at. The rest is history. Peter, thanks for
ınce on an unknown kid.

second story involves an issue of Cell signed supposedly by Ben Lewin
ch I received from Secret Santa during a Walter lab Christmas party. This
ed to be a jibe at my incessant reading of current journals by some disgruntled
ıdent in the lab unable to find time to keep up with the literature. Though a bit
roceeded to read most of the articles in the issue. One article in particular
was the reconstitution of translocation by Gorlich and Rappoport. Absolutely
othing less than a clarification of the whole field through heroic biochemistry.
he identification of Phs1p as the elongation cycle dehydratase the obvious
ame if the entire cycle could be reconstituted from purified components of
mic reticulum membrane. That got me thinking back to the Gorlich paper
arly see myself rereading it on a bench in Berkeley as I outlined the strategy
econstitution.

anks also go to Hiten Madhani for being the other external member of my
ttee and not taking too seriously some of the skits which I orchestrated at the
s oblivious to the norms of advancement in science. To Chris Patil. We
f at first, but over time, for reasons still unbeknownst to me, he thought I
o appreciate the significance of this in my impressionate young mind, you

UCSF LIBRARY

have to realize what it was like growing up in the shadow of cool, smart, and witty people like Chris, Steve McCarroll, and Aaron McGee. They were the epitome of why UCSF graduate students were superior to all others. Chris also was instrumental in shaping my ideas on scientific debate as well as teaching me how to use language in social situations in order to inflict pain. Here's to many more "college days," Chris. To Joe Derisi for always great movie and book recommendations. To Andrew Murray for shaping my romantic view of science and making me realize that there are at least three interpretations of every finding. I died a little when you left. To Dyche Mullins for photography lessons and helping me move when I was homeless. To Dave Morgan for illustrating by example that being a great scientist and a really great person may not be mutually exclusive. To Rosa Marion for being the best thing about the Weissman lab's joint tenure with the O'Shea lab. To the man after my own heart, Hans Luecke, for reinforcing some of my worst fears about most things and turning me onto PyBOP. To Jack Taunton for chatting with me about lipids when I had no one else to talk to, for all the thoroughly enjoyable nights of drinking that managed to distract my mind from its usual worries, and for your friendship over the years. To Mary Matyskiela, my one and only official roton. Take that fact and the fact that Mary was the first person not interested in joining the Weissman lab (after having rotated in it, at least; I'm sure without this qualifier the precedent was set much earlier) and you get a sense of my abilities as a mentor. Somehow we got over that hump and became friends. Mary, you are as cool as Chuck.

UCSF LIBRARY

To my friends Dan, Luke, Garth and Wayne for all those countless times off the field that made graduate school bearable. I know I have been less available lately that I would like to. This is why.

To Elizabeth Clarke for love and support over the last few years. You make everything easier than I ever thought possible. Who knew this stuff could be fun.

Finally, to my mother for her unconditional support of all my big decisions and for immigrating to the United States so that I would have the opportunity to build a better life for myself.

UCSF LIBRARY

ABSTRACT

Very long-chain fatty acids (VLCFAs) comprise a diverse set of lipid species of varying chain lengths that play an essential role in many biological processes. I have identified yeast Phs1p as the founding member of a novel family of ER membrane dehydratases that catalyze the water-removal step in the cyclical elongation of shorter FA species into VLCFAs. With this finding, I was then able to reconstitute the complete elongation cycle using Phs1p in conjunction with several enzyme candidates isolated from yeast ER membranes. Beyond acting as a point of departure for future mechanistic and structural studies into the mechanism of VLCFA synthesis, this work has lead to the characterization of a family of novel condensing enzymes responsible for catalyzing the first step in the elongation cycle. Finally, I have identified a short region within this family that acts as a molecular ruler for determining the length of VLCFAs in yeast. Collectively, these findings raise the possibility that the divergence of this region was the driving force behind the diversification of VLCFA chain-length observed in other species.

The second part of my thesis focused on the question of how terminally misfolded glycoproteins in the endoplasmic reticulum (ER) lumen are distinguished from on-pathway folding intermediates before being targeted for retrotranslocation across the ER membrane and degradation in the cytosol. Yos9p is an ER lectin critical for the ER-associated degradation (ERAD) of luminal substrates. I have shown that Yos9p is able to form a complex with substrates and that this association paradoxically persisted in the

UCSF LIBRARY

absence of substrate sugars as well as upon ablation of the sugar-binding pocket in Yos9p's lectin domain, two conditions that otherwise abolish substrate degradation. These latter findings received a nice explanation when it was observed that Yos9p is part of a multi-protein complex containing Hrd3p, an ERAD component capable of recruiting misfolded forms to the degradation machinery independent of Yos9p. These and other data suggest that Yos9p lies at the core of a surveillance complex that by querying the glycan and folding status of luminal ER proteins selectively commits terminally misfolded glycoproteins for degradation.

UCSF LIBRARY

Jonathan S. Weissman, Ph.D
Thesis Advisor

CONTRIBUTIONS

Portions of the text and figures presented in this thesis are reproduced with rmission from material published previously. Chapter 4 "Exploration of the pological Requirements of ERAD Identifies Yos9p as a Lectin Sensor of Misfolded ycoproteins in the ER Lumen" was published in September 2005 in Molecular Cell l. 19, pp. 741-751. This work was initiated by Dr. Arunashree Bhamidipati who formed the experiments in Figures 1, 2, 3, 5B, 6B, S1, and S3 showing the effects of ng DHFR on the stability of CPY*, the identification of Yos9p as a key component of AD-L, and the crosslinking of CPY*/CPY*^{0000} to Yos9p/R200AYos9p. The sequence nment and structure of the sugar-binding pocket shown Figure 4A and B, ectively, were generated by Dr. Jonathan S. Weissman. Figure 4C showing the cts of Yos9p sugar-binding pocket mutants on CPY* stability was performed by Erin Quan. Chapter 5 "A Luminal Surveillance Complex that Selects Misfolded oproteins for ER-Associated Degradation" was published in July 2006 in Cell Vol. pp. 349-359. Erin M. Quan performed the experiments in Figures 1A-C, 2A-C, 7, 4, S7, and S7 showing the purification of Yos9p complexes, the effect of Hrd1p xpression on CPY* and CPY*^{0000} degradation as well as the dependence of this on RING domain function, and the functional nature of some of the constructs used study. David King and the HHMI Mass Spec Facility carried out the analysis ed in Figure S2.

UCSF LIBRARY

With the exceptions of those items listed above, the work presented in this thesis was performed by its author, Vladimir Denic, under the supervision of Dr. Jonathan Weissman.

UCSF LIBRARY

Dear Mr Denic

We hereby grant you permission to reproduce the material detailed below at no charge in your thesis subject to the following conditions:

1. If any part of the material to be used (for example, figures) has appeared in our publication with credit or acknowledgement to another source, permission must also be sought from that source. If such permission
is not obtained then that material may not be included in your publication/copies.

2. Suitable acknowledgement to the source must be made, either as a footnote
or in a reference list at the end of your publication, as follows:

"Reprinted from Publication title, Vol number, Author(s), Title of article, Pages No., Copyright (Year), with permission from Elsevier".

3. Reproduction of this material is confined to the purpose for which permission is hereby given.

4. This permission is granted for non-exclusive English rights only. For other languages please reapply separately for each one required. Permission
excludes use in an electronic form. Should you have a specific electronic project in mind please reapply for permission.

5. This includes permission for UMI to supply single copies, on demand, of the complete thesis. Should your thesis be published commercially, please reapply for permission.

Yours sincerely

Marion Moss
Senior Rights Assistant
Elsevier Ltd
The Boulevard
Langford Lane
Kidlington
Oxford

UCSF LIBRARY

5 1GB

e: Molecular Cell
nor(s): Bhamidipati et al.
ume: 19
ue: 6
r: 2005
ges: 741 - 751
cle title: Exploration of the Topological Requirement etc.

e: Cell
nor(s): Denic et al.
ume: 126
ue: 2
r: 2006
ges: 349 - 359
cle title: A Luminal Surveillance Complex that Selects etc.

UCSF LIBRARY

TABLE OF CONTENTS

	i-xxi
roduction	1
ntification of the Dehydratase Essential for the Elongation Fatty Acids in the Endoplasmic Reticulum Membrane	11
constitution of the Fatty Acid Elongation Cycle Reveals Molecular Ruler for Determining VLCFA Chain Length	60
bloration of the Topological Requirements of ERAD ntifies Yos9p as a Lectin Sensor of Misfolded ycoproteins in the ER Lumen	75
Luminal Surveillance Complex that Selects Misfolded coproteins for ER-Associated Degradation	117
ımary	167
erences	171

UCSF LIBRARY

LIST OF TABLES & FIGURES

CHAPTER 2

Figure 1	Fatty acid elongation in the ER	49
Figure 2	Depletion of Phs1p results in the accumulation of ceramide precursors and a synthetic growth defect with VLCFA mutants	50
Figure 3	Loss of Phs1p function results in an *elo* phenotype associated with shorter average VLCFA length	51
Figure 4	Reduced overall elongation and accumulation of the 3-hydroxy intermediate in microsomes depleted of Phs1p	52
Figure 5	Microsomes depleted of Phs1p have impaired elongation cycle dehydratase activity	53
Figure 6	Co-immunoprecipitation of Phs1p with the other members of the elongase complex	54
'igure 7	Phs1p catalyzes the dehydration reaction in vitro	55
'igure S1	Deletion of *lcb4* eliminates the formation of phosphorylated LCBs in a *phs1-damp* mutant	56
igure S2	Purification of bacterially-expressed Phs1p-HIS	57
igure S3	PTPLb homologs substitute for the essential function of Phs1p in yeast	58
gure S4	Alignment of Phs1p homologs	59

HAPTER 3

ure 1	Purification of the elongation cycle components	70

UCSF LIBRARY

Figure 2 Sur4p is a condensing enzyme 71

Figure 3 Reconstitution of the individual steps in the elongation cycle 72

Figure 4 Sur4p is unable to substitute for Fen1p in restoring growth of *fen1* mutants in the absence of FAS activity 73

Figure 5 Sur4p but not Fen1p is able to convert C24 into C26 74

CHAPTER 4

Figure 1 Presence of a stable C-terminal DHFR domain provides an impediment to ER-associated degradation of CPY* 101

Figure 2 Yos9p is required for ER-associated degradation of CPY* 102

Figure 3 Yos9p is required for degradation of proteins containing misfolded lumenal but not cytosolic domains 103

Figure 4 Yos9p contains an intact sugar-binding site that is required for its ability to support ERAD 104

Figure 5 Interaction of misfolded ER proteins with Yos9p 105

Figure 6 Sugar-independent recognition of CPY* by Yos9p 106

Figure S1 Stability of DHFR-CPY*-DHFR 113

Figure S2 Yos9p sugar-binding mutants show enhanced association with CPY*-DHFR 114

Figure S3 Yos9p interacts with substrate as part of a large protein complex 115

Figure S4 Yos9p and R200A Yos9p interaction with substrate is unaffected in the absence of Htm1p 116

UCSF LIBRARY

CHAPTER 5

Figure 1	Yos9p associates with the core ERAD machinery at the ER membrane	147
Figure 2	The integrity of the Yos9p-core ERAD machinery complex is not dependent on Der1p, Htm1p or Yos9p's sugar binding pocket	148
Figure 3	Dissection of the Hrd3p/Yos9p interaction by domain mapping/over-expression and a model of how Yos9p interacts with other members of the ERAD machinery	149
Figure 4	Yos9p interacts with CPY* and CPY*0000 in a *HRD3*-independent manner	150
Figure 5	Hrd3p interacts specifically with CPY* and CPY*0000 but not wild type CPY in a *YOS9*-independent manner	151
Figure 6	Sugar-independent association of misfolded carboxypeptidase Y with Usa1p	152
Figure 7	Over-expression of Hrd1p in a *Δhrd3* background results in increased degradation of CPY* and CPY*0000 in a *YOS9*-independent manner	153
Figure S1	Yos9-FLAG genomic is functional for ERAD-L	158
Figure S2	Mass Spectrometry Statistics	159
Figure S3	Yos9 associates with Hrd1p	160
Figure S4	Yos9p/Kar2p association is independent of Hrd3p	161
Figure S5	Deglycosylated Yos9p interacts with deglycosylated Hrd3p	162

UCSF LIBRARY

Figure S6 Yos9p and R200A Yos9p interact with CPY* but not CPY wild type 163

Figure S7 $Hrd3_{1-767}$-MYC is functional for CPY* degradation 164

Figure S8 Usa1p is in a multiprotein complex containing misfolded carboxypeptidase Y prior to cell lysis 165

Figure S9 Degradation of CPY* when Hrd1p is overexpressed in a *Δhrd3* background is suppressed by *Δcue1* 166

UCSF LIBRARY

CHAPTER 1

Introduction

UCSF LIBRARY

n fatty acids (LCFAs) are repetitive hydrocarbon structures that make
c core of all cellular membranes (Schneiter and Kohlwein, 1997).
chemical nature and ubiquitous distribution it is likely that the
a rudimentary fatty acid synthesis apparatus was a key event in the
ion of genetic material from its inanimate surroundings. In all known
d synthesis proceeds by the ordered repetition of four chemical
ndensation of malonyl-Coenzyme A (CoA) with a growing carboxyl
g precursor, reduction of the resulting 3-keto intermediate,
educed 3-hydroxy intermediate, and lastly the reduction of the
termediate into a fully saturated fatty acid product two carbons longer
Vakil et al., 1983). Bacterial LCFA synthesis is usually carried out by
eparate proteins each catalyzing one of the above steps (White et al.,
d on top of this basic catalytic module are several additional activities
ting the cycle, coordinating the transfer of intermediates between the
nd terminating the reaction following several rounds of catalysis.
n is catalyzed by the malonyl-CoA:ACP transacylase and involves
lonyl moiety from the phosphopantetheine arm of the small
ne phosphopantetheine arm of the acyl-carrier protein (ACP). The
edicated to the first condensation reaction then uses an active site
oA from acetyl-CoA and in doing so form a transient acyl-enzyme
of malonyl-ACP into the active site of the condensing enzyme
tion of the acyl-enzyme intermediate and the formation of the

UCSF LIBRARY

nsed 3-keto acyl-ACP and CO_2 products. The 3-keto intermediate is then converted
ıe corresponding fully-saturated product by the movement of ACP from one
tic domain to the next as part of the first reaction cycle. The saturated product
ted by the first round of catalysis is then transferred from ACP to the catalytic
ıe residue of the elongation condensing enzyme which begins another round of
on. Notably, the role of the long phosphopantetheine arm of ACP is not to act as a
ing arm" to deliver substrates between catalytic domains as depicted in most
ks but rather to insert reaction intermediates into the deep hydrophobic clefts of
ites (Jenni et al., 2006; Maier et al., 2006). The intrinsically cyclical nature of the
ı mechanism raises the question of what determines the number of times the
c cycle operates on a growing acyl chain. While it is known that the core catalytic
ery possess some degree of substrate specificity, the molecular basis for this
enon remains unknown. What is clear, however, is that the action of external
ases and acyl-transferases, with defined chain-length specificities, plays a critical
etermining the length distribution of LCFAs in the cell (Schweizer and Hofmann,

eukaryotes, FA synthesis is an enzymatically very similar process with the
that it is typically carried out by large fatty acid synthase (FAS) polypeptides
g multiple domains responsible for catalyzing the separate enzymatic activities
above (Trotter, 2001; Wakil et al., 1983). Furthermore, these multienzyme
ften form oligomeric structures which in the case of fungal FAS comprises two
action chambers each having three copies of all the activities necessary for a

UCSF LIBRARY

nplete reaction cycle (Jenni et al., 2006). More specifically, the ACP domains and all active sites are located on the inside of the chambers thus allowing for efficient nneling of intermediates between catalytic sites that are present at millimolar effective centrations (Jenni et al., 2006).

Considering the many similarities between the prokaryotic and eukaryotic FAS ems, it came as a surprise that, unlike the situation in bacteria, inhibition of yeast cell wth upon depletion of malonyl-CoA cannot be suppressed by the add-back of C16/18 the preferred end products of fungal FAS (Schneiter et al., 1996). These and other rvations lead to the discovery of a comparatively inabundant population of so-called long-chain FAs (VLCFAs) which are now known to be well-suited for orchestrating uniquely eukaryotic biological processes for which LCFAs appear unable to tute (Jakobsson et al., 2006). One notable feature of VLCFAs compared to their r precursors is their much higher structural diversity (Dunn et al., 2004). Namely, ition to the observed variation in chain length, VLCFAs may contain multiple n-carbon double bonds (Beaudoin et al., 2000), as well as a branched hydrocarbon structure (Kniazeva et al., 2004). Moreover, these three forms of structural on can be used in a combinatorial fashion to further expand the array of possible A species. Indeed, in higher eukaryotes different cell types possess distinguishing A signatures suggesting that diversification of these long lipid species has uted to the specialization of tissue function characteristic of multi-cellular ms (Cinti et al., 1992).

What then is the mechanism of VLCFA biosynthesis and what features of the osynthetic apparatus, if any, might help explain the apparent fanning of its products to chemical space? Defining the machinery responsible for synthesis of VLCFAs has en an outstanding question ever since the 1960s when Nugteren demonstrated that LCFA production occurs in the context of the endoplasmic reticulum (ER) membrane ugteren, 1965). Despite this unusual membrane localization of the catalytic machinery underlying reaction mechanism was remarkably similar to that catalyzed by cytosolic S (Nugteren, 1965). One notable distinguishing feature that was later discovered by ward Sprecher and colleagues is that the products of the elongation reaction remain ched to CoA (Bernert and Sprecher, 1979b). This raised some early doubts regarding possibility of a catalytic mechanism involving covalent enzyme substrate rmediates as in the case of classical FA synthesis. Subsequent studies suggested that, e along the lines of bacterial FAS systems, elongation of FAs in the ER was a process ied out by separate polypeptides (Bernert and Sprecher, 1979a). Following these early nces in understanding the enzymology of the elongation reaction, subsequent efforts ochemically identifying the enzymes responsible have been almost entirely ccessful. The integral-membrane nature of the components involved, the generally ersome nature of the enzymatic assays themselves, as well as the presence of minating activities from other membranous compartments all conspired to the ation of the field that lasted well into the 1990s (Bessoule et al., 1989; Cook et al., Domergue et al., 2000; Fehling et al., 1992; Lessire et al., 1999; Puyaubert et al., . It was only then that Martin and colleagues identified *ELO1* as a gene essential for oduction of C16 from exogenously added C14 in the absence of FAS (Toke and

UCSF LIBRARY

Martin, 1996). A subsequent bioinformatical search revealed two close homologs of *ELO1* called *FEN1(ELO2)* and *SUR4(ELO3)* (Oh et al., 1997). While deletion of *FEN1* and *SUR4* together resulted in lethality, individual knock out strains revealed that Fen1p contributes to the synthesis of VLCFAs up to C22 while Sur4p is uniquely able to elongate FAS/Elo1p end-products all the way to C26, the most prevalent very long-chain species in budding yeast (Oh et al., 1997). The fact that Fen1p and Sur4p are generally hydrophobic proteins predicted to span the membrane multiple times and have no overall homology to other enzymes raises the question of what their exact molecular function is the context of VLCFA biosynthesis (Paul et al., 2006). One possible clue to this might the presence of a highly conserved HxxHH motif in the sequence of all homologs of O family. The fact that this motif is also found in desaturases and hydroxylases Shanklin et al., 1994) has lead some researchers to suggest that Elo proteins might act as ter keto or the enoyl reductases in the elongation cycle (Tvrdik et al., 2000). While sequent studies (see below) have implicated two other proteins as better candidates for mes acting at the two reduction steps, the question of whether FEN1/SUR4 act as ificity factors for determining the chain length of elongating substrates, as ponents of the chain termination step of the overall reaction, or perhaps even as the ensing enzymes themselves has been difficult to address with the existing proaches (see below). Nonetheless, the imperative to better understand the molecular ion of these proteins is well illustrated by numerous studies suggesting that the logs of this family are responsible for determining the chemical diversity of FAs in other species (Jakobsson et al., 2006; Leonard et al., 2004).

UCSF LIBRARY

Following the observation that mutations in *FEN1* and *SUR4* can suppress the ım sensitivity of a yeast strain lacking *CSG2*, Dunn and colleagues screened for ional suppressors of this kind in an attempt to identify novel players in VLCFA nthesis. One suppressor, *tsc13,* mapped to an essential gene with homology to enoyl tases (Kohlwein et al., 2001). Indeed, analysis of the VLCFA profile in this mutant ed an increase in the abundance of shorter VLCFA species at the expense of the C26 end-product (Kohlwein et al., 2001). More significantly, ER membranes from utant showed accumulation of the expected enoyl intermediate in the context of an o elongation reaction (Kohlwein et al., 2001). Lastly, bioinformatical screening for rane oxido-reductases in the ER lead to the identification of Ybr159w as the e 3-keto reductase component of the elongation cycle (Beaudoin et al., 2002; Han 002). Finally, the demonstration that Fen1, Sur4p, Tsc13p, and Ybr159w all co-precipitate together raised the possibility that the activities responsible for the ion reaction might physically interact with one another to bring about the ve synthesis of C26 observed in vivo (Han et al., 2002; Kohlwein et al., 2001; al., 2006).

One step in the elongation cycle for which there hasn't been even a candidate suggested has been the dehydration step. This question, of what the molecular the dehydratase is, touches on an even more fundamental issue of what the number of components necessary for a complete elongation cycle is. In the of a biochemical assay for even a single one of the implicated proteins, this is impossible to answer. Nonetheless, it is likely that Ybr159wp is a genuine 3-

UCSF LIBRARY

keto reductase given the fact that a) it is homologous to known oxidoreductases throughout its entire sequence and b) that membranes lacking Ybr159wp accumulate the 3-keto intermediate in an in vitro elongation reaction (Beaudoin et al., 2002; Han et al., 2002). Considering that Tsc13p has homology to enoyl reductases in only the C-terminal portion of its sequence (Kohlwein et al., 2001), it is conceivable that its remaining regions are capable of catalyzing a different step in the cycle. In fact, membranes defective for this putative enoyl reductase accumulate the 3-hydroxy intermediate in addition to the expected enoyl species raising questions about Tsc13p's additional involvement in the dehydration step (Moon and Horton, 2003). Lastly, while genetics has made considerable strides in furthering our understanding of VLCFA biosynthesis, the essential nature of this process poses a significant challenge on our ability to completely inactivate any one of the steps in the cycle by genetic manipulation alone. In fact, upon partial inactivation of the two putative reductase components, the overall level of elongation was hardly diminished and it was largely the observed accumulation of the expected oxidized intermediate that was instrumental in substantiating each assignment (Beaudoin et al., 2002; Han et al., 2002; Kohlwein et al., 2001). This tool, however, does not work in attempting to identify the condensation enzymes as in this case the accumulation of intermediates would correspond to the build-up of shorter saturated fatty acids which are not resolvable by traditional methods for analyzing reaction intermediates. Thus one is left with only a small reduction in the rate of incorporation of malonyl-CoA into the saturated products, a relatively weak argument on its own. In an attempt to overcome these issues and address the role of Fen1p and Sur4p in the elongation cycle a recent study demonstrated that membranes deficient for one

USF LIBRARY

or the other protein have differing abilities to elongate acyl-CoA precursors into longer saturated products that were resolvable by length (Paul et al., 2006). However, the reported effects were often seen only following multiple turnovers of the elongation cycle (as opposed to in the context of a staged single turnover condensation reaction in the absence of externally added reducing cofactors) (Paul et al., 2006). The apparent complexity of these effects and the general dangers of inferring the mechanism of catalysis of a circular biochemical pathway using membranes partially defective for a candidate player in the process, clearly illustrate the need for a defined biochemical system with purified components in order to dissect out the contributions of the various players identified genetically.

As described in Chapter 2, I have identified Phs1p as the long sought-after dehydratase of the elongation cycle. This protein is a founding member of a highly-conserved and novel family of membrane-embedded enzymes that is mutated in the dog model for human centronuclear myopathy and in a plant model for tumorigenesis. My functional characterization of this family now sheds light on the involvement of VLCFAs in myofiber homeostasis and the coordination of cell proliferation and differentiation. Chapter 3 describes how using this finding as my starting point, I reconstituted the complete elongation cycle by integrating Phs1p and additional candidate enzymes purified from yeast ER membranes into synthetic membranes with a defined composition. This has lead to my demonstration that Fen1p and Sur4p are members of a new family of condensing enzymes that dictate the structural diversification (eg. length, degrees of saturation, branching) of VLCFAs in other species. Lastly, I have identified a region

UCSF LIBRARY

within the condensing enzymes that acts a molecular ruler for determining the length distribution of VLCFAs in the cell.

As part of my overall interest in ER homeostasis I have also carried out work on the question of how misfolded proteins are targeted for ER-associated degradation which I describe in Chapters 4 and 5.

UCSF LIBRARY

CHAPTER 2

Identification of the Dehydratase Essential for the Elongation of Fatty Acids in the Endoplasmic Reticulum Membrane

UCSF LIBRARY

s of sphingolipids, very long-chain fatty acids (VLCFAs) play an essential
biological processes, including cell signaling and membrane protein
LCFA synthesis occurs in the endoplasmic reticulum and comprises the
tion of LCFAs by poorly defined molecular machinery. Here, we uncover
sential component required for VLCFA production in yeast. Biochemical
stablishes that Phs1p is the founding member of a unique and conserved
nbrane-embedded enzymes that catalyze the dehydratase step of the
e. Moreover, Phs1p's interacts with both itself and all the remaining
es in the cycle, thus suggesting that it lies at the core of a megasynthase
the structural diversity of VLCFA species in animal and plant tissues.
ons in Phs1p homologs cause tumorigenesis in plants and muscular
a canine model for hereditary centronuclear myopathy. Thus, our
the critical role of VLCFAs in these important disease processes.

UCSF LIBRARY

Introduction

The majority of fatty acids (FAs) in the cell are 16-18 carbons long and, as constituents of glycero-phospholipids, play a structural role in the integrity of biological membranes (Schneiter and Kohlwein, 1997). In addition to this class of long-chain FAs (LCFAs), eukaryotic cells contain smaller amounts of longer species with chain-lengths, in some instances, as great as 30 carbons (Zheng et al., 2005). These very-long chain fatty acids (VLCFAs) are attached to long-chain bases (LCBs) to form ceramides, a diverse set of sphingolipid species involved in cell signaling and the maturation of GPI protein anchors (Futerman and Hannun, 2004; Mayor and Riezman, 2004). Furthermore, ceramides and their more complex sphingolipid derivatives are required for the formation of lipid rafts, membrane microdomains thought to organize large protein signaling complexes and guide the trafficking of transmembrane proteins through the secretory pathway (Rajendran and Simons, 2005; Simons and Toomre, 2000). In the context of multi-cellular organisms, VLCFA synthesis has been co-opted and elaborated for a variety of additional tasks, including wax production and triglyceride oil storage in plants (Kunst and Samuels, 2003), and the synthesis of eicosanoid hormones and development of specialized VLCFA-rich tissues (eg. photoreceptor and Schwann cells) in mammals (Gill and Valivety, 1997; Jakobsson et al., 2006; Leonard et al., 2004). Their key role in numerous biological processes, and the practical benefits associated with manipulating VLCFA levels to alleviate disease (Ferri and Chance, 2005) and engineer commercially useful transgenic plants (Puyaubert et al., 2005), have served as the impetus for defining the molecular mechanism of VLCFA production.

UCSF LIBRARY

advance in anatomizing LCFA synthesis over the last several decades
) has recently culminated in the determination of the high-resolution
acid synthase (FAS) (Jenni et al., 2006; Maier et al., 2006). By
nderstanding of how VLCFAs are synthesized is still rudimentary.
rly as the 1960s, it was demonstrated that, in contrast to LCFA
osol, VLCFA species are generated in the endoplasmic reticulum (ER)
longation of FAS end-products (Nugteren, 1965). Despite this novel
d nature of the elongation machinery, the chemistry of the elongation
to be similar to that catalyzed by FAS and involve the repetitive
on units by the cycling of four reactions (Figure 1): 1) condensation
with malonyl-Coenzyme A (CoA); 2) reduction of the resulting 3-
) dehydration of the reduced 3-hydroxy species; 4) reduction of the
ermediate to yield a saturated FA chain, two carbons longer than its
nlike the multifunctional eukaryotic FAS protein, the individual
n VLCFA synthesis were speculated to originate with separate
ting on a growing acyl chain attached to the pantotheine arm of the
(Bernert and Sprecher, 1979b). Following these early advances,
cal attempts to identify the components of the ER elongation
dered by the integral membrane association of the proteins
rious nature of the enzymatic assays, and by the presence of
erived from contaminating non-ER compartments (Bessoule et al.,

UCSF LIBRARY

1989; Cook et al., 1992; Domergue et al., 2000; Fehling et al., 1992; Lessire et al., 1999; Puyaubert et al., 2001).

Insight into the identity of proteins required for VLCFA synthesis came from a omplementary line of inquiry into the genes involved in fatty acid elongation in *S. erevisiae*. A pioneering study by Martin and co-workers identified *ELO1* as a gene ssential for the conversion of exogenous C14 to C16 FA in the absence of FAS (Toke nd Martin, 1996). A subsequent search for Elo1p homologs led to the discovery of lo2p and Elo3p as key players in the selection of substrates with chain lengths <C26 for ongation to the most prevalent C26 FA species in yeast (Oh et al., 1997). Soon after, an egant leap of genetic reasoning focused attention on *TSC13*, an essential gene with mology to steroid enoyl reductases, which, when partially inactivated, causes the cumulation of VLCFA enoyl elongation intermediates (Kohlwein et al., 2001). Finally, ndidate screening of proteins with homology to oxidoreductases implicated Ybr159wp he major 3-keto reductase involved in the second step of the elongation cycle (Han et 2002). The ER membrane-localized nature of all the above components together with nmunoprecipitation studies further strengthened the idea that they were organized into longase complex (Han et al., 2002; Kohlwein et al., 2001).

The successful identification of genes required for fatty acid elongation in yeast a prerequisite for revealing the conserved nature of VLCFA biosynthesis by lementation of yeast VLCFA mutants with homologs from other species (Gable et 004; Tvrdik et al., 2000). Moreover, analysis of homologs in higher organisms is

UCSF LIBRARY

beginning to uncover a role for VLCFAs in development and disease (Yan et al., Zheng et al., 2005). Finally, enhancement of oil content in plants by xpression of elongase components holds promise as a strategy for satisfying the sing global demand for VLCFAs as precursors to a variety of human consumables ıbert et al., 2005). Given the potential benefits associated with manipulation of A levels toward therapeutically and commercially beneficial ends, it is nental to better understand the underlying mechanism of the elongation cycle. ver, even with the identity of some of the putative yeast catalytic components , reconstitution of the individual steps in the elongation cycle, much less the entire nas not been forthcoming. In the absence of such biochemical evidence, it is also ar whether all the components needed to reconstitute the entire cycle are already Nonetheless, it is likely, given their homology to known reductases, that wp and Tsc13p catalyze the keto and enoyl reduction steps of the cycle, vely (Han et al., 2002; Kohlwein et al., 2001). Additionally, Elo2/3p are strong es for enzymes acting at the first step of the elongation cycle as their absence the formation of 3-keto intermediates and a family of plant condensing enzymes titute for the complete absence of Elo2/3p in yeast (Paul et al., 2006). This, still leaves the question of what the nature of the dehydratase is, a component ngation cycle that has eluded identification for decades.

the present study we report the identification of the long sought-after VLCFA se. Starting with clues contained within the epistatic mini-array profile (E- comprehensive map of genetic interactions, of the early secretory pathway, we

UCSF LIBRARY

demonstrate that this activity in yeast is conferred by the essential and ER-localized membrane protein Phs1p. Shut-off of *PHS1* expression results in reduced average VLCFA chain length that is accompanied by a defect in the dehydratase step of the elongation cycle and a concomitant accumulation of 3-hydroxy elongation intermediates in Phs1p-depleted membranes. Additionally, the finding that Phs1p binds all the other proteins implicated in VLCFA synthesis and has the ability to self-associate, suggests that all the fatty acid elongation activities are assembled into a membrane megasynthase. Critically, we show that bacterially-expressed Phs1p is sufficient to catalyze dehydration of a 3-hydroxy elongation intermediate. Finally, our characterization of the core elongase machinery in yeast provides a context for understanding the molecular basis of myopathy and tumor-like growth in metazoans with mutations in *phs1* homologs (Bellec et al., 2002; Haberer et al., 2002; Pele et al., 2005).

UCSF LIBRARY

Results

PHS1 is an essential gene involved in sphingolipid metabolism

In a previous large-scale genetic analysis of the yeast early secretory pathway (Schuldiner et al., 2005), we reported a set of genetic interactions with a hypomorphic (DAmP) allele of *PHS1(YJL097w)* that led us to propose a role for this essential and uncharacterized ORF in lipid biosynthesis. The DAmP alleles used in that study contained a disrupted 3' untranslated region that served to destabilize the corresponding message. This post-transcriptional lesion did not significantly compromise the ability of *phs1-damp* mutants to grow under normal conditions and thus served as a useful tool for detecting negative genetic interactions. The strongest synthetic growth defect identified in this manner was with a deletion of *LCB3,* the major yeast long-chain base (LCB) phosphatase (Figure 2A) (Mao et al., 1997). *lcb3* mutants are known to have strongly elevated levels of phosphorylated LCB species (LCB-Ps). To test whether the relatively minor increase in LCB-P levels in *phs1-damp* mutants (Schuldiner et al., 2005) was simply due to significant residual activity in the DAmP allele, we analyzed a strain expressing Phs1p under the transcriptional control of the Tetracycline (Tet)-repressible promoter (Mnaimneh et al., 2004). Using an HPLC method for detecting fluorescently labeled LCB species (Lester and Dickson, 2001), we observed that, even in the absence of doxycycline (a non-repressing condition), a tetracycline analog, Tet promoter-driven *PHS1* expression was sufficiently compromised to result in strongly elevated levels of phosphorylated (primarily C18-PHS-P) species (Figure 2B). Additionally, we found dramatically increased levels of nonphosphorylated LCB species (eg. C20-PHS) (Figure 2B), an effect

UCSF LIBRARY

that was not as readily apparent with the weaker *phs1* DAmP allele (Schuldiner et al., 2006). Moreover, shut-off of *PHS1* expression, following the addition of doxycycline, resulted in growth arrest (Supplemental Figure S3) that was accompanied by further increase in the levels of some LCBs (Figure 2B). Thus, loss of the essential function of Phs1p is accompanied by a strong accumulation of ceramide precursors in the cell.

We first excluded the model that Phs1p depletion results in growth arrest due to accumulation of high levels of LCB-Ps. This formal possibility suggested itself based on the observation that the pattern of genetic interactions of *phs1-damp* mutants most resembles that of the deletion of Dpl1p (Schuldiner et al., 2005), the lyase responsible for breaking down LCB-Ps (Figure 2A) (Saba et al., 1997). Simultaneous deletion of *lcb3* and *dpl1* has been shown to inhibit cell growth due to accumulation of intolerable levels of toxic phosphorylated LCBs. Notably, this inhibition was completely suppressed by the concomitant deletion of the major yeast sphingoid kinase, Lcb4p (Figure 2A) (Kim et al., 2000; Zhang et al., 2001). By contrast, *Δlcb4* failed to suppress the accompanying growth defect (data not shown) despite eliminating the LCB-Ps normally associated with depletion of Phs1p (Supplementary Figure S1).

Turning to the observation that *pTet-PHS1* cells have significantly elevated levels of nonphosphorylated LCBs, we next investigated the contribution of Phs1p to other metabolic pathways that could influence the levels of LCBs in the cell. One such anabolic link is the conjugation of LCBs to very long-chain fatty acids (VLCFAs) to form ceramide, the essential precursor of complex sphingolipids (Figure 2A) (Dickson and

UCSF LIBRARY

Lester, 2002). A possible model for the elevated levels of LCBs in *phs1* mutants is that it stems from the reduced consumption of these metabolites as a result of a primary defect in VLCFA synthesis. Further supporting this idea is the observation that Phs1p has an unusually high predicted isoelectric point (pI=10.8), a puzzling biophysical property shared by all the other proteins implicated in VLCFA synthesis (Paul et al., 2006). Additionally, *phs1-damp* has a synthetic genetic interaction with Elo2p (Fen1p) (Schuldiner et al., 2005), a protein involved in determining the substrate specificity of VLCFA production (Oh et al., 1997; Paul et al., 2006). Similarly to *phs1* mutants, deletion of *ELO2* results in a dramatically altered LCB profile (Figure 2C). Moreover, as reported for other VLCFA mutants (Han et al., 2002; Kohlwein et al., 2001), partial loss of function of Phs1p results in a synthetic growth defect with deletions of both *ELO2* and its homolog *ELO3 (SUR4)* (Figure 2D). Collectively, these observations, along with the finding that *elo3* mutants are synthetically lethal with *Δlcb3* (Kobayashi and Nagiec, 2003), suggest that disrupting ceramide synthesis at any one of several levels (eg. VLCFA synthesis, VLCFA coupling to LCB, etc.) results in the shunting of unreacted LCB substrates to LCB-Ps. In turn, the toxic nature of these phosphorylated species implicates the functional assignment of early sphingolipid components to specific branches of the metabolic pathway on the basis of genetic interactions alone.

s1 mutants have impaired fatty acid elongation in vivo

address whether VLCFA synthesis is actually impaired in *phs1* mutants, we inhibited ular fatty acid synthase (FAS) using the small molecule cerulenin (Figure 2A), reby making cell growth absolutely dependent on the addition of LCFAs to the media

ler et al., 2003). The inefficient delivery of exogenous substrates for VLCFA esis, under these conditions, sensitizes cell growth to the efficiency with which substrates are elongated to longer essential species. As expected, wild type growth presence of cerulenin was completely dependent on the addition of either C14 or A (Figure 3A). On the other hand, *elo1* null mutants were unable to grow in the ce of the inhibitor and C14 FA, yet growth was restored to wild type levels by the n of C16 FA, the end-product of Elo1p-mediated C14 to C16 FA elongation e 3A) (Dittrich et al., 1998; Toke and Martin, 1996). Perhaps not unexpectedly, heir partially overlapping substrate preferences (Oh et al., 1997; Paul et al., 2006; et al., 2003), the behavior of *Δelo2* and *Δelo3,* under conditions of FAS on, was more complicated. Deletion of *ELO2* resulted in a strong growth defect n the presence of C14 or C16 FA while *Δelo3* showed a lesser growth defect only resence of C16 FA (Figure 3A). Importantly, LCFAs also showed a compromised o restore the growth of *phs1* mutants in the presence of cerulenin (Figure 3A). By , the behavior of *Δlcb3* in this assay was indistinguishable from that of wild-type t shown), demonstrating that altered LCB levels *per se* are not responsible for the nised elongation of exogenous fatty acids in *phs1* mutants.

o directly test the possibility that Phs1p is required for elongation of FAS end- we analyzed the cellular composition of trans-methylated fatty acids using As reported previously for other elongation mutants (Han et al., 2002; Kohlwein 01; Oh et al., 1997; Rossler et al., 2003), depletion of Phs1p was accompanied ficant reduction in C26 FA (the most abundant VLCFA in wild type cells) and a

UCSF LIBRARY

omitant increase in shorter C20, C22, and C24 FA species (Figure 3B). Notably, the rved reduction of average VLCFA length in *phs1* mutants distinguishes them from hide synthase mutants that, despite similarly elevated levels of LCBs, have an *ase* in C26 FA (Guillas et al., 2001). Together, these findings argue for the role of o in the production of essential VLCFA precursors for ceramide synthesis.

branes depleted of Phs1p are specifically defective in the dehydratase step of ongation cycle

bservation that *phs1* mutants are defective in elongating exogenous LCFAs in the ce of FAS activity (Figure 3A) argues against the interpretation that Phs1p acts y at the level of FAS to promote the production of C26 FA. We therefore wished to ne other events in VLCFA biosynthesis that follow release of LCFAs from FAS for ble defect that could account for the reduced levels of C26 FA in *phs1* mutants e 3B). These include, delivery of activated LCFAs to the ER membrane by acyl-nding proteins (ACBPs), the availability of malonyl-CoA, and the elongation of by the repetitive addtion of two-carbon units derived from malonyl-CoA (Sims et 4). A comparison of Phs1p's cellular localization to the ER membrane with those roteins acting at each of these steps (Huh et al., 2003), suggested that Phs1p's is o act at the level of the elongation cycle (Figure 1). Depletion of Phs1p could s possible involvement at a particular step in the cycle by way of accumulation of gation intermediate preceding that step. Therefore, we incubated Phs1p-depleted mal membranes (ie. derived from *Ptet-PHS1* treated with doxycyline) in the of cold C20-CoA precursor and radiolabeled malonyl-CoA and analyzed the

UCSF LIBRARY

n products by thin-layer chromatography under conditions that have been shown to
of all the elongation intermediates (Kohlwein et al., 2001). As can be seen in
4A, in the absence of reducing cofactors (essential for the second and fourth step
elongation cycle) we observed similar accumulation of the labeled 3-keto species
wild type and *phs1* mutant membranes. This observation argues that Phs1p is
to be necessary for the condensation step of the elongation cycle. However,
e allowed elongation to proceed to completion, by including NAD(P)H in the
, we specifically observed strong accumulation of the 3-hydroxy intermediate in
utant membranes (Figure 4A). Moreover, using membranes prepared under
ns of more complete shut-off of *PHS1* expression (ie. following extended growth
the presence of doxycycline), we saw significantly impaired synthesis of the
elongation cycle end-products (Figure 4B).

he strong accumulation of the 3-hydroxy intermediate in Phs1p-depleted
es argues that Phs1p is required for the dehydratase activity of the elongation
e caveat to this interpretation is that deletion of Ybr159wp, thought to be the
LCFA keto reductase, also results in the accumulation of the dehydratase
(Han et al., 2002). However, a comparison with *Δybr159w* microsomes
hat, in our kinetic regime, Phs1p-depleted membranes accumulated even higher
the 3-hydroxy intermediate without the concomitant build-up of the 3-keto
ate (Figure 5A). This finding suggests that *phs1* mutants are unlikely to have a
ect at the second step of the elongation cycle. Another caveat we wished to
the possibility that accumulation of the 3-hydroxy intermediate in *phs1* mutant

UCSF LIBRARY

somes results from a defect in the enoyl reduction step in conjunction with efficient tion of enoyl intermediates by the reverse activity of an otherwise unaffected ratase (Kohlwein et al., 2001). To test this idea, we incubated membranes with a 3-xy C18-CoA dehydratase substrate synthesized by PyBOP-mediated condensation ydroxyoctadecanoic acid with CoA (Figure 5B). In the absence of reducing ors (thus eliminating the possibility of subsequent reduction of the dehydrated CoA intermediate), we observed by HPLC that wild type membranes converted the te into a slower-eluting enoyl-CoA product peak (see below) more efficiently than utant membranes (Figure 5C). Together, these data argue that the accumulation of ydroxy intermediate in membranes depleted of Phs1p is likely to result specifically defect in the dehydration step of the elongation cycle.

associates physically with all the elongase components

the other proteins implicated in the elongation cycle (Han et al., 2002; Kohlwein 001), Phs1p localizes to the endoplasmic reticulum (Huh et al., 2003). To test Phs1p exists in a complex with the other elongation components, we used a al epitope-tagged version of Phs1p with a triple FLAG tag inserted before the C- KKLI ER-retrieval signal. Following membrane solubilization with detergent, erved specific co-immunoprecipitation of Phs1p with each of the known nts C-terminally tagged with 13xMyc (Figure 6). These interactions are unlikely result of incomplete membrane disruption, as we see no interaction with the ER membrane protein Sec61p (Figure 6). Of the four interactions tested, the Ybr159wp was apparently the weakest perhaps due to the relatively low-

UCSF LIBRARY

ession level of C-terminally tagged Ybr159w. Interestingly, despite being present in arily a faster-migrating cleaved form, only full-length Tsc13p was able to stably ciate with Phs1p. Finally, in the same experiment we observed that differentially ed versions of Phs1p were able to self-associate. These findings, together with ar co-immunoprecipitation studies using different elongase components as bait (Han , 2002; Kohlwein et al., 2001) suggest that the ER membrane activities required for acid elongation are organized into a multi-enzyme megasynthase.

p is the elongation cycle dehydratase

inding that Phs1p can associate with other biochemically uncharacterized proteins cated in VLCFA synthesis along with the fact that it has no obvious homology to dehydratases (see Discussion), raises the question of whether it is directly sible for catalyzing the dehydration step or merely a regulatory/accessory of the dehydratase. To distinguish between these possibilitites, we performed a large- protein purification using microsomes expressing Phs1-FLAG or the control ed protein. Membranes were solubilized under detergent conditions that disrupt the y of the elongase complex (data not shown). Elution with the FLAG peptide d by silver staining demonstrated that Phs1-FLAG (expected MW ~28 kDa) was to apparent homogeneity (Figure 7A). Strikingly, co-incubation of 3-hydroxy A and purified Phs1-FLAG (but not co-incubation with mock-purified Phs1p or AG alone) resulted in the appearance of a slower-eluting product peak (Figure s peak had the same retention time as the one whose formation was impaired in

UCSF LIBRARY

Phs1p-depleted membranes (Figure 5C) and was confirmed by LC/MS to correspond to the dehydrated enoyl C18-CoA product (Figure 7C).

Finally, to exclude the possible presence of highly active trace amounts of a co-purifying dehydratase in our yeast Phs1-FLAG preparations and at the same time facilitate future mechanistic and structural studies of Phs1p, we developed a bacterial expression system. Successful expression of functional eukaryotic membrane proteins in bacteria is challenging and in this case required the use of specialized growth media and relatively long induction times at low temperatures (see Experimental Procedures). Following membrane solubilization, Phs1-HIS was purified by native nickel affinity chromatography in the presence of detergent (Supplemental Figure S2) and, as shown in Figure 7D, catalyzed the dehydration of 3-hydroxy C18-CoA. Collectively, our findings establish that Phs1p lies at the core of the ER fatty acid elongation machinery where it acts as a membrane dehydratase to couple the two reduction steps in the elongation cycle.

ion

elongs to a large family of functionally-conserved eukaryotic proteins. The unity ion within this family is exemplified by the ability of the Pas2 plant homolog et al., 2002), and the human and zebrafish homologs to suppress the lethality d with depletion of Phs1p in yeast (Supplemental Figure S3). This family of has been suggested to be involved in tyrosine phosphorylation (Bellec et al., aberer et al., 2002; Li et al., 2000) based on the presence of a short protein phosphatase-like (PTPL) motif found in the sequence of the human homolog ho et al., 1999). However, sequence alignment of multiple family members is motif to be poorly conserved despite the very high degree of overall sequence ion within the family (Supplemental Figure S4). This observation, along with very that mutations in Phs1p homologs are responsible for the canine model of ntronuclear myopathy and the striking plant tumor-like phenotype (Bellec et al., berer et al., 2002; Pele et al., 2005), underscores the importance of defining the function of this class of proteins.

re, starting with a set of genetic interactions generated as part of a larger effort he epistasis network of the early secretory pathway (Schuldiner et al., 2005), ncovered the essential role of the yeast homolog of this family of proteins in osynthesis. Specifically, we have shown that purified Phs1p acts in vitro as the t-after dehydratase and, as such, it likely completes the minimal list of quired to catalyze a full turn of the elongation cycle. This exciting possibility

UCSF LIBRARY

ımediately relevant to ongoing efforts aimed at genetically engineering plants to mmodate the increasing human demand for synthetic products derived from erucic (a monunsaturated C22 VLCFA) (Puyaubert et al., 2005). Specifically, the limited ıcement in VLCFA production by overexpression of the condensing enzyme alone et al., 2001) may be overcome by the additional overexpression of all the remaining ation cycle activities. Furthermore, our demonstration that bacterially-expressed catalyzes the dehydration step of the elongation cycle represents the first complete stitution of one of the steps in the cycle, and as such serves as the starting point for studies aimed at a more mechanistic and structural understanding of VLCFA esis. Finally, the findings presented here allow us to interpret some of the plant *pas2* t phenotypes (Bellec et al., 2002; Haberer et al., 2002) within the framework of FA function in higher organisms.

The mechanism of LCFA elongation, though superficially similar to that of LCFA sis itself, faces unique challenges associated with synthesizing significantly more hobic species in the context of the ER membrane. Supporting this view is the ation that the two reductase components of the elongation cycle, Ybr159wp and , are homologous to enzymes distinct from the FAS domains catalyzing the onding chemical transformations (Han et al., 2002; Kohlwein et al., 2001). ver, the fact that Elo2 and Elo3p are required for the first step of the elongation et have no homology to known condensing enzymes (Paul et al., 2006), raises the ity that they mediate catalysis of the first step in the elongation cycle by an mechanism. Lastly, here we have shown that Phs1p acts as the founding member

of a unique family of membrane dehydratases. These observations raise a number of questions regarding the underlying mechanism of the elongation reaction. Are the individual steps in the cycle occurring on the cytosolic and/or lumenal leaflet of the ER membrane or are parts of the catalytic machinery embedded in the membrane itself? Indeed, the highly buried nature of the dehydratase component was suggested some time ago (Osei et al., 1989) and is likely made possible by the extreme hydrophobicity of Phs1p's amino acid sequence. Another issue regards the intrinsically reversible nature of the dehydratase reaction (Knoll et al., 1999). One way in which Phs1p might bias the reaction toward dehydration may include the efficient shunting of the 3-hydroxy intermediate to the Tsc13p enoyl reductase, as perhaps evidenced by the relatively robust interaction between these two elongase components (Figure 6). Another factor facilitating dehydration might be the strict exclusion of water molecules by a highly hydrophobic chemical environment surrounding Phs1p's active site. Lastly, the finding that Phs1p is able to self-associate and also interact with the other putative catalytic components is consistent with the large size (>700 kDa) of the elongase complex reported in plant and animal cell detergent extracts (Domergue et al., 2000; Fehling et al., 1992; Grayson and Moldday, 2005; Lessire et al., 1999). This suggests that multiple copies of each catalytic activity are present in a complex that is organized as a homo-oligomer of subcomplexes containing all four elongation cycle activities. Such an arrangement might allow for cooperation between subcomplexes, that, by analogy with FAS (Smith et al., 2003), would be required to complete a full turn of the elongation cycle. These and other questions can be addressed by future studies taking advantage of our ability to purify

active Phs1p from a bacterial source and building on our preliminary reconstitution (V.D. and J.S.W., unpublished observations) of the other steps in the elongation cycle.

In yeast, the biological roles of VLCFAs are becoming increasingly well-defined. However, the question of how basic unicellular processes that are dependent on VLCFAs are integrated into the developmental programs of higher organisms is less clear. A notable trend in the evolution of VLCFA synthesis in mammals has been the proliferation of tissue-specific Elo2/3p homologs (ELOVL). Heterologous expression of certain ELOVL proteins in yeast has demonstrated their ability to drive synthesis of specific VLCFA species that may contribute to their physiological roles in the synthesis of eicosanoid hormones, myelin homeostasis, and the recruitment of brown adipose tissue (Jakobsson et al., 2006). Interestingly, a recent genetic study demonstrated that a loss of function mutation in a *PHS1* homolog is likely responsible for the canine model of centronuclear myopathy (Pele et al., 2005). This disease is characterized by hypotonia (decreased muscle tone), generalized muscle weakness, and increased collapse upon exposure to cold (Bley et al., 2002). Our finding that Phs1p is directly involved in fatty acid elongation suggests a role for VLCFAs in myofiber homeostasis. This together with the finding that individual with mutations in the human homolog of Lcb1p, the enzyme that catalyzes the first step in long-chain base formation, suffer from muscle wasting and weakness (Dawkins et al., 2001), raises the possibility that mutations in the numerous mammalian components of the elongase complex may be responsible for hereditary cases of human myopathies.

n of what role VLCFAs play in plant development is of great interest
e of a large family of fatty acid elongation/keto acyl-CoA synthases
ısing enzymes (Dunn et al., 2004). These proteins have been shown to
eductase/dehydratase/reductase tri-partite catalytic machinery and may
panded repertoire of elongated fatty acid species in plants (Paul et al.,
ely, efforts to understand the full spectrum of plant developmental
ıg from a global alteration in VLCFA levels have been complicated by
st, the restricted expression pattern and narrow substrate specificity of
CS proteins (Fiebig et al., 2000; Millar et al., 1999; Millar and Kunst,
he lack of good conditional alleles that would obviate the problem of
with complete loss of the Ybr159wp homologs in maize (Dietrich et
the presence of additional masking enoyl reductase activities that are
10 (*A. thaliana* Tsc13p homolog) (Zheng et al., 2005).

cation of Phs1p as a key enzyme in the elongation cycle gives insight
ogical role of VLCFAs. In particular, it may provide a molecular
phenotypes caused by mutations in the widely-expressed *A. thaliana*
omolog) (Bellec et al., 2002; Haberer et al., 2002). *Pas2* plants were
n for uncontrolled cellular proliferation, and as such, they serve as a
ding tumorigenesis in plants (Faure et al., 1998). In addition to this
l below, these *pas2* mutants are characterized by severely stunted
presence of deformed leaves, generally poor fertility, and organ
2002; Faure et al., 1998; Haberer et al., 2002). The observed overall

USF LIBRARY

growth defect is likely a reflection of the reported reduction in cell size. Given the mportance of GPI-anchored proteins in cell expansion (Schindelman et al., 2001), one simple molecular explanation for the reduced size of *pas2* plants is that impaired VLCFA ynthesis interferes with the remodeling of GPI anchors that, by analogy to studies in east (Horvath et al., 1994), are likely to be required for proper delivery of GPI proteins o the cell surface. While poor fertility may result from any number of reasons, a lausible mechanism, in this case, might be that alterations in the composition of the LCFA-rich pollen coat result in the disruption of pollen/stigma interactions necessary or successful fertilization. This explanation is analogous to that proposed for plants with utations in *CER6,* a member of the FAE/KCS family (Fiebig et al., 2000). Finally, a stemic defect in VLCFA synthesis could bring about the observed organ fusion henotype in *pas2* mutants by way of mechanical disruption of the VLCFA-rich cuticle, a ructure required to prevent organ fusion (Sieber et al., 2000). Further supporting this gument are plant studies involving more limited reduction in VLCFA levels or more eiotropic alteration of FA metabolism. First, mutations in *FDH* (Lolle et al., 1992; uitt et al., 2000; Yephremov et al., 1999), another member of the FAE/KCS family, ve been shown to result in organ fusions that are recapitulated by administration of fenacet, a herbicide inhibitor of Fdhp (Lechelt-Kunze et al., 2003). Second, organ ion can be induced by spraying adult plants with an inhibitor of acetyl CoA boxylase (*ACC1*), the enzyme responsible for synthesizing malonyl-CoA (Baud et al., 04), a key anabolic precursor in several biochemical pathways, including VLCFA thesis. Incidentally, partial loss-of-function mutations in the essential *ACC1* gene have n shown to be allelic to *pas3* (Baud et al., 2004), a mutant identified in the same

UCSF LIBRARY

screen as *pas2* (Faure et al., 1998). Lastly, the reported organ fusion phenotype in *pas2* mutants is reminiscent of that seen in the *cer10* enoyl reductase mutant (Zheng et al., 2005).

In addition to these developmental defects, seen in many other mutants, *pas* mutants also display a more unique phenotype of tumor-like growth. In light of the findings presented here, this phenotype suggests a novel role for VLCFAs in coordinating cell proliferation and differentiation events in multi-cellular organisms. One explanation for the observed uncontrolled proliferation is that the mechanical disruption of certain VLCFA-rich tissues, that normally act as physical barriers, results in the exposure of nearby cells to ectopic growth factors. Another model is that VLCFAs are required for the synthesis of lipid signaling molecules that regulate major developmental patterning decisions. Related to this is the idea of signaling by LCB-P species. Such a phenomenon has been reported in plants (Coursol et al., 2003), and by analogy to *phs1* mutants (Figure 2B), LCB-Ps are likely to accumulate in *pas2* plants as a result of a global defect in VLCFA synthesis. A further intriguing possibility is that changes in ceramide and sphingolipid metabolism contribute to uncontrolled proliferation by affecting the secretion of plant morphogens. This final possibility is particularly appealing given the recently demonstrated role of auxin in promoting its own efflux from plant cells by regulating the trafficking of its efflux facillitator (Paciorek et al., 2005). Indeed, *pas2* mutants have been reported to have reduced expression of primary auxin response genes (Harrar et al., 2003). Future cytological and biochemical studies should help unravel the

ıtribution of these and other VLCFA-dependent mechanisms to the pathophysiology of ;2 mutants.

More practically, several human disorders are associated with alterations in LCFA metabolism (Wanders, 2004). Specifically, adrenoleukodystrophy (ALD) is a ;ease that in its terminal childhood form is accompanied by severe demyelination of the rvous system (Moser et al., 1992). At a biochemical level, ALD is characterized by :reased production of saturated C26 fatty acids by the elongase complex (Kemp et al., 05; Tsuji et al., 1984; Tsuji et al., 1981). Attempts at ameliorating the disease by ıibiting the elongation machinery with a diet enriched in shorter monounsaturated ecies ("Lorenzo's oil") have met with mixed success (Aubourg et al., 1993). While the :atment normalized the levels of saturated C26 fatty acids in ALD patients, this was companied by a concomitant increase in very-long monounsaturated species (Kemp et , 2005) and a failure to halt neurodegenerative progress. These findings clearly ıstrate the necessity to better understand the underlying mechanism of the elongation :le in order to devise more effective VLCFA-targeted therapeutic strategies.

UCSF LIBRARY

Experimental Procedures

Antisera

Anti-FLAG M2 antibody-coupled resin and free antibody were purchased from Sigma. Anti-Myc 9E10 was purchased from Roche. Anti-Sec61 was a gift from P. Walter (University of California, San Francisco). Secondary antibodies labeled with IR800 dye and Alexa Fluor 680 were purchased from Rockland Immunochemicals and Invitrogen, respectively.

Strains

Δlcb4, Δelo1, Δelo2 (fen1), Δelo3 (sur4) were obtained from the *S. cerevisiae* deletion consortium (Winzeler et al., 1999b). *phs1-damp* mutant construction was previously described (Schuldiner et al., 2005). *Δybr159w* was made by transforming a diploid from a cross between BY4741 and BY4742 (Brachmann et al., 1998) with a PCR product containing the *C. glabrata HIS3* prototrophic marker (Sakumoto et al., 1999). The resulting heterozygote was sporulated to obtain a slow-growing haploid knock-out.

The strain expressing *PHS1* under the control of the Tet-titratable promoter was purchased from Research Genetics. The strain expressing *PHS1* under the control of the *GAL1* promoter was made by transforming a PCR product derived from pFA6a-HIS3 MX6-PGAL1 (Longtine et al., 1998) into a diploid resulting from a cross between *Δlcb4* and BY4742. The resulting double heterozygote was sporulated to obtain a haploid *Gal1-PHS1* segregant (and *Δlcb4* of an α mating type, see below). Dextrose-induced shut-off of Phs1p in this mutant is not sufficiently strong to result in growth arrest but is

UCSF LIBRARY

accompanied by strong accumulation of LCBs. *pGal1-PHS1* was crossed to *Δelo2 (fen1)* and *Δelo3 (sur4)* to generate the strains shown in Figure 2D. *Δlcb4* α was crossed to *phs1* DAmP to generate the strains analyzed for their LCB composition in Supplemental Figure S1.

Δphs1 was made in a W303 diploid strain (MAT a/α homozygous for *leu2-3,-112 his3-11,-15 trp1-1 ura3-1 ade2-1 can1-100*) by *C. glabrata HIS3* PCR knock-out. The diploid heterozygous knock-out strain was transformed with pRS316-Phs1 or pRS316-Phs1-FLAG and sporulated to obtain HIS^+ URA^+ 5-FOA^R segregants.

Elo2/3p, Ybr159wp, and Tsc13p were C-terminally tagged at their respective genomic loci by transformation of PCR products derived from pFA6a-13Myc-kanMX6 (Longtine et al., 1998) into *Δphs1* covered by pRS316-Phs1 or pRS316-Phs1-FLAG. To test the ability of Phs1p to self-associate we transformed *Δphs1* pRS316-Phs1 with the Phs1p Myc-tagging PCR product. The resulting tagged strain was transformed with either pRS314 or pRS314-Phs1-FLAG. All strains altered by genomic deletions, promoter swaps, or C-terminal taggings were checked by colony PCR. The sequences of primers used in these genetic manipulations are available upon request.

Plasmid Construction

pRS316-Phs1 was generated by PCR of the *PHS1* ORF plus ~500bp of upstream and downstream sequences from yeast genomic DNA followed by subcloning into the XhoI/XbaI sites of pRS316 (Sikorski and Hieter, 1989). Next, a polylinker containing

XmaI/ClaI sites was introduced into the C-terminal KVmkSL sequence (between the lower case residues) by subcloning a fusion PCR product into the BglII/SacI sites of pRS316-Phs1. Finally, annealed oligos encoding a triple FLAG tag were inserted into the XmaI/ClaI sites of pRS316-Phs1-polylinker. The TRP-marked variants of pRS316-Phs1 and pRS316-Phs1-FLAG were made by cutting out the XhoI/SacI insert of each and subcloning them into the corresponding sites of pRS314. The bacterial expression vector was made by PCR of the Phs1p coding sequence (without the stop codon) from pRS316-Phs1 followed by subcloning into the NdeI/KpnI sites of pET-29b vector (Novagen). PTPLb human and zebrafish homologs were obtained from Research Genetics as putative full-length clones (EHS1001-6900799 and MDR1734-7599614, repectively). The ORFs were subcloned into the SpeI and BamHI sites of pRS425 containing the SacI/KpnI fragment from p416 MET 25 (Mumberg et al., 1994). This places the ORFs under the control of the strong (in the absence of methionine) MET25 promoter and a strong CYC1 terminator. All PCR-derived inserts were checked by sequencing. The sequences of primers used to generate all the plasmids are available upon request.

UCSF LIBRARY

Growth inhibition with small molecules

Plates used in the growth inhibition experiments were SD complete (cerulenin experiment) or SD-leu-met (doxycycline experiment). In the fatty acid add-back experiment, cerulenin (Sigma) was present at a final concentration of 25 μM. Fatty acids (Matreya) were added to a final concentration of 0.5 mM. Tergitol (Sigma) was included at 1% final concentration to facilitate solubilization. In the homolog complementation experiment, doxycycline was present at a final concentration of 10 μg/ml. For the *pTet-*

PHS1 shut-off experiments, early midlog cells were treated with 10 μg/ml doxycycline for ~4 or ~8-11 hours depending on the experiment.

LCB HPLC analysis

Cellular LCBs were analyzed according to Lester and Dickson, 2001, with some modifications. Most notably, we used a linear elution gradient to resolve the fluorescently labeled species. DEAE (BioRad) fractionation of labeled species prior to HPLC analysis was done exactly as described using disposable mini-columns and gravity flow LCB identity was established by comparison with purchased standards and LCB profiles of deletion mutant strains (eg. *Δdpl1*) documented to have strong accumulation of specific LCB species. Unless otherwise stated, all HPLC analyses were done using an Eclipse XDB-C18 5 μm 4.6x150 mm (Agilent) column attached to a Waters 600S pump, 490E absorbance meter, and 474 fluorescence detector.

GC/MS

Samples were prepared according to Browse et al., 1986. Briefly, midlog cells (~40 OD_{600} units) were washed several times with water and then subjected to transesterification with 1 ml of 1 M methanolic HCl (Sigma) containing 5% v/v 2,2-dimethoxypropane (Sigma) followed by extraction exactly as described. GC/MS spectra were collected on an HP 6890 gas chromatograph outfitted with a J&W DB-XLB column. The data from the HP MSD 5973 (Agilent, Palo Alto) mass spectrometer were analyzed using Chemstation version A.03.00 software (Agilent). Peaks were identified based on co-eluting fatty acid standards (Matreya) and profiling against a database of known compounds.

USC Library

me elongation assay

nes were prepared exactly as described previously (Denic, 2006). 0.1-0.5 mg of nal protein (quantitated in 1% SDS using the Pierce BCA reagent) in 75 µl was 25 µl of 50 mM HEPES KOH pH (6.8), 1 mM MgCl2, -/+ 1mM each NAD(P)H with 40 µM acyl-CoA (Avanti Polar Lipids) and 12.5 µl of C14-labeled CoA (50-60 mCi/mmol, 100 μCi/ml, as supplied by Moravek Radiochemicals). g incubation at 37°C for 10 min, microsomes were saponified and the resulting acids extracted as described previously (Kohlwein et al., 2001). TLC was d as described by Moon et al., 2003 using channeled LK5DF plates purchased atman. Non-radioactive standards were visualized, following film exposure, by plates with bromocresol green (Alltech).

unoprecipitation

lls (~40 OD_{600} units) were grown to late mid-log phase in YPD or selective appropriate. After washing with water, cells were lysed by bead beating in 0.5 S IP buffer (50 mM HEPES-KOH [pH 6.8], 150 mM KOAc, 2 mM MgOAc, 1 l_2, protease inhibitors) containing 0.1% digitonin (Calbiochem). The detergent tion was then raised to 1% in a final volume of 1 ml. The crude lysate was d for 30 minutes at 4°C and then spun at 100,000*g* for 45 minutes. Cleared nt was added to 25 µl of equilibrated anti-FLAG affinity resin and incubated at -3 hours. Immunoprecipitates were washed 4x1 ml with HEPES IP buffer 1% digitonin. Bound material was eluted with equal volume 2x SDS loading

UCSF LIBRARY

5-10 minutes) and resolved by SDS-PAGE followed by Western blotting using the LI-COR Odyssey system.

hesis

C18-CoA was synthesized from Coenzyme A (Sigma) and 3-ecanoic acid (Matreya Inc.), as described previously for short aminoacyl haw et al., 1999). Product formation was monitored by absorbance at 254 LC. Unless otherwise specified, the linear elution gradient used to resolve is as described by Milne et al., 2001. Product-containing fractions from tions were pooled and diluted (in order to reduce the final acetonitrile to about 15%) before being applied to several OPC cartridges (Applied as described below. Following elution and speed vacuuming to dryness, the ct was resuspended in water and stored at -30°C.

dratase assay

osomes prepared as above were added to 25 μL of 50 mM HEPES KOH M MgCl2 with 3-hydroxy C18-CoA (approx. 40 μM). Following a 5 minute 37°C, acyl-CoAs were extracted as previously described (Golovko and). Briefly, following addition of 100 μl of isopropanol, membranes were minute in a waterbath sonicator. This was followed by addition of 12.5 μl onium sulfate and 200 μL of acetonitrile. The samples were vortexed for 5 entrifuged at 1,900*g* for 5 minutes. The upper phase was diluted with 1 ml ium phosphate (pH 4.9) and purified using an OPC cartridge. Once dried,

UCSF LIBRARY

A-containing species were derivatized as previously described (Larson and
l). The fluorescent *etheno* derivatives were monitored using an HPLC
an in-line fluorescence detector set to 230 nm excitation/420 nm emission.
purified PHS1-FLAG or PHS1-HIS, the dehydratase reaction was carried
olume of 20 μL (1:1 dilution of purified protein with buffered substrate as
e). Following incubation at 37°C for 30 minutes, the volume was raised
00 μL and the samples were processed as described above.

f PHS1-FLAG and PHS1-His6

Phs1-FLAG from *Δphs1* p316-Phs1-FLAG membranes was performed
described by Denic et al., 2006, with the following modifications.
re solubilized for several hours at a relatively high detergent to protein
f 1% digitonin HEPES IP buffer per 1000 OD_{600}–worth of purified
ollowing several IP washes, detergent was exchanged to HEPES IP buffer
% BigCHAP (Anatrace). Proteins were eluted with 3xFLAG peptide
CHAP buffer, subjected to SDS-PAGE, and visualized using SilverXpress

sion was done in a BL21 strain. When cells reached ~0.5 OD_{600} at 37°C in
with phosphate and containing 0.5% glycerol, they were shifted to 16°C
n induced with IPTG at 16°C overnight. Phs1-HIS expression was
Western analysis using a polyclonal anti-HIS antibody (Santa Cruz
nc.). Following lysis in a high-salt buffer, the majority of the expressed
nt in the low-speed supernatant. Membranes prepared from this fraction

UCSF LIBRARY

ized overnight at 4°C with 1% dodecylmaltopyranoside (DDM) (Anatrace). membranes were cleared by a high-speed spin before being applied to a Ni- e column (Qiagen). Standard HIS-tagged protein purification was performed owing modifications. Low-stringency imidazole washes were done in the 1% DDM, that was then exchanged for 0.5% BigCHAP, which remained ne remainder of the purification. Eluted proteins were concentrated before l to a desalting column to get rid of the imidazole. Desalted proteins were PES IP buffer containing 0.5% BigCHAP and 10% glycerol, concentrated, -30°C.

l product fractions collected from the dehydratase HPLC assay were to dryness. Each fraction was resuspended in water and injected separately HPLC column outfitted with an MS detector set to record in the positive de (Alliance 2695 Separating Module LC with Micromass ZQMS from lution gradient for resolving the *etheno* acyl-CoA species in this case was tly to accommodate the reduced flow-rate required for MS analysis.

ents

to thank F. Szoka and Y.-A. Moon for general advice on handling lipids; r introducing us to GC/MS; H. Luecke for suggesting PyBOP synthesis as o enzymatic methods; N. Gushwa and J. Garrison for help with LC/MS; Z. vincing us that membrane protein expression in bacteria is feasible and s how to do it; P. Walter and R. Stroud for reagents; B. Tomayama for

UCSF LIBRARY

help with graphics; D. Breslow, C. Patil, J. Newman, R. Farese, K. Ashrafi, and J. Cox for encouragement and helpful discussions. The Howard Hughes Medical Institute supported this work.

ıre Legends

ıre 1. Fatty acid elongation in the ER

gram depicting the chemical transformations associated with each turn of the VLCFA
gation cycle and the putative yeast catalytic components acting at each step.

ıre 2. Depletion of Phs1p results in the accumulation of ceramide precursors and a
hetic growth defect with VLCFA mutants

Diagram depicting sphingolipid metabolism in yeast. See text for details.

Wild type and *pTet-PHS1* cells were treated with 10 μg/ml doxycycline (dox) for 11
rs before analyzing their total fluorescently labeled LCBs with an HPLC apparatus
itted with an in-line fluorescence detector. The various peaks correspond to
tosphingosine (PHS) and dihydrosphingosinse (DHS) LCB species of differing chain
ths and phosphorylation status.

Wild type and *Δelo2 (fen1)* cells were subjected to LCB analysis as in part (B).

pGal1-PHS1 was crossed to *Δelo2 (fen1)* and *Δelo3 (sur4)*. Shown is a representative
type dissected from each cross and struck to single colonies on YPD. *pGal1-PHS1* is
viable in the presence of dextrose but shows a dramatically altered LCB profile that
into an allelic series (based on the total increase in LCB levels) as
DAmP<<*pTet*-dox<*pGal1*dex<*pTet*+dox (data not shown).

e 3. Loss of Phs1p function results in an *elo* phenotype associated with shorter
ge VLCFA length

UCSF LIBRARY

A) Serial dilutions (vertical dimension) of the indicated strains (horizontal dimension) were spotted onto plates -/+ 25 μM cerulenin (cer) along with either carrier, 0.5 mM tetradecanoic (C14 FA), or 0.5 mM hexadecanoic acid (C16 FA).

B) Wild type and *pGal1-PHS1* cells were grown in YPRaffinose and analyzed for total fatty acid methyl ester (FAME) content by GC/MS. Shown are the late time-points of a temperature gradient along which short- and long-chain FAME species elute in the first 10 minutes. The indicated VLCFAMEs were assigned by comparison with co-eluting standards and profiling against a database of small-molecule MS fingerprints.

Figure 4. Reduced overall elongation and accumulation of the 3-hydroxy intermediate in microsomes depleted of Phs1p

A) Microsomes prepared from wild type and *pTet-PHS1* cells (treated with doxycyline for 4 hours) were incubated for 10 minutes in the presence of non-radioactive eicosanoyl-CoA and ^{14}C-labelled malonyl-CoA -/+ NAD(P)H. Labeled fatty acids were separated by TLC and detected by film radiography.

B) Wild type and *pTet-PHS1* microsomes were prepared from cells following a more extended (8 hour) treatment with doxycycline. Microsomes were first normalized for condensation activity in the absence of reducing cofactors (data not shown) and then tested for elongation of palmitoyl-CoA in the presence of reducing cofactors. Shown are three timepoints along a 5-minute time-course.

USF LIBRARY

ure 5. Microsomes depleted of Phs1p have impaired elongation cycle dehydratase vity

Microsomes prepared from wild type, *pGal1-PHS1*, or *Δybr159w* cells grown in D were tested for palmitoyl-CoA elongation as described in Figure 4. *Δybr159w* rosomes were normalized to other samples for condensation activity in the absence of ucing cofactors (data not shown).

After a 2-hour incubation at room temperature, the three syntheses, all containing BOP, and either CoA or 3-hydroxyoctadecanoic acid alone, or the two reactants ether, were analyzed by HPLC. Adduct formation was monitored by measuring orbance at 254 nm. The heterogenous peak at ~32 minutes was also observed in ctions with PyBOP only (data not shown).

Microsomes prepared as in Figure 4B were first normalized for condensation activity he absence of reducing cofactors (data not shown) and then incubated for 5 minutes 3-hydroxy C18-CoA, along with a mock-incubation of 3-hydroxy C18-CoA alone right panel). Following extraction and purification, CoA-containing species were rescently labeled and visualized using an HPLC apparatus outfitted with an in-line rescence detector. The peak labeled with an asterisk is a non-specific breakdown uct of 3-hydroxy C18-CoA (data not shown).

USF LIBRARY

mmunoprecipitation of Phs1p with the other members of the elongase

either untagged Phs1p or Phs1-FLAG in the background of each of the ngase components or Phs1-Myc were lysed and solubilized with 1% wing a high-speed spin, cleared supernatants (total samples) were mmunoprecipitation using anti-FLAG beads. Immunoprecipitates were oading buffer and together with total samples resolved by SDS-PAGE stern analysis with the indicated antibodies.

catalyzes the dehydration reaction in vitro

expressing native Phs1p (-) or Phs1-FLAG (+) were solubilized with a 1% digitonin, cleared, and then affinity-purified using anti-FLAG resin. nd proteins were eluted using FLAG peptide and resolved by SDS- by silver staining.

ed Phs1p or Phs1-FLAG were incubated with 3-hydroxy C18-CoA along bated Phs1-FLAG alone. Following 30-minute incubation, CoA- s were analyzed as described in Figure 5C.

)-(4) containing the substrate and product peaks in part B (labeled with g numbers) were collected and analyzed by LC/MS. Shown are the ordings (SIRs) for the expected molecular weights (adjusted for the cedure) for the $[M-H]^+$ of the 3-hydroxy C18 CoA substrate (1074) and enoyl product (1056). Note the very low (background) total ion count duct fraction derived from co-incubation of 3-hydroxy C18 CoA and

UCSF LIBRARY

mock-purified Phs1p (2). Phs1-FLAG alone yielded a similar profile to that shown for (2) (data not shown). The retention times (indicated by the numbers above the peaks) of the substrate and product peaks are different from those in part (B) due to slightly different gradient conditions required for MS analysis.

(D) Phs1-HIS purified from bacteria and a mock-purified control were incubated with the dehydratase substrate and analyzed as in part (B).

USSH LIBRARY

Denic and Weissman

Figure 1

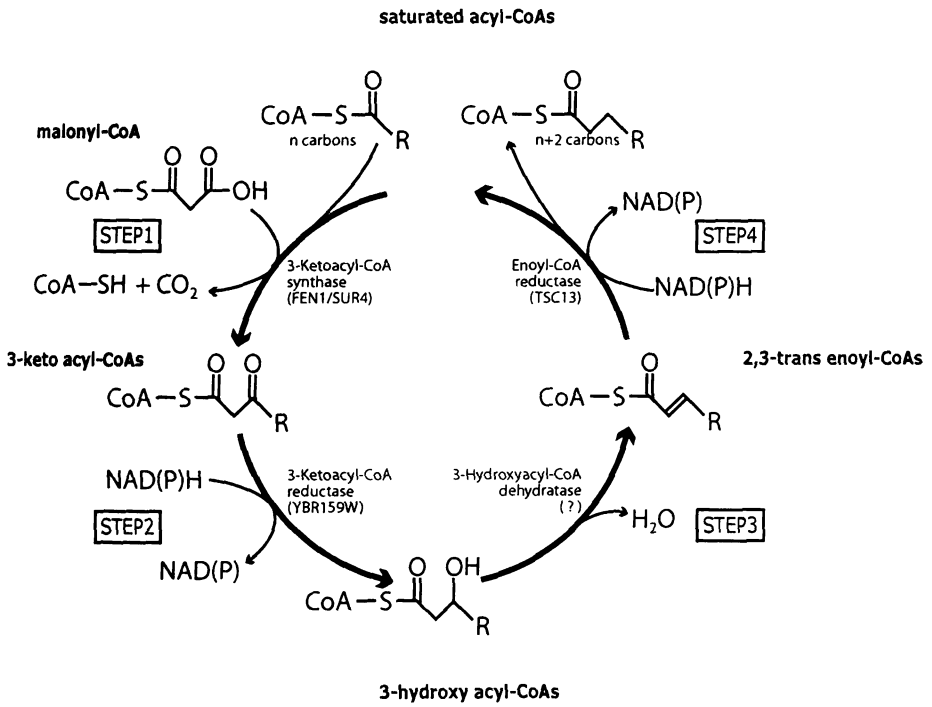

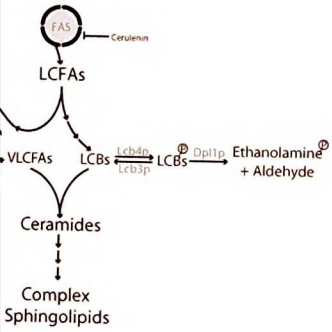

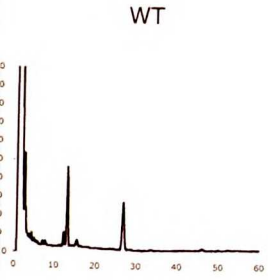

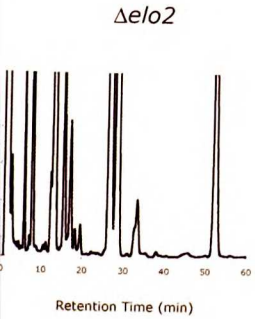

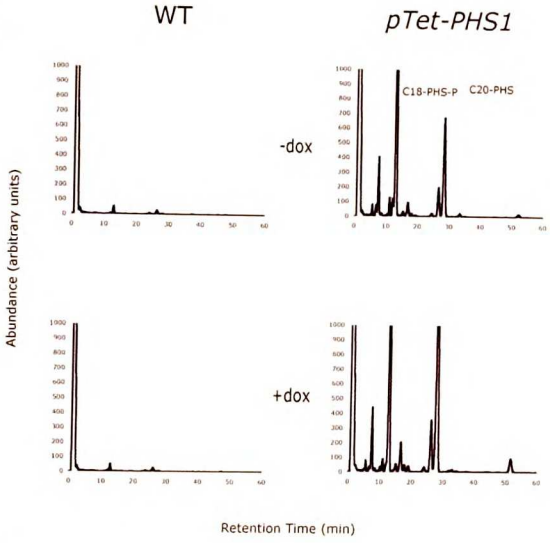

USSF LIBRARY

A

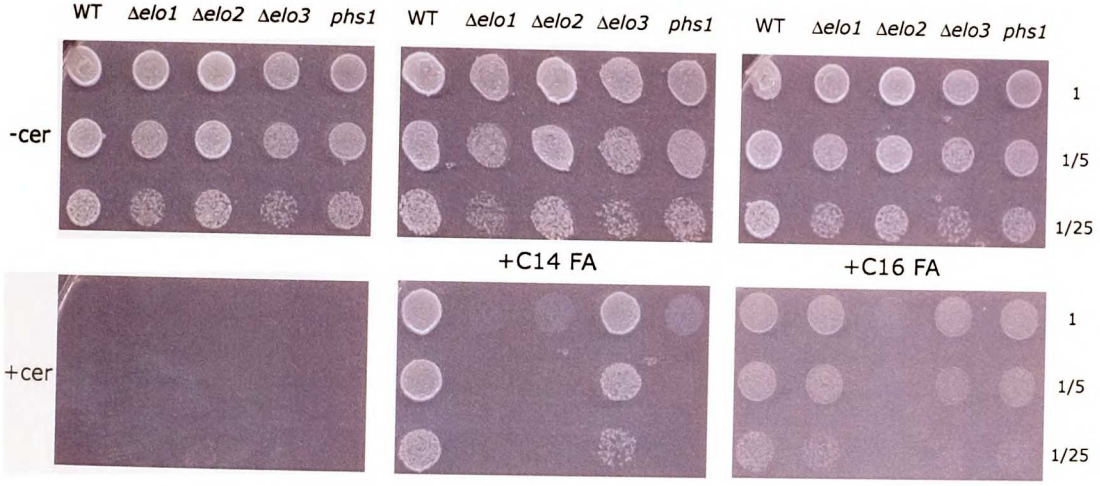
WT Δelo1 Δelo2 Δelo3 phs1
WT Δelo1 Δelo2 Δelo3 phs1
WT Δelo1 Δelo2 Δelo3 phs1
-cer
1
1/5
1/25
+C14 FA
+C16 FA
+cer
1
1/5
1/25

B

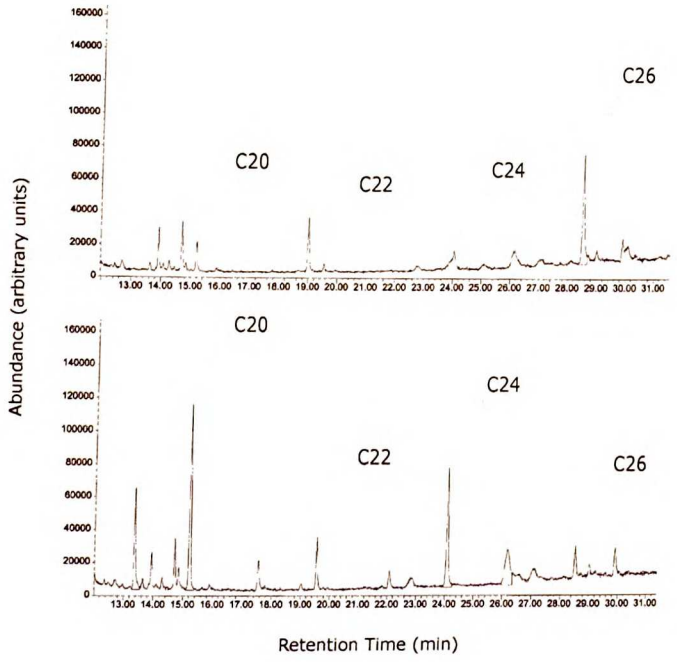
WT
phs1
Abundance (arbitrary units)
C20
C22
C24
C26
Retention Time (min)

A

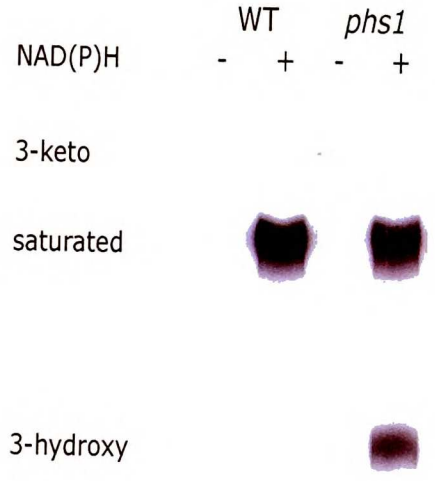
WT
phs1
NAD(P)H
- + - +
3-keto
saturated
3-hydroxy

B

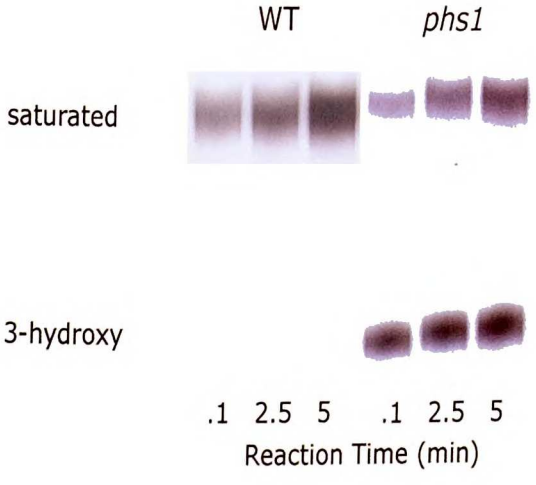
WT
phs1
saturated
3-hydroxy
.1 2.5 5 .1 2.5 5
Reaction Time (min)

Denic and Weissman

Figure 5

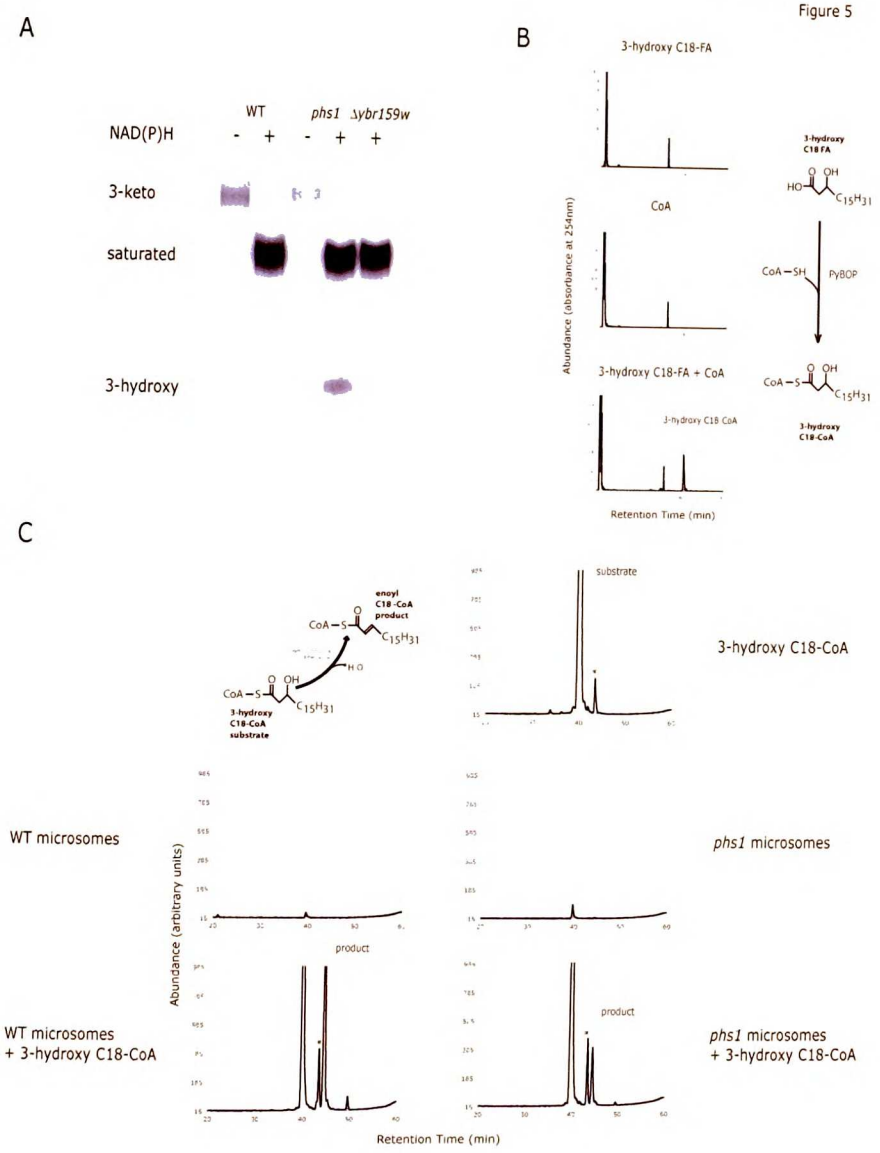

Figure 6

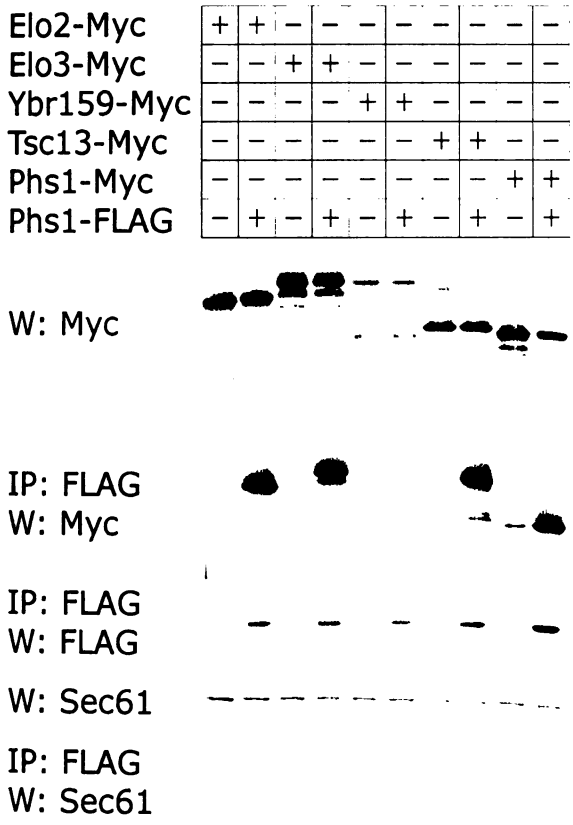
Elo2-Myc + + − − − − − − −
Elo3-Myc − − + + − − − − −
Ybr159-Myc − − − − + + − − −
Tsc13-Myc − − − − − + + − −
Phs1-Myc − − − − − − − + +
Phs1-FLAG − + − + − + − + +
W: Myc
IP: FLAG
W: Myc
IP: FLAG
W: FLAG
W: Sec61
IP: FLAG
W: Sec61

Denic and Weissman

Figure 7

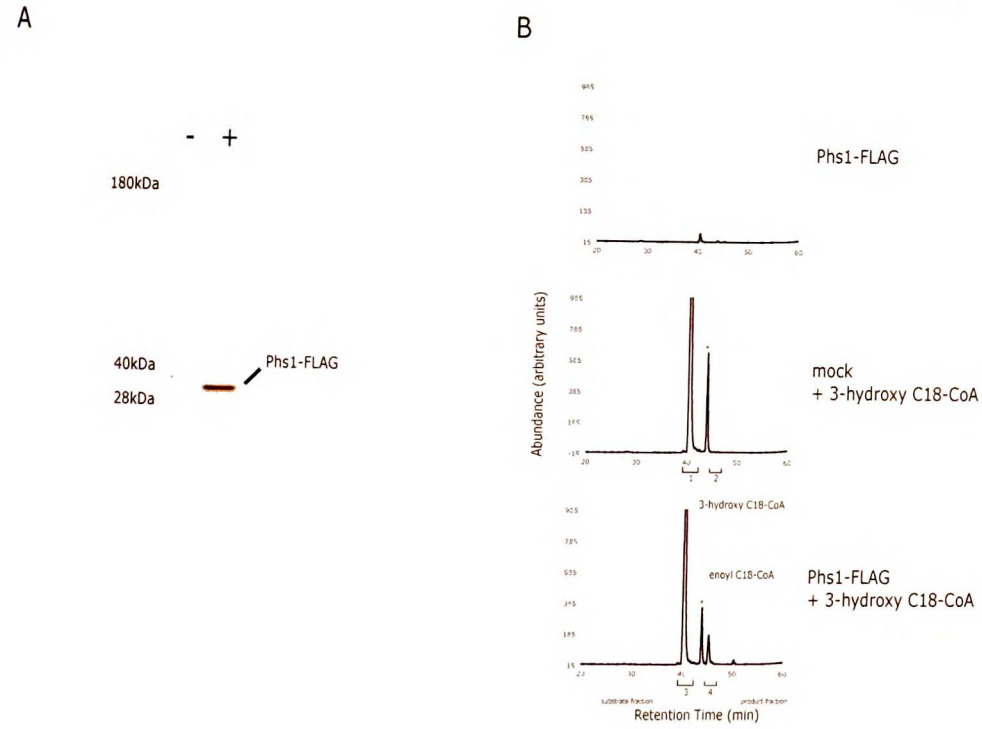

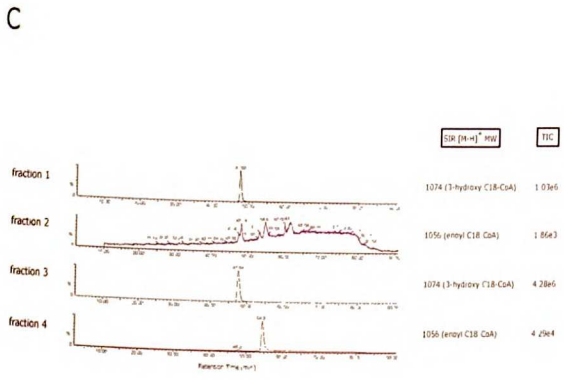

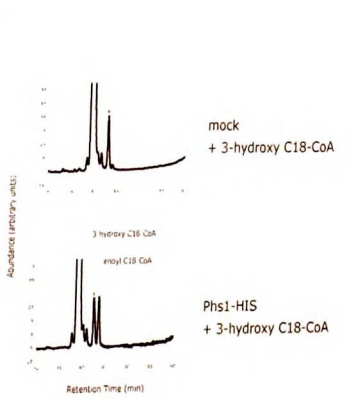

Denic and Weissman

Supplemental Figure S1

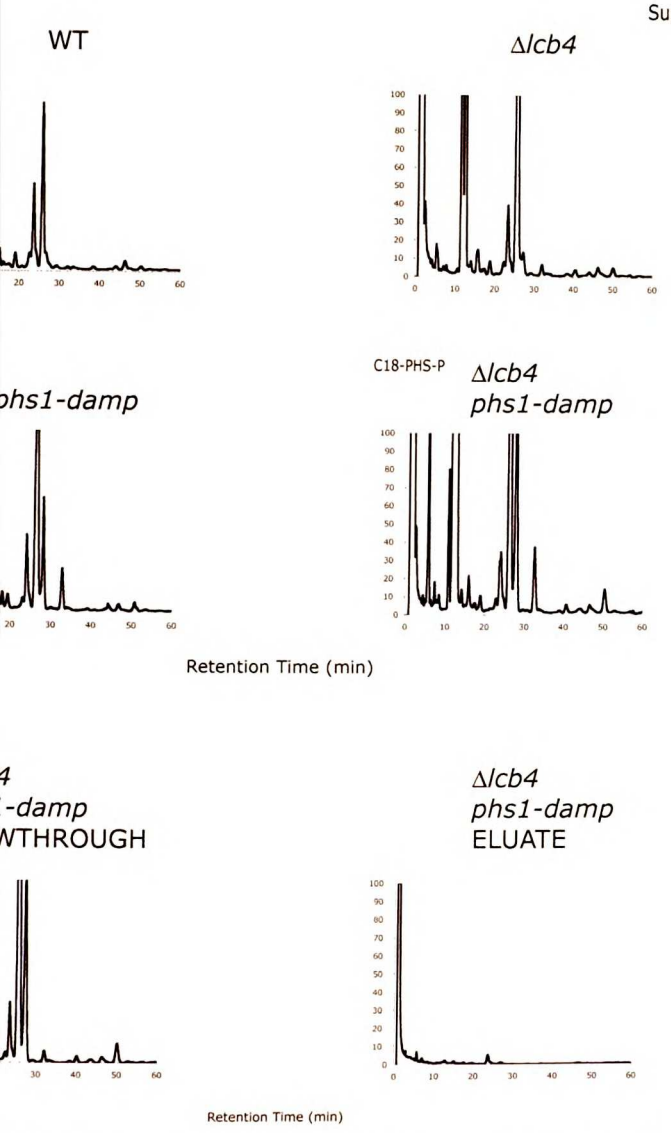

re S1. Deletion of *lcb4* eliminates the formation of phosphorylated
mp mutant

ossed to *phs1-damp* and t he resulting diploid was sporulated and re the LCB profiles of a representative tetratype. Note the absence of cies in the double mutant.

LCBs were extracted from the double mutant in part (A) and passed mn (that specifically retains phosphorylated LCBs) before separately ized amounts of) the flowthrough (containing nonphosphorylated

UCSF LIBRARY

Denic and Weissman
Supplemental Figure S2

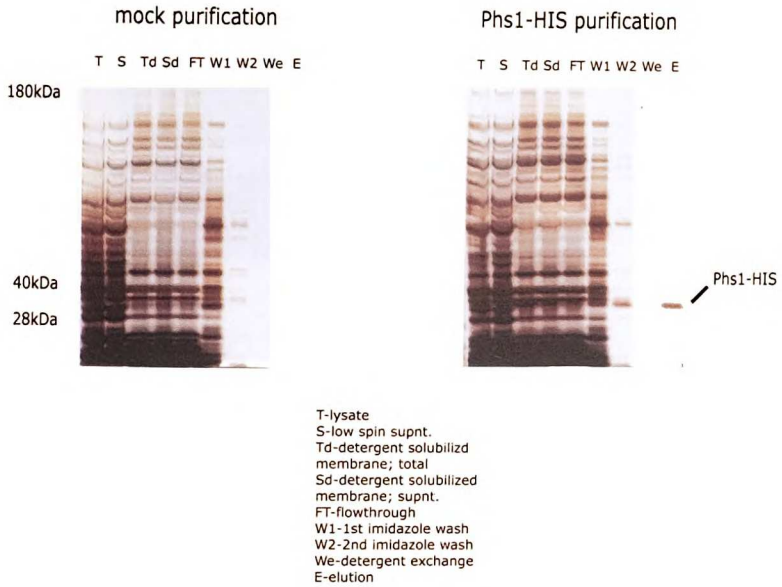

Supplemental Figure S2. Purification of bacterially-expressed Phs1p-HIS

BL21 cells carrying either empty vector or a vector expressing Phs1-HIS were induced and their membrane proteins were solubilized and subjected to nickel affinity chromatography as described in the Experimental Procedures. Purification steps were monitored by Western blotting (data not shown) and by silver staining, as shown here for a representative purification.

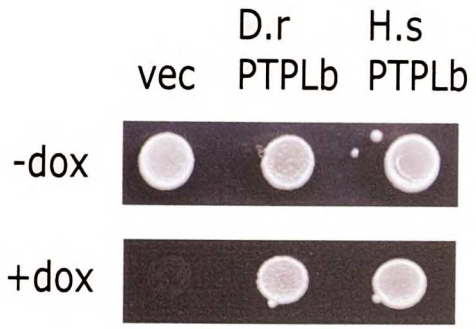

Supplemental Figure S3. PTPLb homologs substitute for the essential function of Phs1p in yeast

pTet-PHS1 was transformed with empty vector (vec) or a vector expressing the zebrafish (D.r) or the human (H.s) PTPLb homolog. Cells were spotted onto the appropriate drop-out plates -/+ 10 µg/ml doxycycline (dox).

Rockefeller University Press

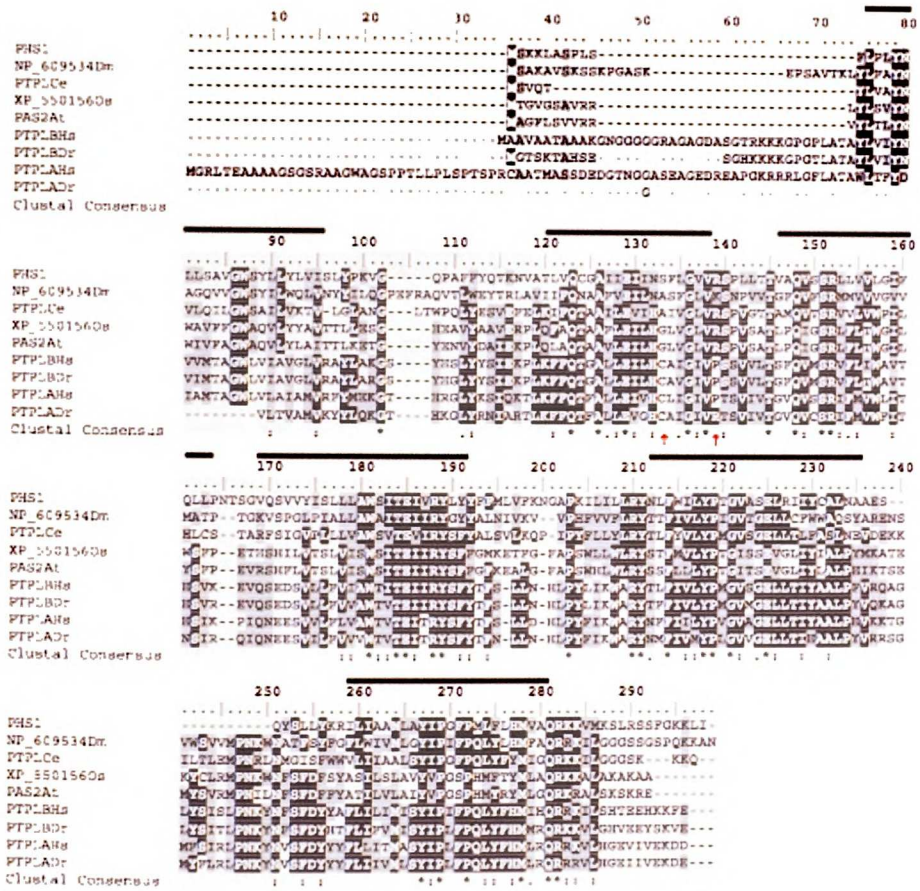

Supplemental Figure S4. Alignment of Phs1p homologs

Shown is the Clustal alignment of the amino acid sequences for the closest Phs1p homologs in flies (Dm), worms (Ce), plants (Os and At), humans (Hs), and zebrafish (Dr). Positions marked with * are absolutely conserved, while : and . denote decreasing degrees of conservation, respectively. Red arrows indicate residue positions critical for the speculated function of the PTPL motif. Black bars indicate the positions of the six Phs1p transmembrane segments predicted by Phobius with the N- and C-terminus (the latter, often containing the dibasic ER-retrieval signal) both residing in the cytosol.

CHAPTER 3

Reconstitution of the Fatty Acid Elongation Cycle Reveals the Molecular Ruler for Determining VLCFA Chain Length

Following the identification of Phs1p as the elongation cycle dehydratase I ed to test the possibility that all the components necessary for reconstituting a plete round of the cycle are now known. Implicit in this argument is the assumption Fen1p and Sur4p are acting as condensing enzymes whereas Ybr159wp and Tsc13p the keto and enoyl reductases, respectively. While these latter two putative nments were likely, a big question mark loomed over the involvement of Fen1p and p in the condensation step of the cycle (see Chapter 1).

orical Influences on the Reconstitution Approach

Previous attempts at biochemically identifying the activities of the elongation have been largely unsuccessful for a variety of reasons (see Chapter 1), not the least hich has been the unwieldy integral membrane association of all the activities. Two ant insights that emerged from some of these earlier purification attempts were that activity was strongly influenced by the concentration and chemical nature of the gent used to solubilize membranes (Bernert and Sprecher, 1979a) as well as by ges in lipid composition during the course of the purification (Bessoule et al., 1989).

In devising a scheme for reconstituting VLCFA biosynthesis I was strongly nced by the reconstituion of protein translocation (Gorlich and Rapoport, 1993) itself was building on earlier work from Blobel and colleagues (Nicchitta and l, 1990; Nicchitta and Blobel, 1993; Nicchitta et al., 1991). The approach I decided

on, at least in principle, is very simple. Each component is first purified separately in the presence of detergent. Detergent is then exchanged for synthetic lipids that reform vesicles around the purified proteins. The vesicles are isolated by ultracentrifugation and assayed for activity.

Strain Construction

Each of the components was first tagged genomically at the C-terminus with a 3xFLAG epitope. The epitope tag did not compromise the activity of the three essential genes (*YBR159w, PHS1,* and *TSC13*) as evidenced by their wild-type growth rate. (Note: for the purpose of this argument I consider the putative ketoreductase to be essential. Formally speaking, the null is alive but grows with a severely reduced growth rate (data not shown). This is due to the presence of a second non-essential ketoreductase that weakly substitutes for the absence of Ybr159wp and that when deleted is lethal in combination with *Δybr159w.* (Han et al., 2002)). Deletion of *FEN1* or *SUR4* alone is not lethal but as I will demonstrate below the epitope-tagged versions of these proteins cover the phenotypes of the corresponding nulls.

Two precautions were taken in order to minimize co-purification of other activities arising from endogenous proteins relative to the activity of the tagged protein alone. First, the endogenous promoter of each tagged protein was replaced with the promoter of yeast *TDH3,* one of the strongest promoters in the yeast genome. This resulted in significantly higher levels (several fold to ten fold, depending on the specific

mponent) of expression relative to endogenous levels (data not shown) Secondly, a rge excess of Triton X-100, a relatively strong detergent, was used in the purification of ajority of the components (see below for exceptions)

otein Purification

Cells overexpressing each of the components were lysed by bead-beating. This sis method differs from the one used in the large-scale purifications described in apters 2 and 4 which instead utilize lyticase to remove the yeast cell wall prior to lysis. ne reason for the switch has been motivated by the observation that the latter method is ss efficient in a side-by-side comparison with the bead-beating method. Morveover, the moval of the cell wall prior to lysis involves the treatment of cells with high ncentrations of a strong reductant, a potentially unfavorable condition for obtaining talytically active proteins that are normally stabilized by disulfide bonds. Following sis, the protein purification procedure becomes essentially as described previously enic et al., 2006) with a few notable modifications. First, 15% glycerol was added to the post-lysis buffers. Secondly, the solubilization detergent (either Triton X-100 or gitonin) was exchanged for 0.5% BigCHAP through a series of wash steps following munopurification (and several washings with the original IP buffer). Lastly, purified terial was eluted two times with 3xFLAG peptide and the two eluates were pooled. pical yields were of the order of 1 μg per liter of culture (YPD, 2 OD_{600}) (Figure 1). tical for obtaining sufficient amounts of catalytically active Fen1p (see below) was the of digitonin (2%) for the solubilization reaction. Purification using Triton X-100

UVSC LIBRARY

virtually no activity. All the remaining components were comparably active in
rgent. The preferred detergent for purifying Phs1p is digitonin as the
ion in this case is more efficient than with Triton X-100 but the level of purity
ed (data not shown).

ıtion

the reconstitution I decided to use a synthetic lipid mixture (all lipids were
individually in chloroform form from Avanti Polar Lipids) approximating the
osition of the yeast ER (Matsuoka and Schekman, 2000). This entailed
the following volumes (transferred using a glass Hamilton syringe with
ı washes in between additions) of lipid stocks (10 mg/ml except PI4P which
ng/ml): PC 16:0/18:1 54 μL; PC di18:1 210 μL; PE 16:0/18:1 23 μL; PE di18:1
S 16:0/18:1 20 μL; PS di18:1 20.5 μL; PI 38.5 μL; PI4P 260 μL; PA di18:1 23
E, PS, PI, PI4P, and PA stand for phosphatidyl choline, phosphatidyl
ne, phosphatidyl serine, phosphatidyl inositol, phosphatidyl inositol-4-
and phospatidic acid, respectively. Di16:0 refers to the fact that the lipid
he phospholipid comprises two palmitoyls whereas 16:0/18:1 corresponds to
oyl and one oleoyl. Lipid stocks were stored under argon at –30 °C in glass
es with teflon caps.

he above chloroform mixture I added 100 μL of 0.5% BigCHAP (in ddH_2O)
of 1M DTT (to prevent oxidation, especially given the prevalence of

double bonds in some of the phospholipid species). The solution was then speed vacuuming at low temperature for 7h. Following removal of organic led 250 μL of 50 mM HEPES-KOH pH 6.8 15% glycerol (LRB) to the nt film on the bottom of the tube. Resuspension was achieved by gentle d waterbath sonication.

der to remove detergent during the reconstitution I used SM2 Biobeads (from The beads would first be wetted in methanol for approximately 10 minutes cause them to contract and settle down nicely at the bottom of the tube) extensively washed with water. The beads would then be split into two washed in either low salt buffer (150 mM KOAc in LRB) or high salt buffer KOAc in LRB). The final bead slurry would comprise ~50% beads (by he corresponding salt buffer. The original use of this approach was to e optimal salt concentration for the reconstitution (as assayed by activity) by us proportions of the two bead stocks. In the end, I settled on using a 1:1 mix ead salt solutions.

nstitutions were initiated by the mixing of all the components together and an incbation on ice for 15-30 minutes. Each reaction had a total volume of d contained either one of the five possible components or 0.5% BigCHAP this mix I then added 5.4 μL of 5% BigCHAP and 11.7 μL of the lipid g with 400 μL of the 1:1 bead solution. Detergent removal was allowed to night at 4 °C with nutation. Given the viscosity of the final mix the preferred

ıbes for this incubation are the 2 mL shallow bottom ones used normally in the lab for rion polymerization reactions.

In the morning tubes are punctured with a short thin syringe needle (25G5/8) in rder to retrieve the fluid components of the reconstitutions in their entirety. This ıvolves first opening the cap of the tube (so as to prevent pressure build-up) and then uncturing the bottom of the tube with just the tip of the needle (so as to prevent the hole rom becoming wide enough to let the beads pass). The punctured tubes are then placed ıto 15 mL Falcon tubes that are spun at 1000g for 1 minute. 250 μL of the eluted ontents are then added to 1.3 ml of cold ddH_2O (to bring down the concentration of any esidual detergent even further) in an ultracentrifuge eppendorf tube. A 10 μL sample is aken at this stage to serve as the total sample in determining the percentage of protein ıcorporated into proteoliposomes. The tubes are spun at 75,000 rpm in a TLA110 rotor or 15 min at 4 °C. A 10 μL sample supernatant sample is taken after the spin. The emaining supernatant is removed except for the final 10 μL (so as to prevent disruption f the loose proteoliposome pellet). Following addition of 20 μL of lysis buffer, roteoliposomes are resuspended by pipetting first with a yellow tip (pressed against the ottom of the tube so as to facilitate shearing of the pellet material) and then with a gel-ading tip. A 1.5 μL pellet sample is taken at this stage. The microsomes are then cubated with 20 μL of an elongase reaction mix of appropriate composition. This mix is ry similar in composition to the one used for analyzing microsome elongase activity ee Chapter 2).

UCT LIBRARY

ın be seen in Figure 2, only Sur4p alone is capable of catalyzing the
a 3-keto intermediate thus suggesting that Elo proteins act as condensing
ote: this is Fen1p made using Triton X-100 which seems to yield an inactive
quent purifications of this component were done using digitonin that seemed
he condensation activity of the enzyme (data not shown)). Strikingly, the
all five components in the reconstitution resulted in efficient formation of the
ed products (Figure 2). To dissect out the contribution of the other
following Sur4p-mediated formation of the condensed 3-keto intermediate, I
reconstitute the ensuing steps in the cycle by sequential addition of the
omponents. Reconstitution of Sur4p in the presence of Ybr159wp resulted in
on of the 3-hydroxy intermediate (Figure 3). As expected, given its
hown in vitro dehydratase activity towards a synthetic 3-hydroxy C18
hapter 2), the additional inclusion of Phs1p in the reconstitution brought
mination of the 3-hydroxy intermediate with the concomitant production of a
ing product that presumably corresponds to the enoyl intermediate. This
waits further confirmation as in the normal phase TLC system used in this
urated product is predicted to run very close to the enoyl intermediate.
ion of Tsc13p is accompanied by an increase in the overall signal strength
esumably because of multiple turnovers of the elongation cycle (and/or
sic activity of the fully intact complex) that is made possible by the presence
talytic activities in the same reconstitution.

Ruler for VLCFA Chain Length

UVic LIBRARY

Lastly, given that Fen1 and Sur4p seem to be acting as members of a new family f condensing enzymes I wished to gain insight into the sequence determinants esponsible for the differential effects of Fen1p and Sur4p on the distribution of VLCFAs vivo. To address this question I generated chimeras between Fen1p and Sur4p. Each onstruct was tagged at its C-terminus with 3xFLAG so as to control for differences in rotein levels and at the same time facilitate future attempts at protein purification The espective Fen-ness and Sur-ness of each construct was assessed by a combination of two ethods. The first assay relies on the fact that Fen1p on a plasmid is able to restore rowth of *Δfen1* cells in the presence of cerulenin and C14 whereas a plasmid-bearing ur4p is a comparatively weak suppressor (Figure 4). In this way the Fen-ness of a himeric construct can be easily assessed. This assay however is not able to distinguish etween a non-functional chimeric protein and one that behaves like Sur4p. To nambigously assess the Sur-ness of the constructs I analyzed the VLCFA profile of a *sur4* strain covered by a plasmid expressing each of the chimeras. In this assay the troduction of Fen1p or a Fen1-like chimera results in a small increase in the production C24 with no apparent reduction in the strong C22 peak characteristic of strains lacking ur4p activity (Figure 5). Importantly, no C26 is made under these conditions. On the her hand, introduction of Sur4p or Sur4-like chimeras is accompanied by a strong duction in the amount of cellular C22 and the appearance of C26 (Figure 6). Using ese two assays I was able to establish that the region of Sur4p uniquely responsible for ongation of C24 species resides in a region predicted to correspond to the short luminal

UVSC LIBRARY

loop preceding the last transmembrane segment of these predicted 7-pass transmembrane proteins.

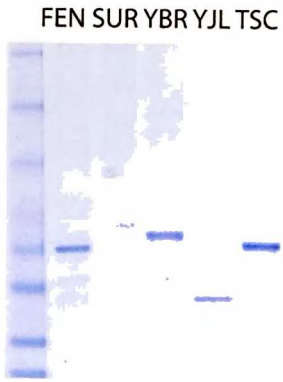

Figure 1 Purification of the elongation cycle components
Each of the indicated proteins was genomically tagged at the C-terminus with 3xFLAG and overexpressed from a TDH3 promoter. Following affinity purification samples were subjected to SDS-PAGE and colloidal blue staining.

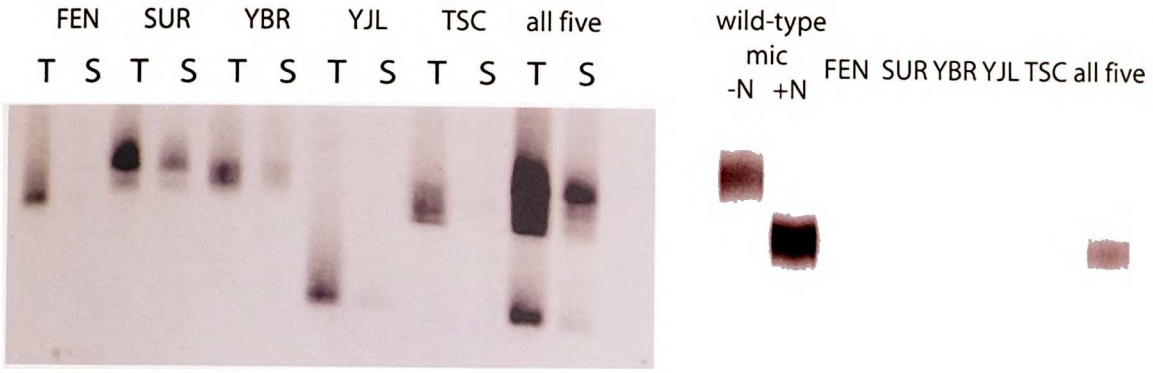

Figure 2. Sur4p acts as a condensing enzyme that acts in conjnction with the remaining candidate components to bring about the full elongation of fatty acids in the ER.
Following detergent removal a total sample (T) of each indicated reconstitution was collected and compared to the supernatant (S) after pelleting of the proteoliposomes. The fractions were analyzed by western analysis. Proteoliposomes were incubated with C20-CoA and radiolabeled malonly-CoA in the presence of reducing cofactors and analyzed by TLC. Wild-type microsomes serve as a control for the accumulation of the 3-keto intermediate in the absence of reducing cofactors (-N) and the formation of a fully saturated product in the presence of reducing cofactors (+N).

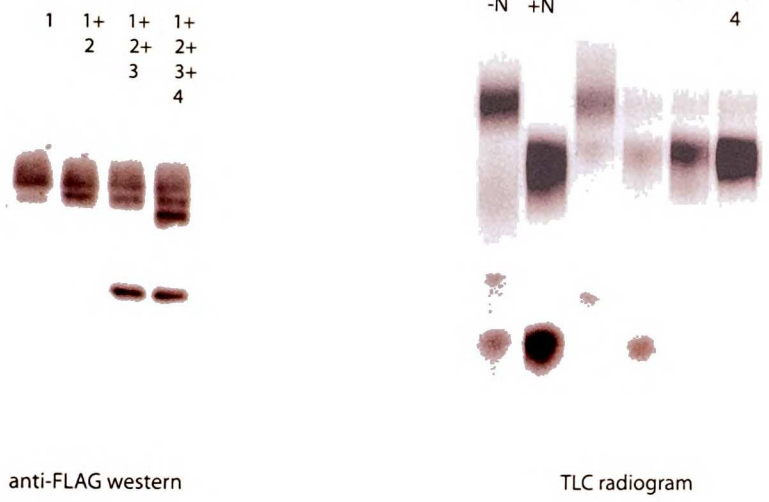

Figure 3. Reconstituion of the individual steps in the elongation cycle
Sur4p (1) was reconstituted in combination with Ybr159wp (2), Phs1p (3), and Tsc13p (4). Proteoliposomes were analyzed for the amount of each component by western and for the accumulation of C20-CoA-derived elongation cycle intermediates (in the presence of reducing cofactors) by TLC. Microsomes (mic) partially depleted of Phs1p were incubated with (+N) or without (-N) reducing cofactors as a control.

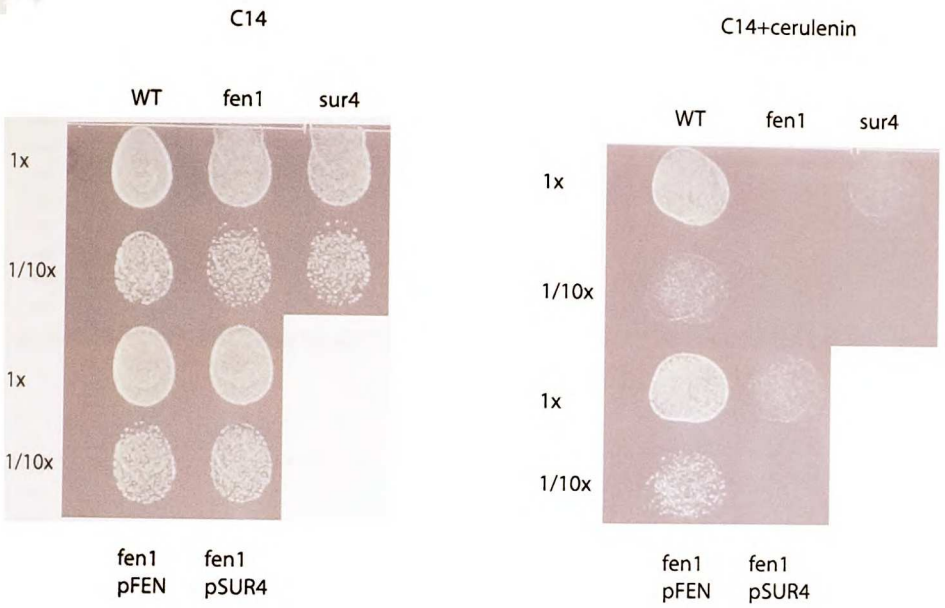

Figure 4 Sur4p is unable to substitute for Fen1p in restoring growth of fen1 mutants in the absence of FAS activity
The indicated strains were spotted onto plates containing either C14 alone or C14 with cerulenin.

UNIVERSITY of LEEDS

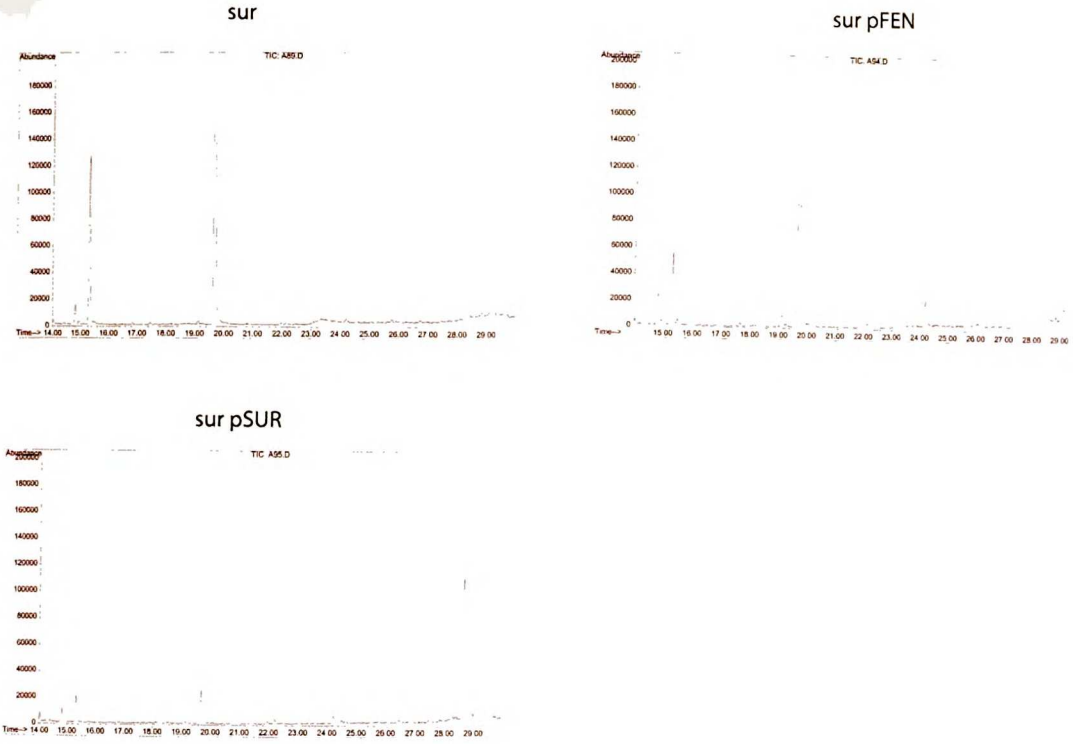

Figure 5 Sur4p but not Fen1p is able to convert C24 into C26

A strain lacking Sur4p (sur) was transformed with either empty plasmid or one expressing Fen1pFLAG (pFEN) or Sur4p-FLAG (pSUR). Total methylated fatty acids were then prepared and analyzed by GC/MS. Only the species eluting at late elution times (x-axis) are shown. C22 elutes just before 20 minutes, C24 elutes just after 24 minutes, and C26 elutes between 28 and 29 muntes.

Brock University Library

CHAPTER 4

Exploration of the topological requirements of ERAD identifies Yos9p as a lectin sensor of misfolded glycoproteins in the ER lumen

UCSD LIBRARY

n of the topological requirements of ERAD identifies Yos9p as a lectin sensor of misfolded glycoproteins in the ER lumen

namidipati, Vladimir Denic, Erin Quan and Jonathan Weissman

es Medical Institute, Department of Cellular and Molecular Pharmacology, California-San Francisco, San Francisco, CA94143-2240, USA

ce:

Weissman

(phone)

(fax)

p.ucsf.edu

UCSF Library

Role of *YOS9* in ER-associated degradation

n permission from Molecular Cell, Vol. 19, 741-751, Bhamidipati, A., n, E. M., Weissman, J. S., Exploration of the topological requirements of s Yos9p as a lectin sensor of misfolded glycoproteins in the ER lumen, 5), with permission from Elsevier.]

Summary

ER-associated degradation (ERAD) of glycoproteins depends on dual recognition of protein misfolding and remodeling of the substrates' N-linked glycans. Following recognition, substrates are retrotranslocated to the cytosol for proteasomal degradation. To explore the directionality of this process, we fused a highly stable protein, DHFR, to the N- or C-terminus of the soluble ERAD substrate CPY* in yeast. Degradation of the C-terminal CPY*-DHFR fusion is markedly slowed and is accompanied by DHFR release in the ER lumen. Thus, folded lumenal domains can impede protein retrotranslocation. The ER lumenal protein Yos9p is required for both release of DHFR and degradation of multiple ERAD substrates. Yos9p forms a complex with substrates and has a sugar-binding pocket that is essential for its ERAD function. Nonetheless, substrate recognition persists even when the sugar-binding site is mutated or CPY* is unglycosylated. These and other considerations suggest that Yos9p plays a critical role in the bipartite recognition of terminally misfolded glycoproteins.

UVa LIBRARY

Introduction

Proteins entering the secretory pathway are first translocated in an unfolded form across the ER membrane (Matlack et al., 1998). Once in the ER, they acquire N-linked glycans and attempt to fold into their native states with the help of a variety of resident chaperone and redox proteins (Helenius and Aebi, 2001). The high flux of proteins through the ER, together with the fact that many secreted proteins have multiple domains and fold slowly, poses a significant recognition problem: how does the ER distinguish between *bona fide* folding intermediates and terminally misfolded proteins? The severity of this problem is illustrated by the fact that even in the absence of acute lumenal stress, a large fraction of nascent ER proteins fails to fold and is consequently targeted for destruction (Casagrande et al., 2000a; Friedlander et al., 2000b; Jensen et al., 1995; Travers et al., 2000; Ward et al., 1995).

In order to avoid accumulation of unsalvageable, misfolded polypeptides that would otherwise impair ER function, the cell has evolved a series of mechanisms, commonly referred to as ER-associated degradation (ERAD), to dispose of such species (Fewell et al., 2001; Hirsch et al., 2004; Tsai et al., 2002). Over the last ten years it has emerged that for lumenal substrates degradation comprises the following sequence of events: recognition of the misfolded protein, targeting for retrotranslocation across the ER membrane and finally ubiquitin-dependent degradation by the cytosolic proteasome. Insight into how the ER distinguishes folding intermediates from terminally misfolded

ns has come from findings that misfolded glycoproteins undergo slow trimming of N-glycans by a variety of glycosidases in the ER (Liu et al., 1999; Spiro, 2004). time-dependent remodeling of N-glycans in conjunction with persistent protein lding is thought to result in a bipartite signal for degradation by the ERAD inery. This affords folding intermediates a protected period of time, before they re remodeled N-glycans, to reach their native state (Wu et al., 2003). Indeed, lete elimination or specific alterations of N-linked glycans leads to severe defects in egradation of a number of substrates (Jakob et al., 1998; Knop et al., 1996b). While equirement for proper glycosylation in ERAD is well established, far less is known how the glycosylation state of substrates is monitored by the ERAD machinery. mportant clue comes from the finding that a conserved ER localized mannosidase- rotein, EDEM/*HTM1*, plays a critical role in ERAD (Hosokawa et al., 2001; Jakob 1998; Molinari et al., 2003; Nakatsukasa et al., 2001; Oda et al., 2003). The nce of a mannosidase-like domain lacking a critical catalytic residue and the ce of any in vitro mannosidase activity (Jakob et al., 2001) have led to the stion that EDEM/*HTM1* acts as a lectin in ERAD. Nonetheless, it remains to be ished whether EDEM/*HTM1* binds specific N-glycans and if such lectin activity butes to its role in substrate degradation.

While such studies have yielded a conceptual and molecular framework for ng about the recognition problem they have, in turn, raised a second one - namely, re misfolded ER proteins transported across the ER membrane to the degradation nery in the cytosol. This separation, while shielding protection to proteolytically ve folding intermediates from being exposed to the protease machinery, poses a

potential problem for terminally misfolded multidomain proteins, since these typically will have stable folded regions that may inhibit the retrotranslocation process. At the heart of this multidomain problem lies the poorly defined process of retrotranslocation itself (Johnson and Haigh, 2000; Lilley and Ploegh, 2004; Ye et al., 2004). To gain insight into this process we generated a series of reporters comprising a highly stable protein, dihydrofolate reductase (DHFR), fused to the N- or the C-terminus of misfolded mutant carboxypeptidase Y (CPY*), the well-characterized soluble ERAD substrate.

Here we show that fusing a stable DHFR domain to the C-terminus markedly slows down degradation, and that degradation is accompanied by the release of free DHFR into the lumen. These studies establish that the ER posseses a mechanism for releasing folded domains from multi-domain proteins prior to completion of retrotranslocation and led us to perform a genetic screen for components necessary for the generation of the DHFR fragments. We further describe the characterization of one such component, Yos9p, a lectin required for the recognition of lumenal misfolded glycoproteins.

Results

Revealing the vectorial nature of retrotranslocation

In order to explore if there is an intrinsic directionality to the process by which lumenal misfolded proteins are recognized and retrotranslocated into the cytosol, we investigated the effects on degradation kinetics of fusing a highly stable protein to either the N- or C-terminus of the well characterized ERAD substrate CPY* (Hiller et al., 1996) (Figure 1A). In each case, the fusion protein was expressed in *S. cerevisiae* from the endogenous CPY promoter on a low copy (CEN/ARS) plasmid and a C-terminal triple HA epitope tag was appended in order to facilitate detection. Fusion proteins were targeted to the ER by the N-terminal signal sequence from *KAR2* (Craven et al., 1996). The logic behind this approach is that if substrate recognition and retrotranslocation require a flexible end then the addition of a stable domain - in our case, *E. coli* dihydrofolate reducatase protein (DHFR) - will provide a physical block to the process. A similar strategy has been used to monitor a range of other biological translocation events including protein import into mitochondria and threading of proteins into the proteolytic chamber of the proteasome (Eilers and Schatz, 1986; Johnston et al., 1995; Lee et al., 2001; Matouschek et al., 1997). Such studies have typically exploited the high stability of mammalian DHFR when complexed with its inhibitor, methotrexate. However, as it was unclear if the charged methotrexate molecule could effectively enter the ER lumen, we used the *E. coli* protein, which is structurally similar to the mammalian protein but folds more rapidly and is significantly more stable (Lee et al., 2001).

We found that fusion of DHFR to the N-terminus did not significantly alter the rate or efficiency of degradation of CPY* or of the CPY*-DHFR C-terminal fusion (Figure 1B and supplemental Figure S1). In contrast, addition of DHFR to the C-terminus of CPY* led to strong stabilization of the fusion protein (Figure 1B). This overall stabilization was a direct consequence of the folded structure of the DHFR protein (as opposed to the presence of the ectopic sequence *per se*) as a similar fusion with mutant form of DHFR [CPY*-DHFR(Pro)] in which the stability of the fold has been disrupted by the mutating three residues to prolines (Ala-29-Pro, Trp-30-Pro and Phe-31-Pro), fails to stabilize CPY* (Figure 1C). Remarkably, during degradation of the CPY*-DHFR fusion, we observe fragments (typically a doublet) that are recognized by both α-HA antibodies as well as α-DHFR antibodies (Figure 1D and data not shown). Moreover, the fragments do not accumulate during degradation of the CPY*-DHFR(Pro) mutant. Full-length CPY*-DHFR and the released DHFR fragments are associated with the microsome fraction and resist proteolysis by proteinase K until the addition of detergent, thus confirming that they remain in the ER lumen (Figure 1E and data not shown).

We observe that degradation of CPY*-DHFR fusion and generation of the DHFR fragments is dependent on two previously identified ERAD components required for cytosolic ubiqitination of CPY*: *HRD1*, a ubiquitin ligase (Bays et al., 2001b), and *DER1*, a four-pass transmembrane protein (Hitt and Wolf, 2004a) that plays a central and conserved role in ERAD (Hiller et al., 1996; Knop et al., 1996a), possibly even in directly facilitating passage across the membrane (Lilley and Ploegh, 2004; Ye et al., 2004) (Figure 1F and data not shown).

The above findings provide a number of novel insights into the mechanism by ıich misfolded proteins are recognized and removed from the ER. First, they monstrate an intrinsic directionality to the process (see Discussion). Second, they ow that the presence of a stable folded lumenal domain can strongly inhibit degradation a partly misfolded multi-domain protein implying that retrotranslocation (or possibly cognition) of folded regions within a misfolded substrate is at least in some instances sfavored or even prohibited. Third, they demonstrate that at least in part, the ERAD achinery circumvents the inhibitory effect of stable lumenal domains by releasing them to the ER lumen through an uncharacterized clipping process. Finally, they establish at liberation of stable folded domains is dependent on the same machinery responsible r the normal degradation of ERAD substrates.

ole for Yos9p in the degradation of lumenal misfolded proteins

We next reasoned that because generation of the DHFR fragments from the PY*-DHFR fusion depended on known components of the ERAD machinery (e.g. er1p, Hrd1p), we could identify novel players acting at or upstream of the clipping ent by looking for yeast mutants that fail to generate the DHFR fragments. To this end, screened a bank of yeast strains, each deleted for one of ~400 nonessential genes own to encode proteins localized to the ER or the early secretory pathway (Huh et al., 03; Kumar et al., 2002). Each strain was transformed with a plasmid carrying CPY*-HFR and the half-life of the fusion protein as well as the release of fragments was onitored by Western blot analysis of cell extracts following inhibition of protein nthesis with cycloheximide. For the remainder of the present work we will focus on a

single protein, Yos9p, identified in this screen (Figure 2A). A full analysis of the results of the screen will be presented elsewhere. Yos9p, previously named on the basis of similarity to a mammalian gene (OS-9) amplified in patients with osteosarcoma (Su et al., 1996), is a poorly characterized protein with two notable features: a mannose 6-phosphate receptor homology (MRH) domain (Munro, 2001) and a C-terminal HDEL sequence which acts as an ER retrieval signal (Pelham et al., 1988) and which is also found in a handful of other lumenal ER resident proteins such as Kar2p and PDI.

An earlier report had suggested that deletion of *YOS9* leads to a modest defect in the trafficking of GPI anchored proteins (Friedmann et al., 2002). However, a more recent analysis (Szathmary et al., 2005; Kim et al., 2005) failed to observe such a defect in a range of different strain backgrounds including those used in the original report. In addition, as this work was being prepared for publication Wolf and co-workers (Buschhorn et al., 2004) reported that Yos9p is required for the ER-associated degradation of glycoproteins. Similarly, we see that loss of Yos9p, in addition to stabilizing the CPY*-DHFR fusion (Figure 2A), results in a profound defect in CPY* degradation, comparable to that caused by the loss of *DER1* (Figure 2B and C). Interestingly, the defect seen in the *Δyos9* strain is considerably stronger than that seen in a *Δmns1* strain (Figure 2B and C). Mns1p is the α–1,2 mannosidase that removes one mannose residue from the core oligosaccharide resulting in the conversion of the $Man_9GlcNAc_2$ form to $Man_8GlcNAc_2$ form. Mns1p acts as a "timer" whose delayed action provides a grace period for proteins to fold before they are subjected to surveillance by the ERAD machinery (Liu et al., 1999; Spiro, 2004). Additionally, the rate of CPY* degradation in the double deletion strain *Δmns1Δyos9* is indistinguishable

from the single *Δyos9* strain. Thus, Yos9p is a critical component of the ERAD machinery whose action maybe enhanced by, but is not fully dependent on, the Mns1p mannosidase timer.

Earlier studies indicated that there are at least two distinct surveillance mechanisms for identifying terminally misfolded ER proteins (Ahner and Brodsky, 2004; Huyer et al., 2004): one (designated ERAD-L) that inspects for proteins like CPY* that contain misfolded lumenal (soluble or membrane tethered) domains and a second (termed ERAD-C) that detects misfolded cytosolic domains of transmembrane proteins. While both of these pathways ultimately converge on the ubiquitin proteosome degradation system, they depend on different sets of ER-associated components to detect misfolded species and deliver them to the cytosol.

To explore the role of Yos9p in these two ERAD pathways, we took advantage of three substrates developed by Ng and co-workers (Vashist and Ng, 2004) that contain misfolded domains oriented to the lumenal and/or cytosolic face. One ERAD-L substrate, KHN, consists of a Kar2p signal sequence fused to the simian virus 5 HA-Neuraminidase ectodomain and like CPY* is a soluble lumenal protein. A second ERAD-L substrate, KWW, consists of KHN fused to the transmembrane domain from the Wsc1p protein such that KHN is oriented to the lumenal side of the ER. A third substrate, KWS, is designed to monitor the ERAD-C process. KWS contains a lumenal KHN domain, the transmembrane Wsc1p domain and a cytosolic domain of the misfolded Ste6-166p mutant. For the two ERAD-L substrates (KHN, KWW), loss of Yos9p led to a profound defect in degradation, comparable to that seen with loss of components of the core ERAD-L machinery (e.g., Der1p and Htm1p) and substantially greater than the defect

absence of Mns1p (Figure 3A, B). In contrast, the degradation of the ERAD-C
KWS, was not affected by loss of Yos9p (Figure 3C). Thus, Yos9p plays a
in the recognition and/or subsequent retrotranslocation of a range of proteins
misfolded lumenal domains.

lectin whose sugar-binding pocket is required for ERAD

presence of the MRH domain in Yos9p is particularly intriguing in light of
nd incompletely understood role that substrate glycosylation plays in allowing
be recognized by the ERAD machinery. While some MRH domains are
nnose 6-phosphate lectins, other MRH domains recognize protein substrates
ndependent manner (Ghosh et al., 2003). In particular, the cation-independent
-phosphate receptor (CI-MPR) contains 15 MRH repeats, only two of which
nd 9) are thought to contain high affinity mannose 6-phosphate binding sites.
nalysis of the single MRH domain in the cation-dependent MPR (CD-MPR)
with mannose 6-phosphate, in conjunction with mutational studies, have
our residues (Gln66, Arg111, Glu133, Tyr143) that are in direct contact with
e sugar and are critical for carbohydrate recognition (Hancock et al., 2002;
, 1999) (Figure 4A and B). These residues provide a strong signature
f sugar binding activity as they are highly conserved among the MRH repeats
PR that tightly bind mannose 6-phosphate (repeats 3 and 9) but diverge
e MRH repeats not involved in sugar binding (Ghosh et al., 2003). Of these
re residues, the final three are located at well defined positions relative to
ysteines and thus their location in Yos9p (Arg200, Glu223, Tyr229) and its

Figure 4A) can be unambiguously determined despite the weak overall
etween the various MRH domain-containing proteins. Significantly, we find
ative changes (Glu-to-Asp, Tyr-to-Phe, Arg-to-Ala) to these signature
ngly inhibit or completely abrogate CPY* degradation (Figure 4C). Thus,
alysis in conjunction with mutational studies strongly supports the notion that
ctin and that this sugar binding activity is critical to its ability to support

ient recognition and degradation of misfolded glycoproteins requires the
specific oligosaccharide structures on the substrate polypeptide (Jakob et al.,
, in principle, the degradation defect seen in a strain lacking Yos9p could be
consequence of either failure to properly synthesize N-linked core
ides or failure to correctly trim such oligosaccharides. To exclude the
hat Yos9p is required for the synthesis of the core oligosaccharide, we
glycosylation state of mature wild type CPY. As noted previously (Jakob
failure to generate full-length high mannose sugars (e.g., caused by deletion
or *ALG12* genes) leads to reduced efficiency of N-glycosylation of wild type
oligosaccharyltransferase, resulting in a ladder of hypoglycosylated CPY
ntrast, no such ladder is seen in a *Δyos9* strain, indicating that Yos9p is not
he production or transfer of full-length high mannose oligosaccharides to
eptide chains (data not shown). Secondly, as it is known that interfering
trimming of N-glycans can lead to stabilization of CPY* (Hitt and Wolf,
et al., 1998) we wished to exclude such a role for Yos9p. This concern was
finding that glucosidase II, one of the enzymes, that catalyzes trimming of

s also contains an MRH domain (Munro, 2001). However, in contrast to mutants, the ERAD defect caused by loss of Yos9p is not suppressed by a n in the gene (*ALG6*) responsible for the biosynthetic glucosylation of the oligosaccharide (Jakob et al., 1998) (data not shown). Finally, as noted AD defect in a strain deleted for both *YOS9* and *MNS1* is considerably e one seen in a strain deleted for *MNS1* alone, even though *MNS1* delete complete failure to undergo trimming to convert $Man_9GlcNAc_2$ forms to arguing against the idea that Yos9p is performing a function linked solely ident mannose trimming (Jakob et al., 2001). Taken together, the above n that the lectin activity of Yos9p is required for its ability to support lation but that Yos9p nonetheless acts downstream of generation of the charide structure required for ERAD.

gnition by Yos9p

ss whether Yos9p is involved in directly recognizing substrates, we noprecipitation experiments using a tagged version of Yos9p. We tagged ple FLAG epitope inserted immediately prior to the C-terminal HDEL ssed it on a high-copy (2μ) plasmid under the control of its natural onstruct was able to complement the ERAD defect of a *Δyos9* strain . Additionally, in order to facilitate detection of what would most likely eraction with a short-lived CPY* substrate, we performed all strain deleted for downstream ERAD components, either *Δhrd1* or ch conditions, solubilization of a crude cellular membrane fraction with

photeric detergent CHAPS revealed that Yos9-FLAG interacts specifically well with both CPY* and CPY*-DHFR (Figure 5A). This latter observation t the degradation defect caused by fusing DHFR to the C-terminus of CPY* ult from an inability to interact with Yos9p and is thus likely to result from with a downstream step in ERAD such as retrotranslocation.

interaction between CPY* and Yos9p was confirmed using a cross-linking rdner et al., 2000b). Here, we treated intact microsomes with a short (12 Å) oss-linker (DSP) and immunoprecipitated CPY* and any covalently-roteins under denaturing conditions. We then reversed the cross-link and os9-FLAG. As seen in Figure 5B, Yos9-FLAG interacts with CPY* and specific and cross-linker dependent manner. Interestingly, when these were repeated with non-reversible cross-linkers (DSS and DSG), both CPY* ere found in a large (>200kDa), discrete complex (supplemental Figure S3) at multiple copies of Yos9p or CPY* or other proteins are involved in the complex.

e have shown that Yos9p's lectin activity is required for its ERAD function, test if the Yos9p-substrate interaction we see is also abolished by sugar-tions in the MRH domain. Unexpectedly, the lectin mutants were still able th the substrate (Figure 5C, and supplemental Figure S2 and S4), and this anything, was more pronounced (relative increase in pull down efficiency y native IP, see Methods) than the one seen with the wild-type Yos9p (see We also find that the interaction between CPY* and both wild type Yos9p A mutant persists in the absence of Htm1p (Figure 5D and supplemental

ure S4), a putative lectin involved in ERAD. To exclude the possibility that the ability
ubstrate to bind the Yos9p lectin mutants resulted from additional sugar-dependent
acts, we subjected the native immunoprecipitates to digestion with
glycosidaseH, which cleaves off all but one residue of N-linked core
osaccharides. This treatment quantitatively deglycosylated the substrate but failed to
ish the interaction with the wild type Yos9p (data not shown) as well as with the
0A lectin mutant (Figure 6A). It remains a formal possibility that a small fraction of
* bound to Yos9p is resistant to endoH treatment. We therefore confirmed that the
-Yos9p interaction did not depend on sugar recognition by using a mutant of CPY
Y*0000) in which the four glycosylation sites have been removed. CPY*0000 has a
slow rate of degradation in wild type cells, which is unaffected by the loss of Yos9p
chhorn et al., 2004). Consistent with the above results, CPY*0000 could be
unoprecipitated with Yos9p and this interaction was more pronounced in the R200A
9p lectin mutant (Figure 6B). Taken together, these data strongly argue that Yos9p is
to interact with a misfolded protein independent of its lectin domain or the presence
y N-glycans on the substrate.

Discussion

The "signal hypothesis" (Blobel and Dobberstein, 1975), first formulated 30 years ago, has served as a conceptual framework for understanding how proteins are targeted for translocation across a variety of cellular membranes. By contrast, the reverse process by which misfolded ER proteins are targeted back into the cytosol for destruction remains poorly understood. This problem seems all the more challenging as it is known that lumenal ERAD substrates have their N-terminal signal sequences cleaved and completely disengage from the translocon prior to being recognized by the ERAD machinery (Plemper et al., 1999b). Moreover, the physical properties and exposed epitopes of terminally misfolded proteins are likely to resemble those found in productive folding intermediates. Thus, two outstanding questions in the field are one of information flow (i.e, what are the signals that mark proteins for destruction) and one of mechanics (i.e., how do substrates, once recognized, engage the retrotranslocation apparatus and emerge on the cytosolic side).

The multidomain nature of secreted proteins provides a particular mechanical challenge to retrotanslocation, as many misfolded proteins may contain stably folded lumenal domains. Thus, retrotranslocation requires either that the cell is capable of transporting such native domains intact across the ER membrane or alternatively that there are mechanisms to unfold or proteolytically remove such domains prior to or during the process of retrotranslocation. While there is evidence that the former possibility is used in some cases (Fiebiger et al., 2002; Tirosh et al., 2003), here we establish that the presence of folded lumenal domains can provide a strong impediment to the degradation

of misfolded ER proteins. In particular, addition of the highly stable protein, *E. coli* DHFR, to the C-terminus of the well characterized soluble ERAD substrate CPY* (Hiller et al., 1996) greatly slows its rate of degradation. This inhibition is due specifically to the presence of the structured region and not the DHFR sequence *per se* as a destabilized mutant of DHFR fails to have an effect on the CPY* degradation kinetics. The block in degradation appears to occur after substrate recognition as the presence of the DHFR domain does not inhibit interaction of CPY* with Yos9p, the lumenal lectin we show to play a critical role in ERAD (see below).

As part of the ERAD process, DHFR can be clipped from the remainder of CPY* and the released DHFR fragments remain in the ER lumen. In addition to facilitating degradation of proteins with stable lumenal domains, proteolytic release may also be important in preventing such substrates from occluding the available retrotranslocons. The mechanism by which this clipping occurs remains an interesting open question; for example, are there lumenal proteases dedicated to releasing stable domains or is the clipping a result of incomplete proteasomal degradation of a partially retrotranslocated substrate?

The DHFR fusion strategy also reveals a strong directionality to the recognition and retrotranslocation of CPY*, as the C-terminal fusion showed marked inhibition of degradation whereas the N-terminal fusion had no effect. The observation that fusing DHFR to both termini of CPY* does not completely block degradation (supplemental Figure S1) indicates that an unfolded domain of a multidomain protein can be recognized even when sandwiched between two stable folded regions. These observations suggest that retrotranslocation can be initiated internally, even though in the absence of structured

s there may typically be a strong preference for commencing this process at one or f the termini. Extension of the fusion strategy used in the present work should help ıte what types of sequence/structural information (e.g., conformation of the ded region, N-linked glycans or ubiqutination sites) lead to such a bias.

A search for factors required for generating the DHFR fragments of the CPY*- fusion identified the resident ER protein Yos9p, which contains a mannose 6- ıate receptor homology (MRH) domain. Consistent with a recent report from the ab (Buschhorn et al., 2004), Yos9p is required for the degradation of a range of nt glycoproteins that contain lumenally exposed misfolded domains. Yos9p may ute directly to the recognition of misfolded substrates as it can be efficiently co- oprecipitated with CPY* under native conditions and can be cross-linked with using the short (12 Å) cross linker DSP.

YOS9 was originally identified on the basis of its sequence similarity to alian OS-9. However, in light of our current findings regarding Yos9p's critical ERAD of lumenal misfolded glycoproteins, two earlier studies raise significant as to whether OS-9 is a functional homolog of Yos9p. First, in contrast to Yos9p's l disposition (Friedmann et al., 2002), OS-9 has been shown to be peripherally ted with the cytosolic face of the ER where it transiently interacts with meprin β tate its trafficking along the early secretory pathway (Litovchick et al., 2002). ly, a recent report demonstrated that OS-9 interacts with and promotes the tion of the cytosolically localized protein hypoxia-inducible factor 1α (HIF-1α) t al., 2005). While these data argue that OS-9 is performing a distinct function os9p, the presence of an MRH domain in OS-9 raises the interesting question of

nction such a domain, with its sugar-binding pocket intact, would be performing
ytosol. Thus, either a fraction of OS-9 is localized to the ER, or OS-9 recognizes
oteins that have escaped from the ER in a role possibly similar to the one
d for the E3 lectin Fbs1 (Yoshida et al., 2002). The human genome contains a
protein (XTP3-tranactivated protein B [XTP3-B]) with similarity to Yos9p that is
ttractive candidate for a true functional homolog of Yos9p. XTP3-B contains
H domains and shows greater similarity to Yos9p compared to OS-9. The
ion of XTP3-B proteins is unknown but close homologs are found throughout
ns including a *C. elegans* protein (WP:CE34218) with a C-terminal HEDL which
nfers residence in the ER lumen.

The presence of an MRH domain in Yos9p is particularly intriguing in light of the
ole that substrate glycosylation plays in protein degradation. While only a subset
domains are competent to bind sugars (Ghosh et al., 2003), our analysis of
nd related sequences together with the structure of the MRH domain complexed
nnose argues strongly that the sugar binding site is intact and conserved in
Moreover, this sugar-binding pocket is required for Yos9p function, as
tive mutations in solvent exposed residues known to be critical for sugar
on abrogate the ability of Yos9p to degrade CPY*. Despite the critical role of
p lectin activity, interaction between Yos9p and substrate persists even when the
ding site is mutated or the substrate is deglycosylated, suggesting that Yos9p
s misfolded polypeptides in a sugar-independent manner. Indeed, MRH
have been found to be involved in sugar-independent interactions (Ghosh et al.,

What then is the role of the Yos9p lectin in ERAD? Three distinct possibilities for Yos9p's role in the bipartite recognition of terminally misfolded proteins ving both substrate recognition and read out of the glycosylation status: 1) Binding RAD substrates by Yos9p involves both recognition of sugars and direct interaction the substrate and this latter mode is sufficient to support co-immunoprecipitation in resence of the mild detergent CHAPS. Consistent with the notion that sugar binding ibutes to Yos9p-substrate interactions, Szathmary et al. (2005) find that in the nce of Triton X-100, co-immunoprecipitation Yos9p and CPY* is not observed in strains containing mutations in some of the *ALG* genes which alter the structure of ked glycans. 2) Substrate recognition by Yos9p predominantly involves direct, n-independent recognition of misfolded species. Yos9p then queries the sugar status e substrate to determine whether the N-glycans are in a configuration instructive for -off to downstream effectors (eg., they have undergone proper time-dependent ning). 3) Carbohydrate binding by Yos9p is required for its productive interaction downstream ERAD components but not involved in substrate binding. In accordance this intriguing possibility, we consistently find a marked increase in the amount of ate co-immunoprecipitated with Yos9p when its sugar-binding site is ablated. dless, identification of Yos9p as a critical lectin that is required for ERAD and that cts with substrates provides a key tool for understanding the molecular basis of how R quality control machinery distinguishes right from wrong.

xperimental Procedures

lasmid Construction

CPY* and the indicated derivatives of CPY* were expressed from the natural romoter based on a CEN/ARS plasmid (see supplemental section).

Untagged Yos9p and R200A, E223D, Y229F *YOS9* lectin mutants were expressed rom the *YOS9* endogenous promoter on a CEN/ARS plasmid. Flag tagged *YOS9* onstructs were generated on a high copy 2μ plasmid (see supplemental section).

KHN-HA, KWS-HA, KWW-HA (Vashist et al., 2001; Vashist and Ng, 2004) and on-glycosylated CPY* were a gift from Davis Ng.

trains

Δprc1, *Δyos9* and *Δrpn4Δpdr5* were derived from W303-1A (MATa; *leu2-3, -112 s3-11, -15 trp1-1 ura3-1 ade2-1 can1-100*). *PRC1*□nd *YOS9* were deleted using imeric PCR (Longtine et al., 1998) with the *TRP1* and *HIS3* auxotrophic markers. *rpn4Δpdr5* was generated by sequentially deleting *RPN4* and *PDR5* with *HIS3* and *EU2* auxotrophic markers.

Δyos9, Δder1, Δhrd1Δmns1, Δhtm1, Δalg6, Δalg9, Δalg12 are derivatives of 4741: S288c background (*MATa his3Δ1 leu2Δ*□*met15Δ*□□*ura3Δ0)* or Y3656 47□□can1*Δ*□□MFA1pr-HIS3-MFα1pr-Leu2 *his3Δ1 leu2Δ*□□*met15Δ*□□□*ura3Δ0* 'Δ0). Deletion strains in MATa were generated by the *S. cerevisiae* deletion

eler et al., 1999a) using a Kanamycin resistance cassette. Deletion
were generated using a NAT antibiotic resistance cassette (pFA6-NAT-
and McCusker, 1999). Double deletions were generated by crossing
ypes using standard yeast manipulation techniques (Guthrie and Fink,

immunoprecipitations (IPs), *YOS9* was deleted with *MET15* in the
strain (Ghaemmaghami et al., 2003). This strain was then crossed to
Δhrd1Δyos9 isolate obtained from this was used for native IPs with
d *YOS9* lectin mutants. The *Δhtm1Δhrd1Δyos9* triple mutant was
ng *Δhrd1Δyos9* with *Δhtm1::Kan*.

hase Degradation Assay

hide chase degradation assays were done as previously described
00b) with minor modifications (see supplemental section).

on Assays

otection experiments were done in a W303-1A *Δrpn4Δpdr5* strain, but
observed in the wild type background. Microsomes from cells
DHFR-HA were prepared as described in the supplemental section and
esence or absence of 10μg/ml proteinase K and with or without 1%
for 10 min. The reaction was terminated by the addition of PMSF to a

ntration of 0.05mM. Samples were analyzed by SDS-PAGE electrophoresis
/ Western blotting with 12CA5 mouse α -HA and goat α -mouse antibodies.

ıg Experiments

se experiments were done as described before (Gardner et al., 2000b) with
ications (see supplemental section).

ıunoprecipitations

ıative IPs, 25 OD_{600} units of mid-log phase cells were spheroplasted using the
cribed under protease protection assays. The spheroplasts were washed in LB
) containing 0.7M sorbitol and lysed in 1.25ml cold lysis buffer containing
s pH6.8, 150mM KOAc, 2mM $Mg(OAc)_2$, 1mM $CaCl_2$ and protease
he lysate was cleared at 21,000g for 10 min at 4^0C. The pellet was
in 1.25ml LB containing 0.5% CHAPS. The samples were incubated on ice
nd centrifuged at 21,000g for 10 min. BSA was added to 0.1% to the
and 1ml of this was subjected to IP with protein A/G agarose prebound to α -
es (combination of Roche 12CA5 and Santa Cruz HA probe Y11) at 4^0C for
ting. IPs were washed 4 times with 1ml of LB containing 0.5% CHAPS and
ml of 0.1% DOC/SDS. Each wash lasted 2 min. Immune complexes were
ling the beads in SDS-PAGE sample buffer and analyzed by SDS-PAGE
sis and Western blotting. Protein bands were detected by using fluorescent
d the LI-COR Odyssey detection system.

were

into

incu

the

elu

mu

For EndoH treatment, 20μl of 100mM NaCitrate pH5.5 and protease inhibitors ere added to duplicate IPs after the final wash. The duplicate IPs were pooled and split to two. They were incubated with or without 1μl of EndoH (Roche; 1U [200ul]) and ːubated at 37^{0}C for 30 min with occasional mixing. The supernatant was taken out and ː beads were washed with LB containing 0.5% CHAPs. Immune complexes were ıted as described above.

The relative efficiency of interaction of wild-type Yos9p (WT) vs R200A lectin ıtant was determined using the following formula :

$$\{IP_{FLAG(R200A)}/[(IP_{CPY*(R200A)})(Total_{FLAG(R200A)})]\} \div \{IP_{FLAG(WT)}/[(IP_{CPY*(WT)})(Total_{FLAG(WT)})]\}$$

CPY* and total amount of wild-type Yos9p or R200A lectin mutant varied by at ɔst 20%. IP_{FLAG} is the amount of FLAG tagged Yos9p or R200A lectin mutant mmunoprecipitated. IP_{cpy*} is the amount of CPY* pulled down. $Total_{FLAG}$ is the amount FLAG tagged Yos9p or R200A present in the reaction prior to the addition of ibodies used for immunoprecipitation.

Acknowledgments

We are grateful to D. Ng and C. Jakob for communicating results to us prior to publication; to R. Kopito and J. Christianson for helpful discussions; to members of the O'Shea and Weissman labs for helpful discussions; J. Hollien, M. Kulp, J. Newman, and M. Schuldiner for helpful comments on the manuscript; M. Schuldiner and M. Noble for the ER knockout library; S. Ghaemmaghami and A. Belle for technical help with the cycloheximide degradation assay screen. We are grateful for the support from American Cancer Society (A. Bhamidipati), National Science Foundation (E. Quan) and Howard Hughes Medical Institute.

A

DHF

CPY

CPY*
(HA)3
FR
CPY*
(HA)3
CPY*
DHFR
(HA)3

B

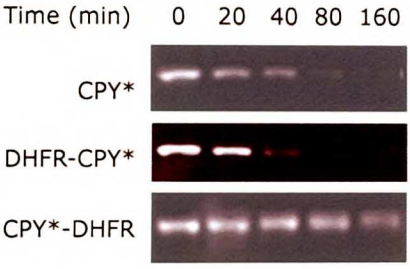
Time (min)
0
20
40
80
160
CPY*
DHFR-CPY*
CPY*-DHFR

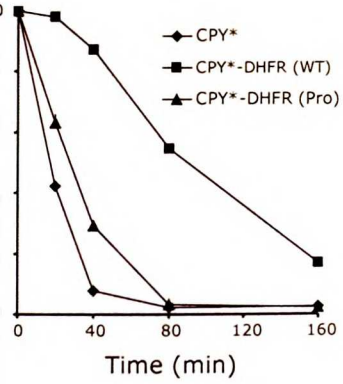
CPY*
CPY*-DHFR (WT)
CPY*-DHFR (Pro)
0
40
80
120
160
Time (min)

D

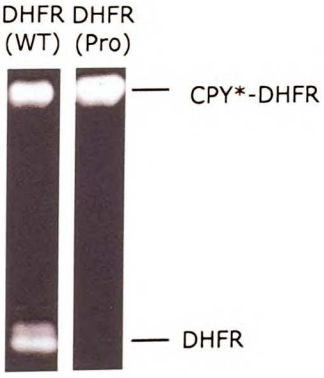
DHFR
(WT)
DHFR
(Pro)
CPY*-DHFR
DHFR

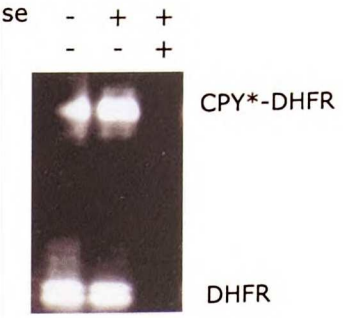
se
-
+
+
-
-
+
CPY*-DHFR
DHFR

F

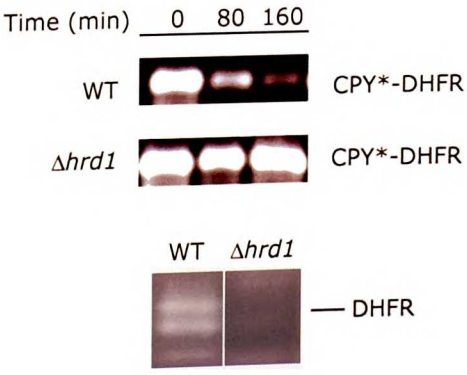
Time (min)
0
80
160
WT
CPY*-DHFR
Δhrd1
CPY*-DHFR
WT
Δhrd1
DHFR

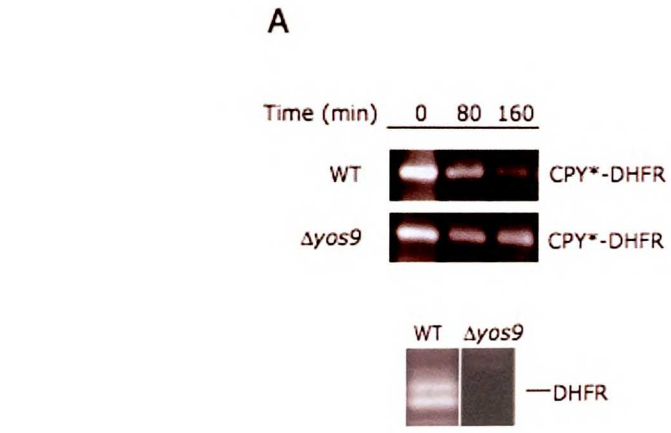
A
Time (min) 0 80 160
WT
CPY*-DHFR
Δyos9
CPY*-DHFR
WT Δyos9
DHFR

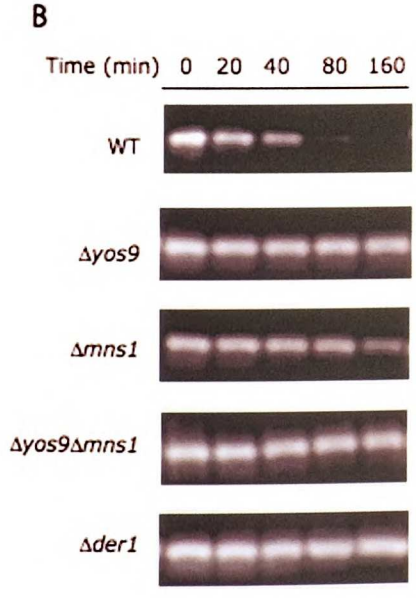
B
Time (min) 0 20 40 80 160
WT
Δyos9
Δmns1
Δyos9Δmns1
Δder1

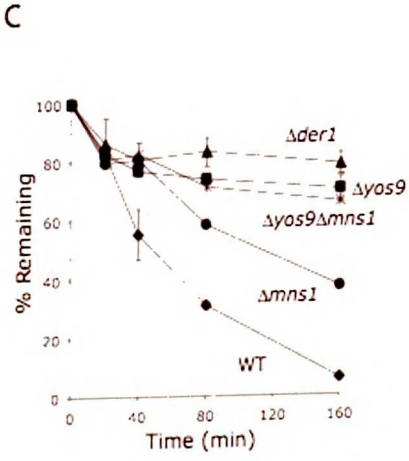
C
% Remaining
Time (min)
Δder1
Δyos9
Δyos9Δmns1
Δmns1
WT

A

B

Bhamidipati et al. Figure 3

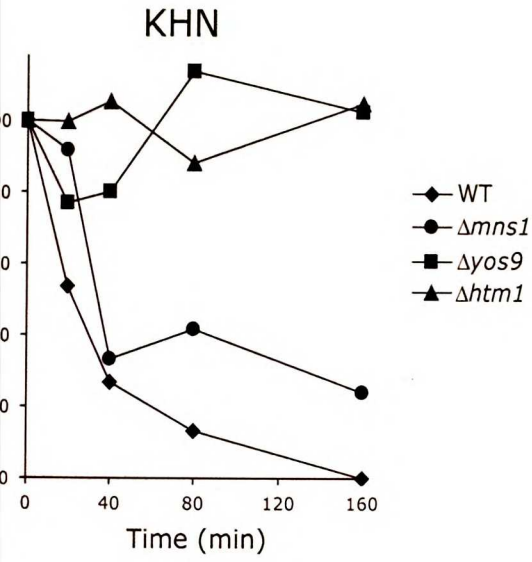

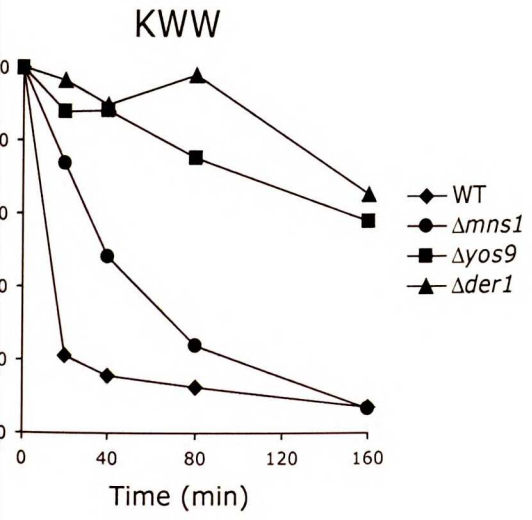

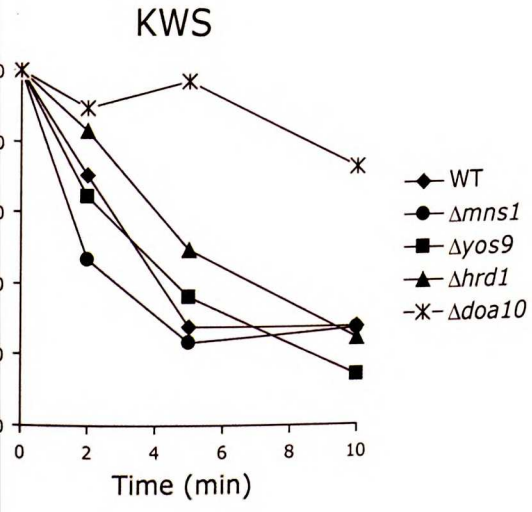

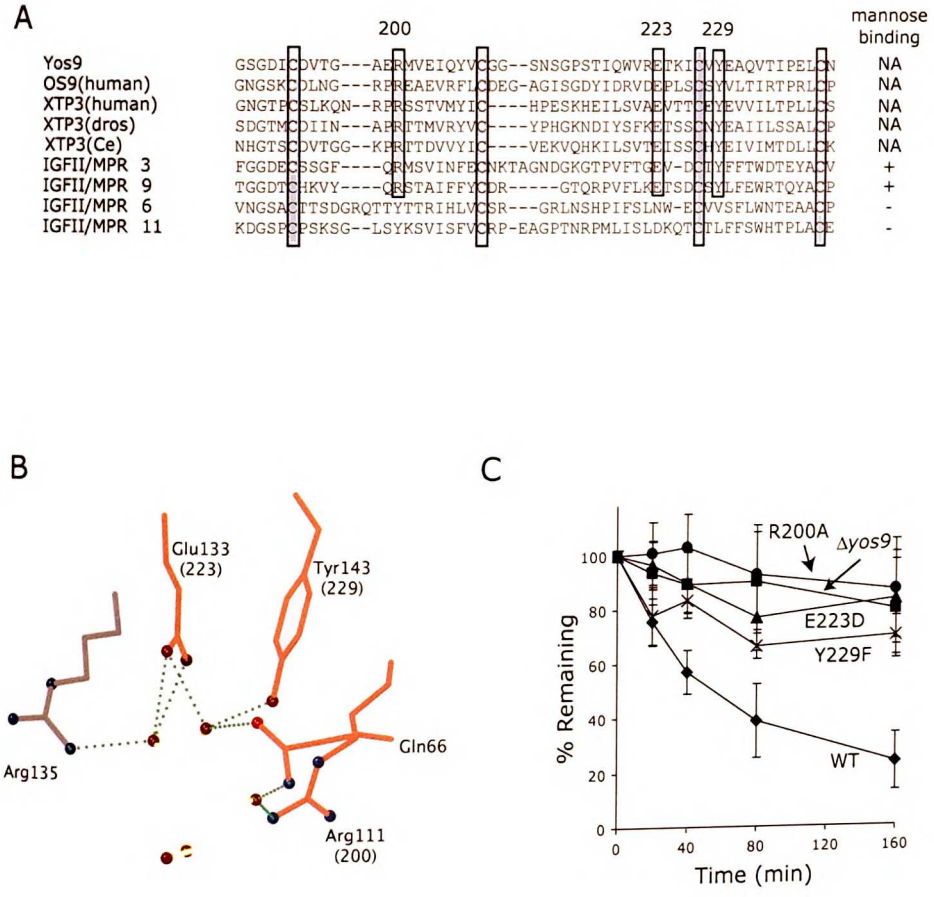
A
200
223
229
mannose binding
Yos9 GSGDICDVTG---AERMVEIQYVCGG--SNSGPSTIQWVRETKIDMYEAQVTIPELCN NA
OS9(human) GNGSKCDLNG---RPREAEVRFLCDEG-AGISGDYIDRVDEPLSCSYVLTIRTPRLCP NA
XTP3(human) GNGTPCSLKQN--RPRSSTVMYICG----HPESKHEILSVAEVTTGEYEVVILTPLLCS NA
XTP3(dros) SDGTMCDIIN---APRTTMVRYVCG----YPHGKNDIYSFKETSSCNYEAIILSSALCP NA
XTP3(Ce) NHGTSCDVTGG--KPRTTDVVYICG----VEKVQHKILSVTEISSCHYEIVIMTDLLCK NA
IGFII/MPR 3 FGGDECSSGF----QRMSVINFECNKTAGNDGKGTPVFTGEV-DCTYFFTWDTEYACV +
IGFII/MPR 9 TGGDTCHKVY----QRSTAIFFYCDR-----GTQRPVFLKETSDCSLFEWRTQYACP +
IGFII/MPR 6 VNGSACTTSDGRQTTYTTRIHLVCSR---GRLNSHPIFSLNW-ECVVSFLWNTEAACP -
IGFII/MPR 11 KDGSPCPSKSG--LSYKSVISFVCRP-EAGPTNRPMLISLDKQTCTLFFSWHTPLACE -
B
Glu133 (223)
Tyr143 (229)
Gln66
Arg135
Arg111 (200)
C
R200A
Δyos9
E223D
Y229F
WT
% Remaining
Time (min)
0
20
40
60
80
100
0
40
80
120
160

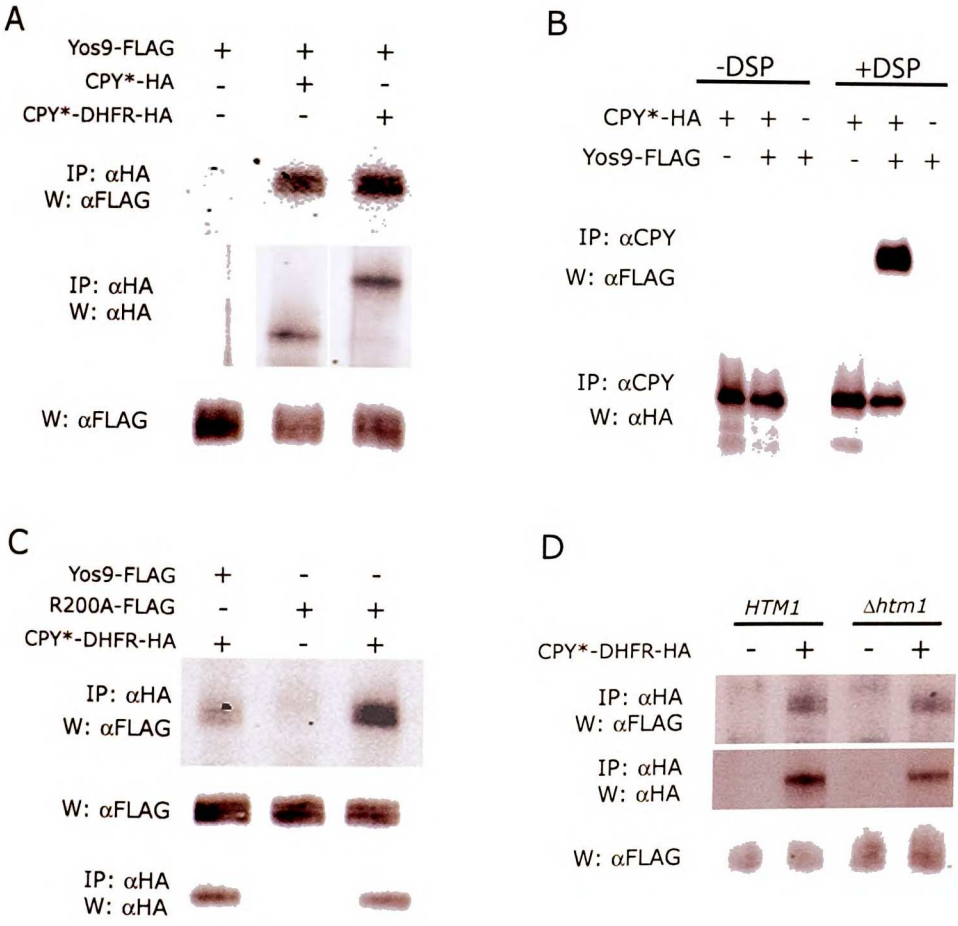
A
Yos9-FLAG + + +
CPY*-HA - + -
CPY*-DHFR-HA - - +
IP: αHA
W: αFLAG
IP: αHA
W: αHA
W: αFLAG
B
-DSP
+DSP
CPY*-HA + + - + + -
Yos9-FLAG - + + - + +
IP: αCPY
W: αFLAG
IP: αCPY
W: αHA
C
Yos9-FLAG + - -
R200A-FLAG - + +
CPY*-DHFR-HA + - +
IP: αHA
W: αFLAG
W: αFLAG
IP: αHA
W: αHA
D
HTM1
Δhtm1
CPY*-DHFR-HA - + - +
IP: αHA
W: αFLAG
IP: αHA
W: αHA
W: αFLAG

A

A

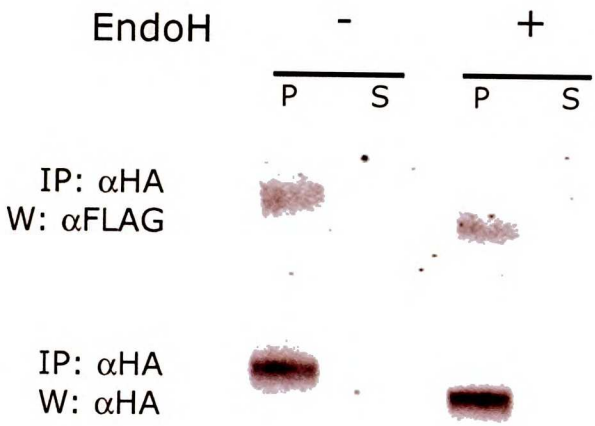
EndoH
-
+
P
S
P
S
IP: αHA
W: αFLAG
IP: αHA
W: αHA

B

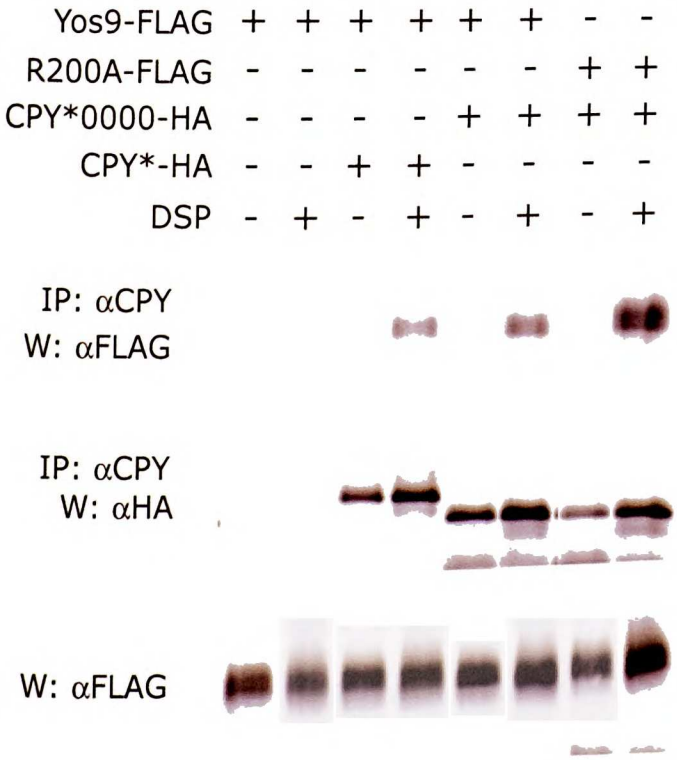
Yos9-FLAG + + + + + + - -
R200A-FLAG - - - - - - + +
CPY*0000-HA - - - - + + + +
CPY*-HA - - + + - - - -
DSP - + - + - + - +
IP: αCPY
W: αFLAG
IP: αCPY
W: αHA
W: αFLAG

SUPP

Exper

Plasm

expe

leng

end

dow

and

sub

ba

up

d

d

V

SUPPLEMENTAL MATERIAL

Experimental Procedures

Plasmid Construction

To facilitate construction of CPY* fusion proteins for retrotranslocation experiments a modular system was generated on a low copy CEN/ARS plasmid. Full-length *S. cerevisiae* CPY cDNA encoding wild type CPY (*PRC1*) along with its endogenous promoter (500bp upstream of start codon) and terminator (300bp downstream of stop codon) was cloned into *Kpn1* and *EcoR1* sites of pRS316 (Sikorski and Hieter, 1989). Quikchange mutagenesis (Stratagene) was used to make an amino acid substituition G255R that transforms wild type CPY to the ERAD substrate CPY*. PCR based mutagenesis techniques were used to introduce an *Sph1* restriction site immediately upstream of the start codon. *Eag1* and *Xho1* sites were introduced immediately downstream of the CPY signal sequence and *HindIII* site was introduced immediately downstream of the stop codon. A triple HA epitope tag with a stop codon at the 3' end was obtained by PCR and cloned into the *HindIII* site to generate a C-terminally tagged CPY*. *Sal1* and *Nhe1* restriction sites were introduced just upstream of the HA tag via the forward primer.

Constructs for directionality experiments were generated in the following manner: CPY*-HA was obtained by replacing the endogenous signal sequence flanked by *Sph1* and *Eag1* in the modular system with the *KAR2* (BIP) signal sequence (Craven et al., 1996). We replaced the endogenous post-translational CPY signal sequence with the co-translational *KAR2* signal sequence as it allowed for a greater fraction of the fusion proteins to enter the ER. The PCR fragment encoding the *KAR2* signal sequence was

PCR a

and c

Sal1-

to ge

obtai

by a

term

cop

we

FL

sit

in

tr

r

PCR amplified from yeast genomic DNA. *E. coli* DHFR was amplified by colony PCR and cloned into *Eag1-Xho1* sites of CPY*-HA to generate DHFR-CPY*-HA or into *Sal1-Nhe1* sites to generate CPY*-DHFR-HA or into the *Eag1-Xho1* and *Sal1-Nhe1* sites to generated DHFR-CPY*-DHFR-HA. The CPY*-DHFR(Pro)-HA proline mutant was obtained by changing A29, W30 and F31 to prolines by fusion PCR.

An untagged Yos9p expression construct (pRS315-Yos9) was generated by amplifying *YOS9* along with its endogenous promoter (500bp upstream of start) and terminator (300bp downstream of stop) and cloning it into *Xma1-Sac1* sites of the low copy CEN/ARS plasmid pRS315. Untagged R200A, E223D, Y229F *YOS9* lectin mutants were generated by fusion PCR using pRS315-Yos9 as a template. To construct the FLAG tagged *YOS9* (pRS425-Yos9-FLAG), the gene was subcloned into *Xma1-Sac1* sites of the high copy 2μ plasmid pRS425. Subsequently, *Eag1* and *Xho1* sites were introduced upstream of the *YOS9* HDEL sequence by fusion PCR. Oligos encoding a triple FLAG tag were synthesized and cloned into *Eag1-Xho1* sites. FLAG tagged mutants R200A-FLAG, E223D-FLAG, Y229F-FLAG were generated by cutting out *BglII–SpeI* fragments from the pRS425 Yos9-FLAG construct and replacing them with the corresponding fragments from the pRS315 mutant constructs.

Cycloheximide Chase Degradation Assay

For Figures 1B, C and D *Δprc1* strain was used and for Figure 4C *Δyos9::HIS3* strain was used. Yeast transformed with the indicated constructs were grown to mid-log phase in selective media. Cycloheximide (Sigma) was added to a final concentration of 100μg/ml – 200μg/ml (time 0) to terminate protein synthesis. Time

ints were taken by adding TCA to a final concentration of 10% to 0.6-0.8 OD_{600} units cells. TCA precipitates were washed with 100% cold acetone twice, air dried for 20 in, and resuspended in 100μl of SDS boiling buffer. Cells were lysed by vortexing with ass beads at the maximum setting at 4°C. Lysates were cleared by centrifugation at ,000g and boiled. 12μl of the samples were subjected to SDS-PAGE electrophoresis on 15% tris-glycine gels and analysed by Western blotting with 12CA5 mouse α-HA tisera (1:1000, Roche) and goat α -mouse (1:3000, Bio-Rad) antibodies. Nitrocellulose ots were incubated in Super Signal West Femto Maximum Sensitivity hemiluminescent Substrate (Pierce) and protein bands were visualized using emiluminescence and a CCD camera (FluorChem 8800) and quantitated.

For Figures 1F and 2A, 1ml of cells were removed at each time point and the cloheximide chase was terminated by flash-freezing cell pellets in liquid nitrogen. For gure 4C chase was terminated at indicated times by the addition of 250μl of cold 5x EP and 25μl of 1:1 mix of 1M NaF and NaN_3. Cells were immediately pelleted at 4^0C d flash frozen in liquid nitrogen. Pelleted cells were thawed and lysed by the addition hot SDS-PAGE sample buffer followed by boiling for 5 min. Bands were visualized ing fluorescent secondary antibodies (Molecular Probes) and the LI-COR Odyssey stem.

otease Protection Assays

Microsomes for protease protection assays were prepared in the following nner. Cells containing CPY*-DHFR-HA were grown to mid-log in SD-Ura medium.

ycloheximide was added to 200μg/ml to 30 OD_{600} units of mid-log cells and incubated 30° for 90 min. NaN_3 was added to 10mM and cells were harvested. Cells were ashed with water and pretreated in 1ml of buffer containing 100mM Tris pH 9.4, 10mM TT at room temperature (RT) for 5 min. Cells were pelleted and incubated in 1ml of pheroplasting buffer containing 10mM Tris pH7.5, 0.7M sorbitol, 100mM NaCl, 1mM TT, 10mM NaN_3 and 100μl lyticase at 30°C for 30 min with occasional mixing. pheroplasts were pelleted at 2500g for 3 min and subsequently washed gently in 1ml of uffer containing 50mM NaP pH 7, 0.7M sorbitol. Spheroplasts were resuspended in 5mls of cold lysis buffer containing 25mM NaP pH7, 0.2M sorbitol, 10mM NaCl, 1mM DTA, and protease inhibitors and lysed by douncing. Lysate was cleared by entrifugation at 1000g for 10 min at 4°C twice. The supernatant was used to obtain a 13 fraction for protease protection assays.

rosslinking Experiments

Yeast cells transformed with desired constructs were used to make ER-rived microsomes as described previously (Brodsky et al., 1993) with a few odifications. 600 OD_{600} units of mid-log phase cells grown in selective media were rvested by centrifugation. Cells were washed in water and pretreated in 16ml of buffer ntaining 100mM Tris pH9.4, 10mM DTT at RT for 15 min. Cells were pelleted and suspended in 8ml of lyticase buffer (50mM Tris pH7.8, 1M sorbitol, 5mM βMe). 5ml of lyticase was added to the resuspended cells and the cells were incubated at RT til 70% spheroplasting efficiency was achieved. Spheroplasting was checked by the op in OD_{600} units. Spheroplasts were pelleted for 4 min at 4°C and resuspended in cold

15ml

1mM

about

4°C.

(270

in b

aliq

car

(D

80

cr

P

t

15ml of lysis buffer (25mM Hepes pH6.8, 10mM NaCl, 200mM sorbitol, 1mM $MgCl_2$, 1mM $CaCl_2$ and protease inhibitors). Resuspended spheroplasts were incubated in ice for about 15 min and lysed by douncing on ice. Lysates were cleared at 160g for 8 min at 4^0C. Supernatants were subjected to two rounds of ultracentrifugation at 194,400g (27000rpm, Ti 70 rotor) for 24 min at 4^0C. The final microsome pellets were resuspended in buffer 88 (20mM Hepes, 150mM KoAc, 250mM sorbitol and 5mM $Mg(OAc)_2$. 150μl aliquots of the microsomes were flash frozen in liquid nitrogen and stored at –80.

150μl of microsomes were used for each crosslinking reaction. Reactions were carried out with or without the reversible crosslinker, DSP (Dithiobis[succinimidlypropionate], Pierce), which was added to a final concentration of 800μg/ml, and incubated at RT for 30 min. For some experiments non-reversible crosslinkers, DSS (Disuccinimidyl suberate, Pierce) and DSG (Disuccinimidyl gluterate, Pierce) were at concentrations ranging from 200μg/ml-800μg/ml. Tris pH7.5 was added to a final concentration of 40mM to quench the crosslinker. Microsomes were centrifuged at 21,000g for 5 min at 4^0C and resuspended in 100μl urea boiling buffer (50mM Tris pH7.5, 1mM EDTA, 1% SDS, 2M Urea). Microsomes were disrupted by vortexing at maximum setting with glass beads at 4^0C. 900μl of Tween IP buffer (50 mM Tris pH7.5, 150mM NaCl, 0.5% Tween-20, 0.1mM EDTA) were added to each reaction and rabbit polyclonal α–CPY antisera made using full-length protein (1:100, Covance Research Products) was used for immunoprecipitating crosslinked species. Protein A/G beads (Santa Cruz) were used to capture immune complexes. The beads were boiled with SDS-PAGE sample buffer to release immune complexes which were then analyzed by SDS-PAGE electrophoresis and Western blotting. Western blots were probed with

mouse α-HA 12CA5 antibodies or mouse α-FLAG (M2 Monoclonal antibody, Sigma) antibodies. Protein bands were visualized by using chemiluminescence and a CCD camera (FluorChem 8800) or by using fluorescent secondary antibodies and the LI-COR Odyssey detection system.

Property of
Cornell University
Library

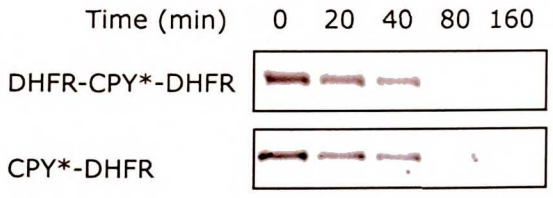

Figure S1. Western blots monitoring the degradation of DHFR-CPY*-DHFR (top panel) in which DHFR was fused to the N-terminus of CPY*-DHFR-HA and CPY*-DHFR-HA (lower panel).

[illegible]

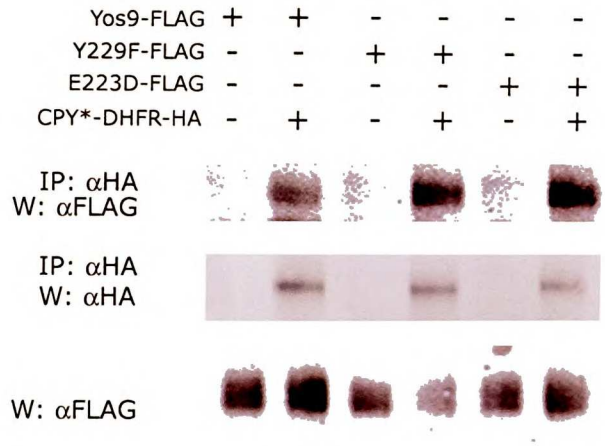

Figure S2. Δ*hrd1*Δ*yos9* cells expressing CPY*-DHFR-HA, and Yos9-FLAG or a Yos9-FLAG variant in which one of the residues implicated in mannose binding in CD-MPR has been mutated (E223D, Y229F). Transformed cells were subjected to native IP and samples were analyzed by SDS-PAGE and Western blotting as described for Figure 5A.

[illegible]

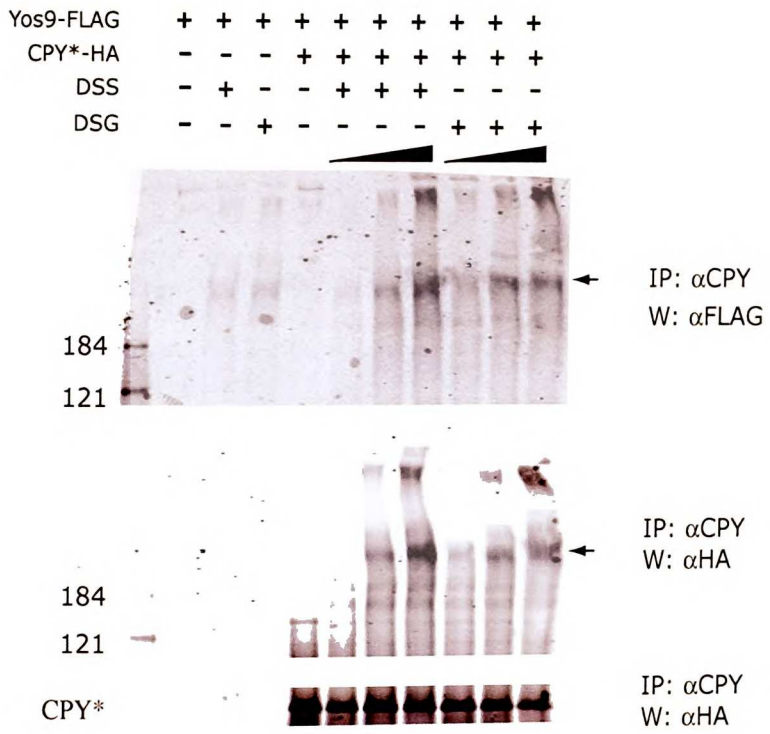

Figure S3. Microsomes derived from Δ*hrd1*Δ*yos9* cells expressing Yos9-FLAG with or without CPY*-HA were incubated in the presence or absence of non-cleavable cross-linkers DSS (disuccinimidyl suberate) or DSG (disuccinimidyl gluterate) followed by denaturing IP as described in Figure 5B. Cross-linkers were used at 800μg/ml for the negative controls and increasing concentrations were used (200μg/ml-800μg/ml) in the strains expressing CPY*-HA. A cross-linker specific high molecular weight species (indicated by arrow) can be detected by both α-HA and α-FLAG antibodies. In addition, a much larger aggregate that does not enter the main body of the gel becomes prominent as the cross-linker concentration is increased. Molecular weight markers (kDa) are shown on the left.

[illegible]

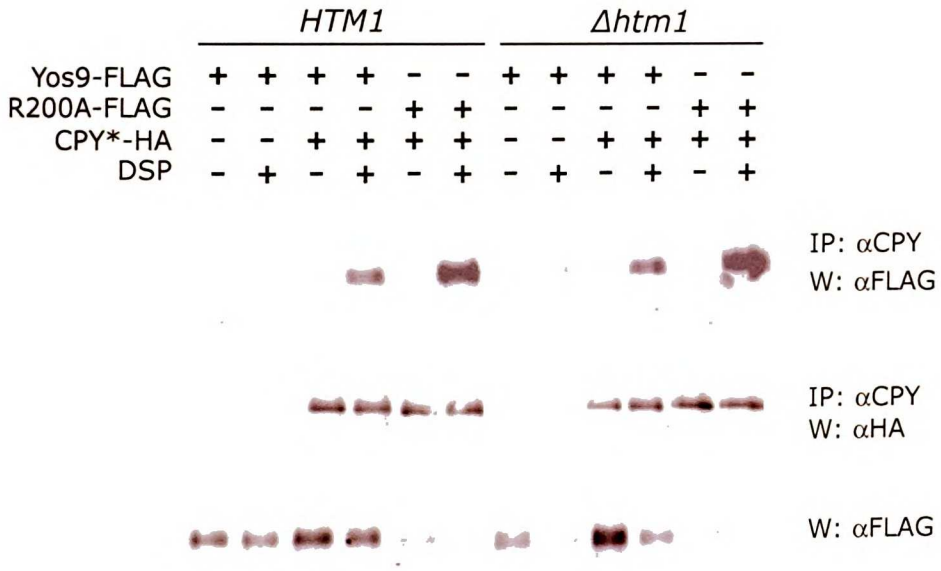

Figure S4 *Δhrd1Δyos9 (HTM1)* or *Δhrd1Δyos9Δhtm1 (Δhtm1)* cells expressing either Yos9-FLAG or the MRH mutant of Yos9, R200A-FLAG, with or without CPY*-HA were subjected to cross-linking with the cleavable cross-linker DSP followed by denaturing IP as described in Figure 5B.

CHAPTER 5

A Luminal Surveillance Complex that Selects Misfolded Glycoproteins for ER-Associated Degradation

A Luminal Surveillance Complex that Selects Misfolded Glycoproteins for ER-Associated Degradation

Vladimir Denic*, Erin M. Quan* and Jonathan S. Weissman

Howard Hughes Medical Institute, Department of Cellular and Molecular Pharmacology, University of California-San Francisco and the California Institute of Quantitative Biomedical Research, San Francisco, CA 94143-2542, USA

Correspondence:

Jonathan S. Weissman

415-502-7642 (phone)

415-514-2073 (fax)

weissman@cmp.ucsf.edu

Running title: Role of Yos9p and Hrd3p in ERAD-L

[Reprinted with permission from Cell, Vol. 126, 349-359, Denic, V., Quan, E. M., Weissman, J. S., A Luminal Surveillance Complex that Selects Misfolded Glycoproteins for ER-Associated Degradation, Copyright (2006), with permission from Elsevier.]

nary

he ER-associated degradation (ERAD) machinery accurately identifies terminally ded proteins is poorly understood. For luminal ERAD substrates, this recognition ds on their folding and glycosylation status as well as on the conserved ER lectin . Here we show that Yos9p is part of a stable complex that organizes key nents of ERAD machinery on both sides of the ER membrane including the embrane ubiquitin ligase Hrd1p. We further demonstrate that Yos9p, together Kar2p and Hrd3p, forms a luminal surveillance complex that both recruits non- proteins to the core ERAD machinery and assists a distinct sugar-dependent step ary to commit substrates for degradation. When Hrd1p is uncoupled from the surveillance complex, degradation can occur independently of the requirement for ylation. Thus, Yos9p/Kar2p/Hrd3p acts as a gatekeeper, ensuring correct ication of terminally misfolded proteins by recruiting misfolded forms to the machinery, contributing to the interrogation of substrate sugar status, and ting glycosylation-independent degradation.

Introd

Protei

proce

form

the

inev

(Ca

20

El

(E

s

Introduction

Proteins that traverse the secretory pathway fold in the endoplasmic reticulum (ER). This process is assisted by ER-resident chaperones, addition of N-linked glycans, and formation of disulfide bonds (Helenius and Aebi, 2001). The high flux of proteins into the ER together with the complicated multi-domain nature of many secreted proteins inevitably results in some fraction of proteins becoming terminally misfolded (Casagrande et al., 2000b; Friedlander et al., 2000a; Jensen et al., 1995; Travers et al., 2000; Ward et al., 1995). To protect cells from the deleterious effects of such forms, the ER employs a series of mechanisms collectively referred to as ER-associated degradation (ERAD) to bring about their efficient disposal (Romisch, 2005). In most instances, substrates are first specifically identified and then targeted for ubiquitination in preparation for their destruction in the cytosol by the proteasome (Meusser et al., 2005; Nishikawa et al., 2005; Romisch, 2005; Sayeed and Ng, 2005; Tsai et al., 2002). Depending on the position of the misfolded lesion, the recognition step can occur either on the luminal side (ERAD-L), the cytosolic side (ERAD-C), or in the context of the ER membrane itself (ERAD-M) (Bonifacino et al., 1990; Taxis et al., 2003; Vashist and Ng, 2004). For luminal targets, Kar2p (the major ER-localized Hsp70), has been shown to keep substrates in an ERAD-competent soluble state (Kabani et al., 2003; Nishikawa et al., 2001) and additionally participates in a second less well-defined step of bringing them to the retrotranslocation machinery (Kabani et al., 2000), which then delivers substrates across the membrane to the cytosolically-located catalytic sites of the ubiquitin conjugation machinery. Following ubiquitination by membrane-associated ubiquitin

ligases (e.g., Hrd1p and Doa10p in yeast)(Bays et al., 2001a; Deak and Wolf, 2001; Swanson et al., 2001), substrates are typically extracted from the membrane by the Ubx2p-recruited Cdc48p-Npl4p-Ufd1p AAA ATPase (Jarosch et al., 2002; Neuber et al., 2005; Schuberth and Buchberger, 2005; Ye et al., 2001), which together with other ubiquitin-binding proteins escorts substrates to the proteasome (Richly et al., 2005).

Our understanding of the more downstream events in ERAD is becoming increasingly sophisticated. By comparison, detailed information is lacking on how proteins are initially selected for degradation and subsequently delivered to the ubiquitination/extraction machinery. The significance of understanding how the ER scans through the abundance of folding intermediates for terminally misfolded proteins is well illustrated by a recent study showing that the most dangerous variants of an amyloidogenic protein are those whose mutations are not so destabilizing as to trigger detection by the ERAD system (Sekijima et al., 2005). The complexity of the recognition problem is further underscored by the risk of over-vigilance, which can lead to the degradation of imperfect but potentially functional proteins, as appears to be the case for the CFTR chloride channel (Drumm et al., 1991).

Degradation of ERAD-L substrates depends not just on substrate misfolding but also on the presence of substrate sugars (Kostova and Wolf, 2005; Spear and Ng, 2005). The molecular basis of this dual requirement and how this information is communicated to the downstream ERAD machinery is unclear. Htm1p, a putative ER lectin required for ERAD-L, may contribute to sugar recognition (Jakob et al., 2001; Nakatsukasa et al., 2001). More recently, Yos9p has been identified as a conserved ER lectin with a critical role in the recognition of luminal misfolded glycoproteins (Bhamidipati et al., 2005;

Buschhorn et al., 2004; Kim et al., 2005; Szathmary et al., 2005). Furthermore, it was shown that Yos9p can associate with the prototypical ERAD-L substrate CPY* even when its sugar-binding site (critical for its ERAD function) is mutated and the substrate is deglycosylated (Bhamidipati et al., 2005). This suggests that Yos9p lies at the core of a poorly defined bipartite recognition machinery that specifically targets for retrotranslocation only those proteins that are simultaneously misfolded and have the correct sugars.

Following recognition, ERAD-L substrates are delivered to the cytosol, where they undergo ubiquitination by Hrd1p (Bays et al., 2001a; Deak and Wolf, 2001). This membrane-bound ubiquitin ligase is associated stoichiometrically with another key component of ERAD-L, Hrd3p, whose presence is required to prevent Hrd1p from undergoing self-destruction (Gardner et al., 2000a; Plemper et al., 1999a). The highly conserved, large (~80 kDa) nature of the Hrd3p luminal region suggests that it may play an additional role in early ERAD-L events. Counteracting this view, however, is the finding that simply restoring Hrd1p levels by over-expression suppresses the substrate degradation defect associated with the loss of Hrd3p (Gardner et al., 2000a; Plemper et al., 1999a).

In the present study we investigate the molecular mechanism by which ERAD-L substrates are recognized and targeted for destruction. Specifically, we demonstrate that Yos9p, Hrd3p, and Kar2p, form a luminal surveillance complex that recognizes misfolded substrates independent of their glycosylation status and brings them to the downstream ubiquitination/extraction machinery. Degradation, however, requires a distinct commitment step that is dependent on substrate sugars and Yos9p's sugar-

binding site. Finally, we show that in addition to its positive role in enhancing recruitment of bona fide ERAD-L substrates, the surveillance complex also helps eliminate basal, indiscriminate degradation which otherwise leads to cellular toxicity.

Re

Yo

ma

Pr

su

T

Y

(

s

(

Results

Yos9p forms a stable complex with the transmembrane and cytosolic ERAD machinery

Previous studies have shown that Yos9p associates with the misfolded, luminal ERAD substrate, CPY* (Bhamidipati et al., 2005; Kim et al., 2005; Szathmary et al., 2005). This recognition event is likely to occur in the context of a multiprotein assembly as Yos9p is membrane-associated but does not itself contain a transmembrane domain (Friedmann et al., 2002; Kim et al., 2005). Furthermore, crosslinking experiments suggested that substrate-associated Yos9p was part of a discrete high molecular weight complex (Bhamidipati et al., 2005). To gain insight into the composition of this complex, we used an affinity purification approach, taking advantage of a yeast strain expressing a functional 3xFLAG epitope-tagged version of Yos9p expressed from its endogenous locus (Supplementary Figure S1). Specifically bound proteins were isolated from detergent-solubilized microsomes and subjected to SDS-PAGE and Coomassie Blue staining, thus identifying several abundantly-associated polypeptides. Mass spectrometry (Supplementary Figure S2) indicated that the Yos9p-specific bands consisted of the following proteins: Cdc48p, Hrd3p, Kar2p, Yos9p/Ubx2p (co-migrating), Hrd1p, and Emp47p (Figure 1A). Additionally, this complex contained Usa1p, a new ERAD component identified and characterized in the accompanying paper (Carvalho et al., 2006). Strikingly, with the exception of Emp47p (the significance of whose association with Yos9p will be addressed elsewhere), all the Yos9p-associated proteins are known to be required for Yos9p-dependent ER-associated degradation and include luminal

(Kar2p), transmembrane (Hrd1p, Hrd3p, Ubx2p, Usa1p) and fully cytosolic (Cdc48p) ERAD components (Romisch, 2005). Thus, Yos9p is part of a stable complex that organizes a series of key components of ERAD machinery on both sides of the ER membrane.

We performed further experiments to address two specific issues regarding the integrity of the complex. First, two membrane proteins critical for ERAD-L, Der1p and Htm1p, (Jakob et al., 2001; Knop et al., 1996a; Nakatsukasa et al., 2001) were not identified in our affinity purification. To exclude the possibility that these were integral components of this membrane complex whose presence was obscured for technical reasons, we repeated the purification using strains deleted for *der1* or *htm1*. These deletions had no apparent effect on the molecular composition of the Yos9p complex (Figure 2A and 2B). Second, we wished to explore the role of Yos9p's sugar-binding pocket in complex assembly. This was motivated by our previous finding that point mutations specifically ablating this region strongly eliminated Yos9p's ability to support ERAD-L but did not interfere with substrate interaction (Bhamidipati et al., 2005). We therefore repeated the purification with a sugar-binding mutant (R200A) but detected no changes in the composition of the complex with the apparent exception of a slight decrease in Coomassie staining of the Yos9p/Ubx2p region (Figure 2C). However, we demonstrated that the Yos9p/Ubx2p association was not affected by directly monitoring levels of coimmuniprecipitated Ubx2p using Western blotting (Figure 2D). These data suggest that sugar recognition by Yos9p acts at a step downstream of substrate binding and complex assembly.

Yos9p/Kar2p/Hrd3p form a luminal subcomplex

Since Yos9p is a strictly luminal protein, we wished to determine the contribution of other members in the complex to Yos9p's ability to associate with Cdc48p on the cytosolic side. The multi-pass transmembrane protein Hrd1p was a good candidate for allowing communication between the complex components on opposing sides of the membrane (Deak and Wolf, 2001; Gardner et al., 2000a). Indeed, when we repeated the purification procedure using a *hrd1* deletion strain, we observed a complete loss of Yos9p-associated Cdc48p (Figure 1B). In contrast, Hrd3p association remained unaffected. Together with IP-Western data confirming the presence of Hrd1p in the Yos9p immunoprecipitations (Supplementary Figure S3), this finding demonstrated that despite its faint appearance by Coomassie staining, Hrd1p is nonetheless absolutely required for Cdc48p's ability to associate in a complex with Yos9p.

The fact that Hrd3p has a large (~80 kD) luminal domain and exists in a 1:1 complex with the Hrd1p ubiquitin ligase (Gardner et al., 2000a) suggests that Hrd3p might be responsible for anchoring Yos9p to Hrd1p/Cdc48p. In accordance with this idea, we observed a total absence of Cdc48p when we purified Yos9p from a Δ*hrd3* strain (Figure 1C). Given that Kar2p and Yos9p closely migrate by SDS-PAGE, we confirmed by Western blotting that the Kar2p/Yos9p interaction is independent of the presence of Hrd3p (Supplementary Figure S4) and Cdc48p (Figure 1C). Additionally, we demonstrated that the Kar2p-Yos9p interaction is still observed even when endogenous *KAR2* has been replaced by the *kar2-1* peptide-binding mutant (Figure 1D)(Kabani et al.,

2003). This suggests that Kar2p's association with Yos9p is not solely mediated through Kar2p's ability to interact with unfolded proteins.

We further explored the Yos9p-Hrd3p interaction using truncations of Hrd3p. Hrd3p comprises a luminal region, consisting of domains A (residues 1-390) and B (residues 390-767), that is attached to a transmembrane anchor and a cytosolic tail (residues 767-833) (Gardner et al., 2000a) Figure 3A). To investigate which of these regions was responsible for the observed interaction with Yos9p, we generated strains expressing from the endogenous locus, C-terminally tagged variants of Hrd3p and tested their ability to co-immunoprecipitate Yos9p. As shown in Figure 3B, both full-length and A-B (1-767) Hrd3p (but not the A domain alone) were able to pull down Yos9p indicating that the B domain is required for Yos9p binding while the transmembrane anchor and the cytosolic tail are dispensable. We further find that strong over-expression of either Yos9p or Hrd3p alone results in only a minor enhancement in the amount of Hrd3p pulled down with Yos9p (Figure 3C). However, concomitant over-expression of both proteins resulted in a synergistic ~20 fold increase in Yos9p/Hrd3p complex formation (Figure 3C). Moreover, this interaction persisted even following deglycosylation of both proteins by EndoH (Supplementary Figure S5). Thus the observed Yos9p interaction with Hrd3p is sugar-independent and unlikely to be bridged by other dedicated ERAD components.

Collectively, these findings lead us to propose the following model for the molecular organization of the complex (Figure 3D). Yos9p, Kar2p, and the luminal domain of Hrd3p form a complex, which is anchored to the transmembrane Hrd1p ubiquitin ligase (Gardner et al., 2000a). In turn, Hrd1p, in a manner that depends on its

ligase activity, recruits Ubx2p-tethered Cdc48p (Gauss et al., 2006; Neuber et al., 2005; Schuberth and Buchberger, 2005), a cytosolic protein shown to be required for the extraction of substrates from the ER membrane (Jarosch et al., 2002; Ye et al., 2001). The transmembrane proteins Der1p and Htm1p are central players in ERAD, but our results establish that they are not required for the integrity of the Yos9p complex described here.

Yos9p and Hrd3p can recruit misfolded proteins independently of each other

We next wanted to explore how ERAD-L substrates are recruited to the Hrd1p ubiquitin ligase complex. First we tested whether the Yos9p-substrate interaction is dependent on Hrd3p. As previously reported, Yos9p co-immunoprecipitated with the prototypical ERAD-L substrate CPY*, and this interaction did not depend on substrate sugars, either alone or in combination with the R200A Yos9p lectin mutant (Figure 4A and 4B) but was specific for the misfolded form (Bhamidipati et al., 2005; Kim et al., 2005; Szathmary et al., 2005) Supplementary Figure S6). Importantly, these interactions persisted even in strains lacking *HRD3*, suggesting that they were being mediated directly by Yos9p and/or Kar2p.

To investigate the simple model that Hrd3p is acting as a passive scaffold for bridging the Yos9p/Kar2p/substrate complex with the downstream ERAD machinery, we asked whether Yos9p was required for the ability of substrate to be co-immunoprecipitated with Hrd3p (Gardner et al., 2001; Gauss et al., 2006). We initially found that various N- or C- terminally tagged versions of full-length Hrd3p either gave very weak Western signals or were non-functional (data not shown). However, as

demonstrated in the case of HMG-CoA Reductase 2 degradation (Gardner et al., 2000a), Hrd3$_{1-767}$-MYC efficiently supported CPY* degradation when tagged at the C-terminus (Supplementary Figure S7) and robustly interacted with Yos9p (Figure 3B, 3C). As expected, based on its association with Yos9p, Hrd3p was able to interact with both CPY* as well as with an unglycosylated variant of CPY* (CPY*0000) which is not subject to ERAD-L (Figure 5A) (Kostova and Wolf, 2005; Spear and Ng, 2005). Surprisingly, we still observed coimmunoprecipitation of Hrd3p with CPY* and CPY*0000 in a strain deleted for *YOS9* (Figure 5A). This interaction is likely to be direct because it was observed even in the absence of Der1p, Htm1p, and Hrd1p (which is responsible for anchoring the Hrd3p luminal domain) (Figure 5A, 5B). Furthermore, we observed that over-expression of Hrd3p leads to a proportional increase in the amount of Hrd3p-CPY* complex recovered by immunoprecipitation (Figure 5C). Several lines of evidence argue for the validity and specificity of this interaction. First, the observed association between Hrd3p and substrate is unlikely to be an artifact of inadequate membrane disruption as we solubilized lysates using a large excess of Triton X-100, a strong non-ionic detergent and we observed no interaction with the abundant ER membrane protein Sec61p (Figure 5A, 5B). Second, this interaction is not due to the formation of a large substrate aggregate that non-specifically incorporates other proteins, because it remains in the supernatant even after clearing the solubilized lysates at 100,000xg for 45min. Finally, the interaction is highly specific for the misfolded form of carboxypeptidase Y, since we could vastly increase the amount of native CPY in the ER by deleting the gene for its ER export receptor, Erv29p (Belden and Barlowe, 2001), without observing a significant interaction with Hrd3p (Figure 5D). We therefore

conclude that Yos9p/Kar2p and Hrd3p independently recognize misfolded ER luminal proteins.

Substrate engagement with the multi-protein Hrd1p ligase complex is sugar-independent

The observation that the Yos9p lectin mutant (R200A) interacted with both substrates (Figure 4) and downstream ERAD components (Figure 2D) suggests that recognition and commitment to degradation are mechanistically separable events. To test this idea further, we made use of a recently identified ERAD-L component (Carvalho et al., 2006) Usa1p. As expected based on Usa1p's association with Yos9p and Hrd3p (Carvalho et al., 2006), we show that Usa1p can be co-immunoprecipitated with CPY* in a Hrd3p-dependent manner (Figure 6). Notably, despite the fact that CPY*0000 cannot be degraded by the ERAD-L system, it nonetheless is part of a multiprotein complex including Usa1p (Figure 6, Supplementary Figure S8). These data suggest that substrate recruitment to the ERAD core machinery can be mechanistically distinguished from a subsequent commitment to degradation. It is this commitment step in the ERAD process which confers dependence on substrate glycosylation and Yos9p's sugar-binding site.

Hrd1p gating by Yos9p/Hrd3p prevents promiscuous degradation

Our finding that Hrd3p plays a key role in bringing Yos9p to the ubiquitin degradation machinery and independently recognizing substrates seems at odds with previously published reports indicating that the strong substrate degradation defect in a Δ*hrd3* mutant is bypassed by over-expression of Hrd1p (Gardner et al., 2000a; Plemper et al.,

1999a). To explore this apparent discrepancy, we first recapitulated the phenomenon by placing Hrd1p under the control of a strong (*TDH3)* promoter (Gardner et al., 2000a) and confirmed that CPY* stabilization in a *hrd3* delete is in fact partially alleviated by over-expression of Hrd1p (Figure 7A). Next, we examined the contribution of Yos9p to substrate recognition in the context of Hrd1p over-expression and found that deleting *YOS9* had no effect on Hrd1p's ability to stimulate CPY* degradation (Figure 7A). This is in marked contrast to the strong CPY* stabilizing effect of deleting *YOS9* in strains with regulated Hrd1p function (Bhamidipati et al., 2005; Buschhorn et al., 2004; Kim et al., 2005; Szathmary et al., 2005) Supplementary Figure S1). In light of the above suggestion that the sugar-binding site of Yos9p acts at a commitment step that is downstream of substrate recruitment to the complex, we wanted to reinvestigate the requirement for glycosylation in this Hrd1p over-expression bypass regime. We first confirmed that the removal of substrate sugars leads to a dramatic stabilization of CPY*, comparable to that observed when *HRD3* or *YOS9* are deleted. Strikingly, under conditions of Hrd1p over-expression in a *hrd3* deletion mutant, we saw significant degradation of CPY*0000, such that its degradation was now similar to that of CPY* (Figure 7B). This promiscuous destruction of an otherwise stable protein could account for our observation that over-expression of Hrd1p causes S288C yeast strains to grow at a reduced rate (Figure 7C). In order to confirm that this effect was indeed due to deregulated ubiquitin ligase activity, we deleted *CUE1,* the ER membrane anchor for the Ubc7p E2 enzyme (Biederer et al., 1997), and observed suppression of both the promiscuous degradation (Figure 7D and Supplementary Figure S9) and the growth phenotype (Figure 7C). Taken together, these data suggest that uncensored Hrd1p activity

caus

of

lea

caused by the disruption of the Hrd3p/Yos9p gating mechanism results in the destruction of proteins normally spared by the rules and restrictions of ERAD-L recognition, thus leading to impaired cellular viability.

Discussion

The ER must specifically identify terminally misfolded proteins in an environment dominated by structurally similar on-pathway folding intermediates. Compounding the complexity of this substrate selection problem is the fact that surveillance has to be enforced on three topological fronts (luminal, membrane, and cytosolic). Accordingly, the ER-associated degradation system comprises multiple converging pathways (Romisch, 2005; Sayeed and Ng, 2005). At the top of this arborized organization is a multiplicity of recognition factors in charge of initiating substrates down increasingly narrow paths that culminate in their degradation by the cytosolic proteasome machinery. While there have been substantial advances in understanding how in mammalian cells viruses target for destruction specific folded endogenous proteins such as class I MHC heavy chains (Lilley and Ploegh, 2004; Lilley and Ploegh, 2005; Ye et al., 2005; Ye et al., 2004), it remains poorly understood how recognition of terminally misfolded proteins is accomplished and coupled to shared downstream ERAD components.

In the present study we address this substrate selectivity issue for ERAD-L, a major conserved pathway responsible for the degradation of luminal misfolded glycoproteins (Vashist and Ng, 2004). In order to focus on a single, coherent branch of the ERAD system, we started with a top-down approach centered on Yos9p, a luminal lectin thought to act early in the pathway. This led to the identification of a Yos9p/Kar2p/Hrd3p surveillance complex that brings ERAD-L substrates into contact with the downstream Hrd1p ubiquitin ligase and the accompanying Ubx2p-recruited Cdc48p. Remarkably, both Yos9p/Kar2p and Hrd3p can individually recognize the

[illegible]

prototypical ERAD-L substrate CPY* in a manner that depends on the folding status but not the glycosylation state of the substrate. The above recruitment step tethers putative substrates to the ubiquitination/extraction machinery on the other side of the membrane by way of the Hrd3p/Hrd1p interaction. Substrate degradation requires a distinct commitment step which is dependent on both the substrate sugars and an intact Yos9p sugar-binding site. The mechanism by which this commitment step allows substrates to proceed down the ERAD-L pathway remains unclear. One intriguing possibility is that Yos9p, possibly together with Htm1p, queries the sugar status of the substrate and, for glycoproteins judged to be legitimate ERAD substrates, allows for the participation of Der1p in the subsequent retrotranslocation step. Interestingly, recent studies suggest physical interaction between glycosylated ERAD substrates and Der1p/Derlin (Gauss et al., 2006; Oda et al., 2006) arguing for the possible existence of distinct substrate recognition events that are not mediated by the Yos9p/Hrd3p recruitment complex. It remains to be established how this multiplicity of recognition events are coordinated to bring about the substrate commitment to degradation.

Why has such a baroque mechanism evolved for selection of ERAD substrates? While the exact structural and kinetic features of misfolded proteins that lead to their recognition by the ERAD machinery are not well delineated, it now appears that recognition does not simply involve assessment of a protein's thermodynamic stability (Sekijima et al., 2005). The cooperation of two interacting complexes (Hrd3p and Yos9p/Kar2p), each of which are individually capable of binding misfolded forms, could allow for a more sophisticated probing of the biophysical properties of non-native proteins. For example, dual binding would be expected to favor recognition of substrates

with extended or multiple non-native epitopes. On a more speculative note, the use of a two step process (i.e., recruitment and commitment) could allow for enhanced specificity by a kinetic proofreading mechanism especially if the two steps are separated by an irreversible process (Hopfield, 1974) such as, for example, sugar trimming (Hirao et al., 2006) or ATP hydrolysis by Kar2p. Additionally, there may be proofreading steps upstream and/or downstream of the Yos9p/Hrd3p recruitment process studied here.

More concretely, we demonstrate that the Yos9p/Kar2p/Hrd3p surveillance complex promotes specificity by acting as a gatekeeper of the Hrd1p ubiquitin ligase, ensuring that only legitimate substrates are degraded. It acts to enhance the delivery and degradation of bona fide ERAD-L substrates, while on the other hand repressing indiscriminate degradation of ER proteins. The significance of suppressing the basal degradation activity is illustrated by the slow growth phenotype that results when upstream recognition is bypassed in a *hrd3* deletion mutant over-expressing Hrd1p. Such deleterious effects are elegantly avoided in wild type cells by the fact that Hrd1p has a built in auto-destruction mechanism when it is not complexed with Hrd3p (Gardner et al., 2000a; Plemper et al., 1999a). This reduced specificity for retrotranslocation caused by Hrd1p over-expression is reminiscent of bacterial translocon mutants that are able to promiscuously export polypeptides in a signal sequence-independent manner (Flower et al., 1994).

More practically, manipulating the specificity of the ERAD system could yield an attractive therapeutic strategy (e.g. for supporting degradation of a mutant allele). However, such efforts are hampered by the broad protective role of the ERAD systems and the fact that many ERAD components are shared with other biological processes

[illegible]

(Adams, 2002). Because the ERAD-L surveillance complex is dedicated to channeling only a subset of ERAD substrates for degradation, a better understanding of this targeting step may aid in the development of future pharmacological approaches with enhanced selectivity for specific disease processes.

UCSF LIBRARY

Experimental Procedures

Plasmid and Strain Construction

See Supplemental Experimental Procedures.

Antibodies

Sec61p and Kar2p antisera were a gift from Randy Schekman (University of California, Berkeley) and Peter Walter (University of California, San Francisco). HA epitope was detected using 12CA5 monoclonal antibody (Roche). In Figure 4B, HA epitope was detected using polyclonal Y11 HA-probe (Santa Cruz Biotechnology). Anti-CBP TEV-N Peptide, anti-FLAG M2 monoclonal antibody, anti-hexokinase and anti-CPY mouse monoclonal 10A5 were purchased from Bethyl Laboratories Inc, Sigma, US Biologicals, and Molecular Probes, Inc, respectively. MYC tag was detected by 9E10 monoclonal antibody(Roche). Secondary Antibodies labeled with IR800 dye and Alexa Fluor 680 were purchased from Rockland Immunochemicals and Molecular Probes, Inc, respectively.

Native Immunoprecipitations (large scale)

ER derived microsomes were prepared from late mid-log phase yeast cells (~2800 OD_{600} units) grown in YPD (The strains in Figure 2C were grown in selective media) and harvested by centrifugation. The cells were washed with water, resuspended in 50ml of 100mM Tris-HCL [9.4] buffer containing 10mm DTT and incubated for 5 minutes at room temperature. The cells were pelleted and resuspended in 20ml lyticase buffer

[illegible]

(50mM Tris-HCL [7.8], 1M sorbitol, 5mM βMe, 100mM NaCl). 3ml of lyticase made using a plasmid that was a gift from Randy Schekman (University of California, Berkeley) was added and the cells were incubated at 30 degrees until at least 80% spheroplasting efficiency was achieved. The spheroplasts were pelleted at 3000g for 4 minutes at 4°C and washed with lyticase buffer before being resuspended in 25ml of cold lysis buffer (25mM HEPES-KOH[6.8], 10mM NaCl, 200mM sorbitol, 1mM $MgCl_2$, 1mM $CaCl_2$, protease inhibitors). The cells were then incubated for 15 minutes on ice and lysed by douncing. The lysates were cleared twice at 1000g for 8 minutes and the resulting supernatant was subjected to a high speed spin at 50,000g. The microsome pellet was washed once before being solubilized in 5ml HEPES IP buffer (50mM HEPES-KOH [6.8], 150mM KOAc, 2mM MgOAc, 1mM $CaCl_2$, protease inhibitors) plus 1% Triton X-100 for 1hr at 4°C. The solubilized microsomes were spun for 22 minutes at 50,000g. 120-150µl pre-equilibrated anti-FLAG resin (Sigma) was added to the supernatant and incubated at 4°C for 3hr. The immunoprecipates were washed with 4x5ml of IP buffer plus 1% Triton X-100. The bound protein was eluted with 60-75ul of 3X FLAG peptide (Sigma) resuspended in IP buffer plus 1% Triton X-100 to a final concentration of 1mg/ml and mixing on ice for 30 minutes. SDS loading buffer was added to half of the eluate and run on 4-12% SDS PAGE gels followed by staining overnight with Colloidal Blue stain (Invitrogen), referred to as Coomassie blue in the text.

For Figure 1A, protein bands were excised from the gel and analyzed by Arnie Falick, David King and Sharleen Zhou at the Howard Hughes Medical Institute Mass Spectrometry Laboratory, University of California, Berkeley. Gel slices were trypsinized

(Promega) and mass spectra were acquired on a Bruker Reflex III MALDI-TOF mass spectrometer. Proteins were identified by searching NCBInr database using MS-Fit program on Protein Prospector (UCSF, http://prospector.ucsf.edu) (Jimenez et al., 1998).

Native Immunoprecitations (small scale)

Yeast Cells (40-80 OD_{600} units depending on experiment) were grown to late mid-log phase in selective media. After being washed in water, cells were lysed by bead beating in 0.5ml HEPES IP buffer containing 0.1% Triton X-100. The detergent concentration was then raised to 1% in a final volume of 1ml. The crude lysate was solubilized for 30 minutes at 4°C and then spun at 100,000g for 45 minutes (except for Figure 3B which was done at 21,000g for 10 minutes). The cleared supernatant was added to 25µL of equilibrated affinity resin and incubated at 4°C for 1-3 hours. The immunoprecipitates were washed 4x1ml with HEPES IP buffer plus 1% Triton X-100. Bound material was eluted by boiling in SDS loading buffer and subjected to SDS-PAGE followed by western blotting and detection using the LI-COR Odyssey system.

An alternative lysis protocol was used for Figures 4A, 4B, and S6. Here the cells were first spheroplasted (Bhamidipati et al, 2005) before being lysed by bead beating in HEPES IP buffer containing 0.2M sorbitol (without detergent). The lysate was spun at 21,000g for 10 minutes and the resulting crude membrane fraction solubilized in 1ml of HEPES IP buffer plus 1% Triton X-100 for 30 minutes at 4°C. The resulting solubilized membranes were cleared and processed exactly as indicated above.

EndoH treatment was performed as described (Bhamidipati et al., 2005).

[illegible]

Cycloheximide Chase Degradation Assay

Cycloheximide chase degradation assays were performed as previously described (Bhamidipati et al, 2005). In brief, log phase cells were treated with 200ug/ml cycloheximide to terminate protein synthesis. Timepoints were aliquoted into cold YEP (to facilitate subsequent pelleting) and 10mM NaF/NaN_3 followed by pelleting and flash freezing in liquid nitrogen. The cells were then lysed with boiling SDS loading buffer, subjected to SDS PAGE and immunoblotted as described above. Bands were visualized using the LI-COR Odyssey system (which allows for two color detection) and subsequently quantitated with LI-COR Odyssey software. Following normalization to the hexokinase loading control, the values were plotted as averages ± standard deviation of 4 measurements (2 independent experiments done in duplicate) with timepoint 0 set to 100%.

Boston Public Library
Copley Square

Figure Legends

Figure 1. Yos9p associates with the core ERAD machinery at the ER membrane

Microsomes were prepared from late mid-log phase cells expressing genomic copies of either untagged Yos9p (A) or Yos9-FLAG (A-C) in wild type, *Δhrd1* or *Δhrd3* strain backgrounds as shown. The microsomes were solubilized with Triton X-100 and affinity purified using anti-FLAG beads. Immunoprecipitates were eluted with 3xFLAG peptide and resolved by SDS-PAGE followed by Coomassie blue staining. The identity of bands in (A) was determined by mass spectrometry. * denotes the position of missing bands. Molecular weights are labeled according to a prestained protein ladder.

(D) As indicated, wild type or *kar2-1* cells were transformed with empty vector or pRS425 expressing Yos9-FLAG. Prior to harvesting, cells were shifted to the nonpermissive *kar2-1* temperature (37°C) for 1 hour. Subsequently, total cell lysates were solubilized with 1% Triton X-100, cleared, and immunoprecipitated with anti-FLAG resin. Bound proteins were eluted by boiling in SDS loading buffer and along with total cell lysates were resolved by SDS-PAGE followed by Western blot analysis with the indicated antibodies.

Figure 2. The integrity of the Yos9p-core ERAD machinery complex is not dependent on Der1p, Htm1p or Yos9p's sugar binding pocket

Microsomes were made from wild type, *Δder1*, or *Δhtm1* log phase cells expressing genomic Yos9-FLAG (A-B), or Yos9-FLAG and R200AYos9-FLAG from a plasmid (C) as indicated. Microsomes were solubilized and Yos9p was immunoprecipitated as

described in Figure 1A. Note: Usa1p comigrates with Hrd3p. We did not explicitly test for the presence of Usa1p in the various deletion strains.

(D) Wild type or *UBX2-TAP::HISMX6* cells were transformed with either an empty vector, pRS425-Yos9-FLAG or pRS425-R200AYos9-FLAG as indicated and subjected to immunoprecipitation as described in Figure 1D. Anti-CBP was used to visualize the TAP fusion protein while anti-Sec61p served as a negative control.

Figure 3. Dissection of the Hrd3p/Yos9p interaction by domain mapping/over-expression and a model of how Yos9p interacts with other members of the ERAD machinery

(A) Schematic of Hrd3p. Domain boundaries are demarcated with their amino acid position in the Hrd3p sequence. Tm denotes the transmembrane domain.

(B) A 13MYC tag was inserted at the *HRD3* locus following amino acids 390, 767 or 833 in a strain expressing Yos9 genomic FLAG. The cells were immunoprecipitated with anti-MYC as described in Figure 1D.

(C) Strains expressing endogenous or over-expressed (symbolized with ↑ indicating *TDH3* promoter driven expression) tagged versions of Yos9p and $Hrd3_{1\text{-}767}p$ were mated as shown, and subjected to immunoprecipitation as described in Figure 1D. The numbers in parentheses indicate the levels of each protein relative to the control strain expressing endogenous levels of both proteins.

(D) Proposed model of how Yos9p associates with other ERAD components in the ER membrane and cytosol. Hrd1p anchors at least a portion of the Yos9p/Kar2p/Hrd3p surveillance complex to the ER membrane and interacts with Ubx2p which recruits Cdc48p to the membrane complex (the dependence of Cdc48p recruitment on Hrd1p's

ubiquitin ligase activity is not depicted in the figure). Der1p and Htm1p may associate but are not important for the integrity of the complex. Ubc7p and its membrane anchor Cue1p are necessary for the ubiquitination of substrates by Hrd1p.

Figure 4. Yos9p interacts with CPY* and CPY*0000 in a *HRD3*-independent manner

(A) *Δyos9Δder1HRD3* or *Δyos9Δder1Δhrd3* cells were transformed with pRS425-Yos9-FLAG, together with an empty vector, or one expressing CPY* or CPY*0000 as indicated. Following spheroplasting and lysis by bead beating, crude membranes were solubilized with 1% Triton-X100 and subjected to immunoprecipitation with anti-HA essentially as described in Figure 1D.

(B) *Δyos9Δder1HRD3* or *Δyos9Δder1Δhrd3* cells were transformed with pRS425-R200AYos9-FLAG together with an empty vector or a vector expressing CPY*0000, as indicated. Spheroplasting and immunoprecipitation were performed as described in Figure 4A.

Figure 5. Hrd3p interacts specifically with CPY* and CPY*0000 but not wild type CPY in a *YOS9*-independent manner

(A)*Δder1YOS9HRD1, Δder1Δyos9HRD1,* or *Δder1Δyos9Δhrd1* cells expressing Hrd3$_{1-767}$-MYC were transformed with an empty vector or a vector expressing CPY* or CPY*0000, as indicated, and subjected to immunoprecipitation as in Figure 1D.

(B) The indicated strains expressing Hrd3$_{1-767}$-MYC were transformed with an empty vector or a vector expressing CPY* or CPY*0000 as shown and subjected to immunoprecipitation as in Figure 1D.

(C) Strains expressing endogenous or over-expressing tagged versions of Hrd3$_{1-767}$-MYC were transformed with empty vector or a vector expressing CPY* and subjected to immunoprecipitation as in Figure 1D. Upward arrow indicates *TDH3* promoter driven expression.

(D) *Δder1Δerv29YOS9* or *Δder1Δerv29Δyos9* cells expressing Hrd3$_{1-767}$-MYC were transformed with an empty vector or a vector expressing CPY* or wild type CPY, as indicated, and subjected to immunoprecipitation as described in Figure 1D.

Figure 6. Sugar-independent association of misfolded carboxypeptidase Y with Usa1p
Wild type or *Δhrd3* cells expressing C-terminally tagged Usa1-MYC were transformed with an empty vector or a vector expressing CPY* or CPY*0000, as indicated, and subjected to immunoprecipitated as in Figure 1D.

Figure 7. Over-expression of Hrd1p in a *Δhrd3* background results in increased degradation of CPY* and CPY*0000 in a *YOS9*-independent manner

(A) Degradation of CPY* in (♦) wild type (WT), (□) *Δhrd3↑HRD1* (upward arrow indicates *TDH3* promoter driven expression), (Δ) *Δhrd3Δyos9↑HRD1*, and (●) *Δhrd3* backgrounds was monitored by the cyloheximide chase degradation assay. Equal amounts of cells were removed at the indicated timepoints following addition of cycloheximide and subjected to SDS-PAGE followed by Western blotting with anti-HA and anti-hexokinase antibodies. Each timepoint represents the average and standard deviation of 4 measurements (2 independent experiments done in duplicate) normalized to a loading control.

(B) Degradatio

indicates *TDH*

Δhrd3↑*HRD1*

(C) *Δcue1* an

Δhrd3↑*HRD1*

Δcue1Δhrd3↑

(D) Degradat

Δhrd3 ↑*HRD*

Δcue1Δhrd3

(B) Degradation of CPY* in (♦) wild type (WT), (□) *Δhrd3 ↑HRD1* (upward arrow indicates *TDH3* promoter driven expression) cells, or CPY*0000 in (●) wild type, (**Δ**) *Δhrd3↑HRD1* was monitored as in Figure 7A.

(C) *Δcue1* and *Δhrd3↑HRD1* were crossed and sporulated. Wild type (WT), *Δhrd3, Δhrd3↑HRD1* (upward arrow indicates *TDH3* promoter driven expression), and *Δcue1Δhrd3↑HRD1* cells were grown on minimal media lacking tryptophan.

(D) Degradation of CPY* in (♦) wild type (WT), or CPY*0000 in (●) wild type, (□) *Δhrd3 ↑HRD1* (upward arrow indicates *TDH3* promoter driven expression) cells, or (**Δ**) *Δcue1Δhrd3↑HRD1* was monitored as in Figure 7A.

[illegible]

Acknowledgments

We thank M. Bassik for experimental assistance; A. Falick, D. King and S. Zhou for mass spectrometry analysis; T. Rapoport for communicating results prior to publication; J. Brodsky, R. Hampton, D. Ng, R. Schekman and P. Walter for reagents; A. Bhamidipati, D. Breslow, J. Brodsky, J. Christianson, R. Hampton, J. Hollien, R. Kopito, and K. Tipton for helpful discussion; B. Toyama for help with graphics. We are grateful for the support from the National Science Foundation (E.Q.) and the Howard Hughes Medical Institute.

A
113.7 kDa
80.9 kDa
63.8 kDa
C

Figure 1

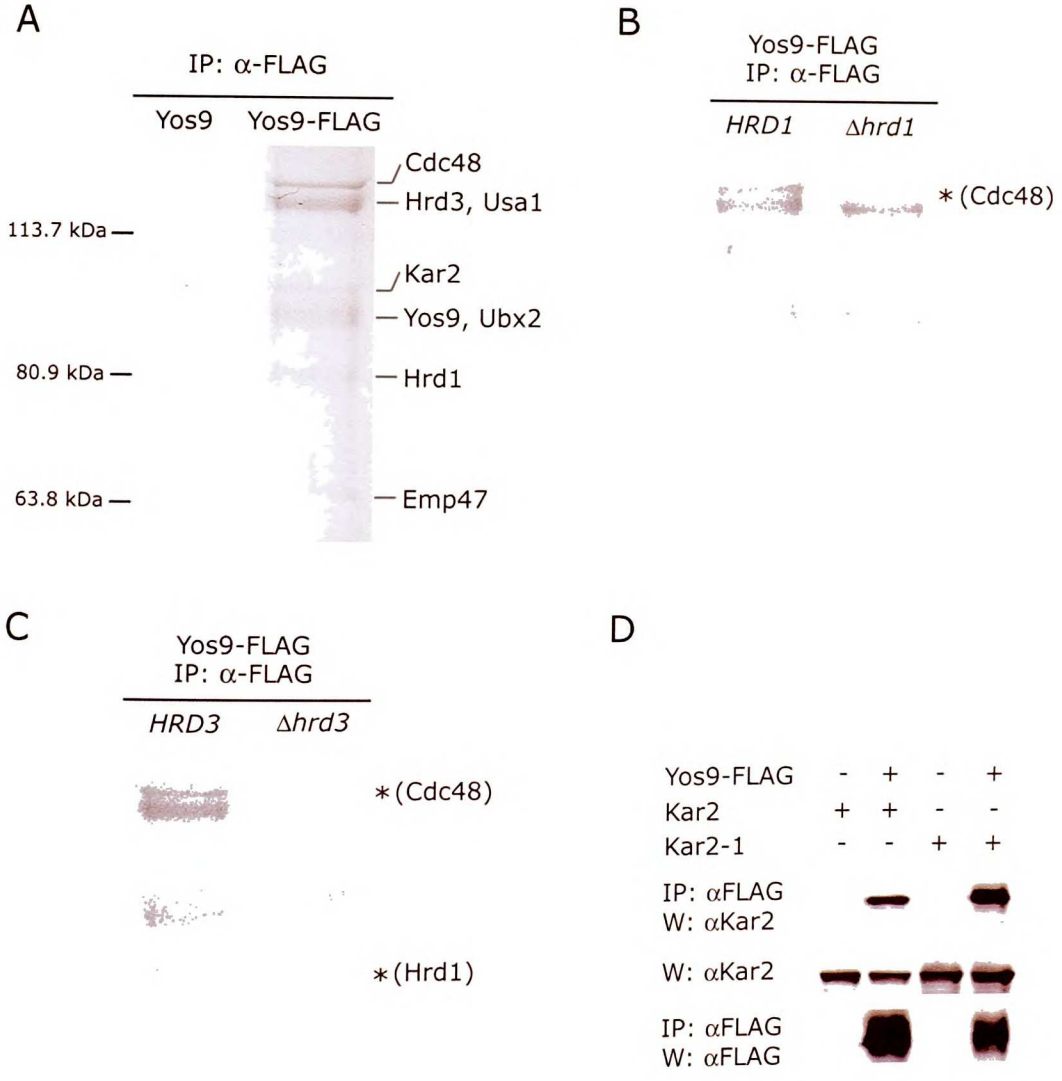
A
IP: α-FLAG
Yos9
Yos9-FLAG
Cdc48
Hrd3, Usa1
113.7 kDa
Kar2
Yos9, Ubx2
80.9 kDa
Hrd1
63.8 kDa
Emp47
B
Yos9-FLAG
IP: α-FLAG
HRD1
Δhrd1
*(Cdc48)
C
Yos9-FLAG
IP: α-FLAG
HRD3
Δhrd3
*(Cdc48)
*(Hrd1)
D
Yos9-FLAG - + - +
Kar2 + + - -
Kar2-1 - - + +
IP: αFLAG
W: αKar2
W: αKar2
IP: αFLAG
W: αFLAG

A
Yos9-FL
IP: α-Fl
DER1
C
Yos9-
IP: α
YOS9

Figure 2

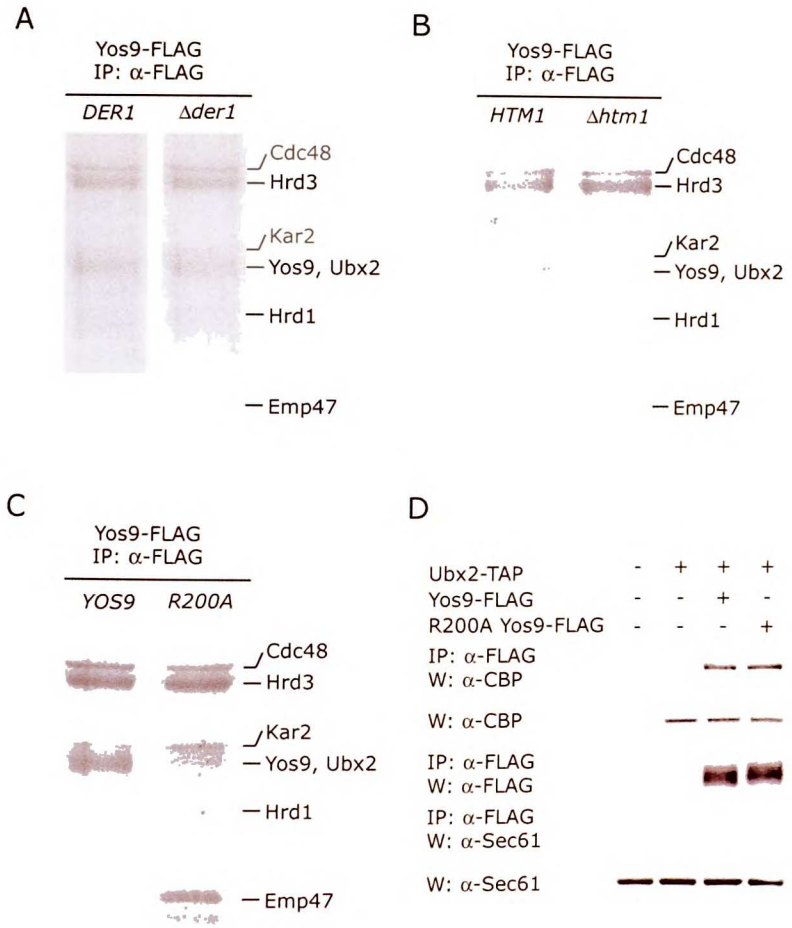
A
Yos9-FLAG
IP: α-FLAG
DER1
Δder1
Cdc48
Hrd3
Kar2
Yos9, Ubx2
Hrd1
Emp47
B
Yos9-FLAG
IP: α-FLAG
HTM1
Δhtm1
Cdc48
Hrd3
Kar2
Yos9, Ubx2
Hrd1
Emp47
C
Yos9-FLAG
IP: α-FLAG
YOS9
R200A
Cdc48
Hrd3
Kar2
Yos9, Ubx2
Hrd1
Emp47
D
Ubx2-TAP - + + +
Yos9-FLAG - - + -
R200A Yos9-FLAG - - - +
IP: α-FLAG
W: α-CBP
W: α-CBP
IP: α-FLAG
W: α-FLAG
IP: α-FLAG
W: α-Sec61
W: α-Sec61

B
Yos9-FLAG
Hrd3-MYC
Hrd3$_{1-767}$-MY
Hrd3$_{1-390}$-MY
IP: α-MYC
W: α-FLAG
W: α-FLAG
IP: α-MYC
W: α-MYC
IP: α-MYC
W: α-Sec6
W: α-Sec6

Figure 3

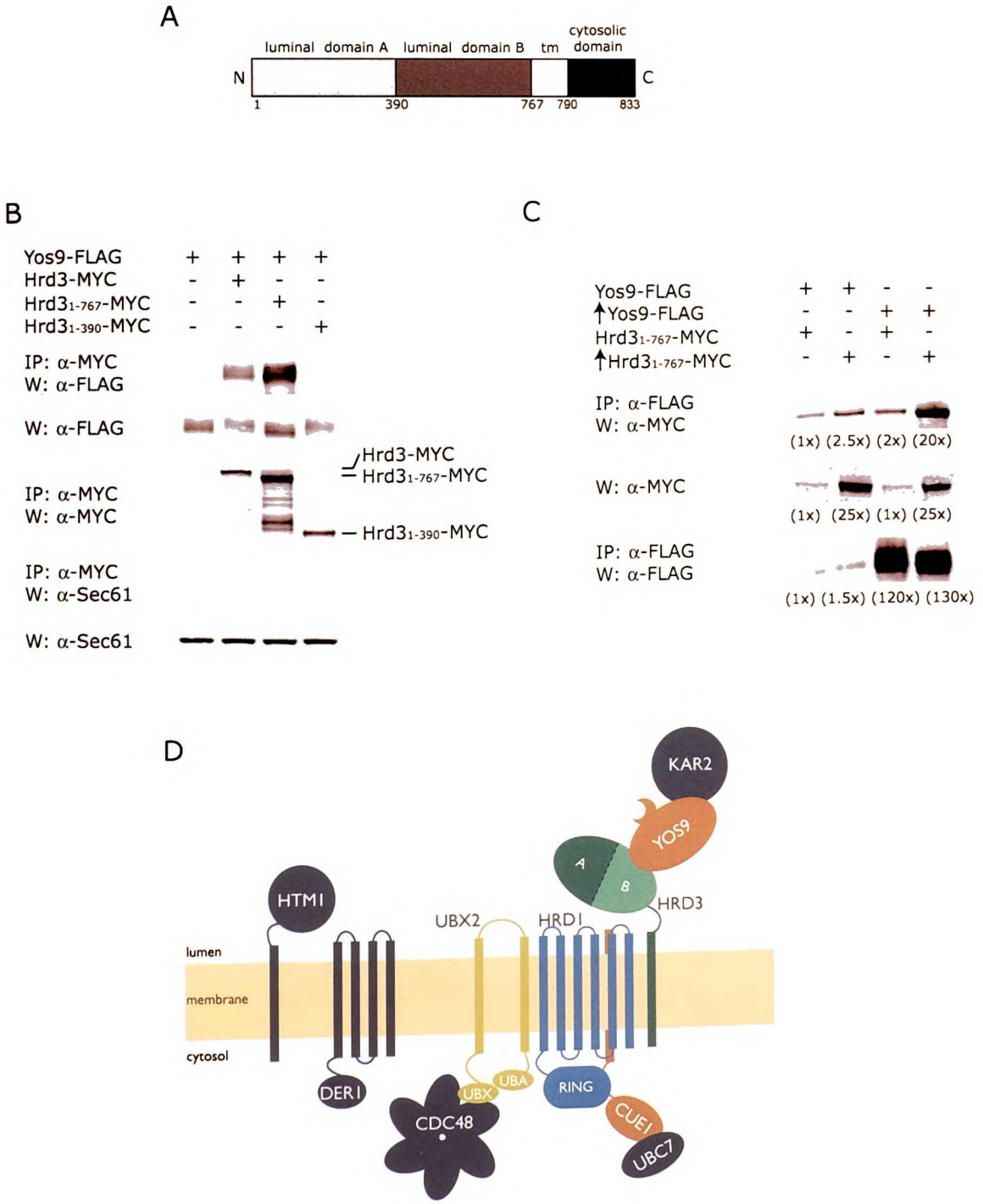
A
luminal domain A
luminal domain B
tm
cytosolic domain
N
C
1
390
767
790
833
B
Yos9-FLAG + + + +
Hrd3-MYC - + - -
Hrd3₁-₇₆₇-MYC - - + -
Hrd3₁-₃₉₀-MYC - - - +
IP: α-MYC
W: α-FLAG
W: α-FLAG
Hrd3-MYC
Hrd3₁-₇₆₇-MYC
IP: α-MYC
W: α-MYC
Hrd3₁-₃₉₀-MYC
IP: α-MYC
W: α-Sec61
W: α-Sec61
C
Yos9-FLAG + + - -
↑Yos9-FLAG - - + +
Hrd3₁-₇₆₇-MYC + - + -
↑Hrd3₁-₇₆₇-MYC - + - +
IP: α-FLAG
W: α-MYC
(1x) (2.5x) (2x) (20x)
W: α-MYC
(1x) (25x) (1x) (25x)
IP: α-FLAG
W: α-FLAG
(1x) (1.5x) (120x) (130x)
D
KAR2
YOS9
A
B
HRD3
HTM1
UBX2
HRD1
lumen
membrane
cytosol
DER1
UBX
UBA
RING
CUE1
CDC48
UBC7

A
CPY*-HA
CPY*00
Yos9-FL
IP: α-HA
W: α-FL
W: α-FL
IP: α-H
W: α-H
B
CPY*
R200A
IP: α-
W: α-
W: α-
IP: α
W: α

Figure 4

A

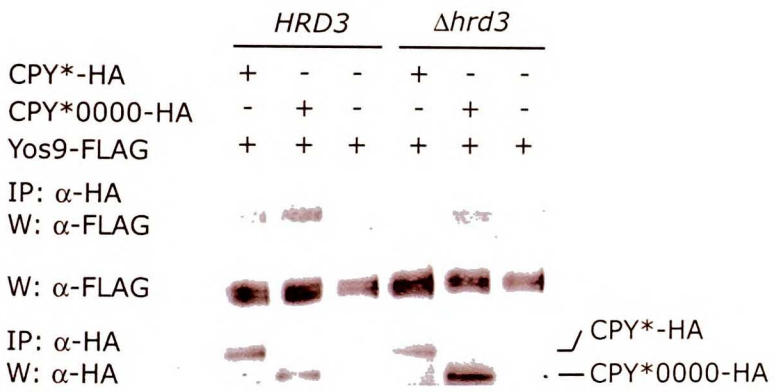
HRD3
Δhrd3
CPY*-HA + - - + - -
CPY*0000-HA - + - - + -
Yos9-FLAG + + + + + +
IP: α-HA
W: α-FLAG
W: α-FLAG
IP: α-HA
W: α-HA
CPY*-HA
CPY*0000-HA

B

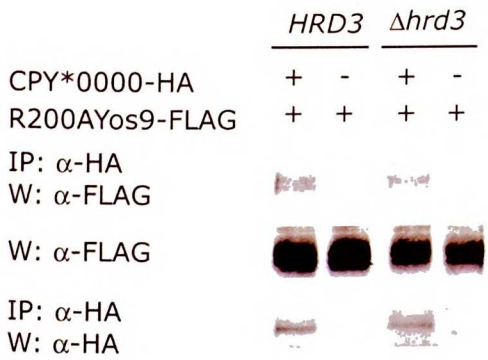
HRD3
Δhrd3
CPY*0000-HA + - + -
R200AYos9-FLAG + + + +
IP: α-HA
W: α-FLAG
W: α-FLAG
IP: α-HA
W: α-HA

A
B
C
Hrd3
Hrd3
CPY*-F
IP: α-F
W: α-M
W: α-M
IP: α-
W: α-

Figure 5

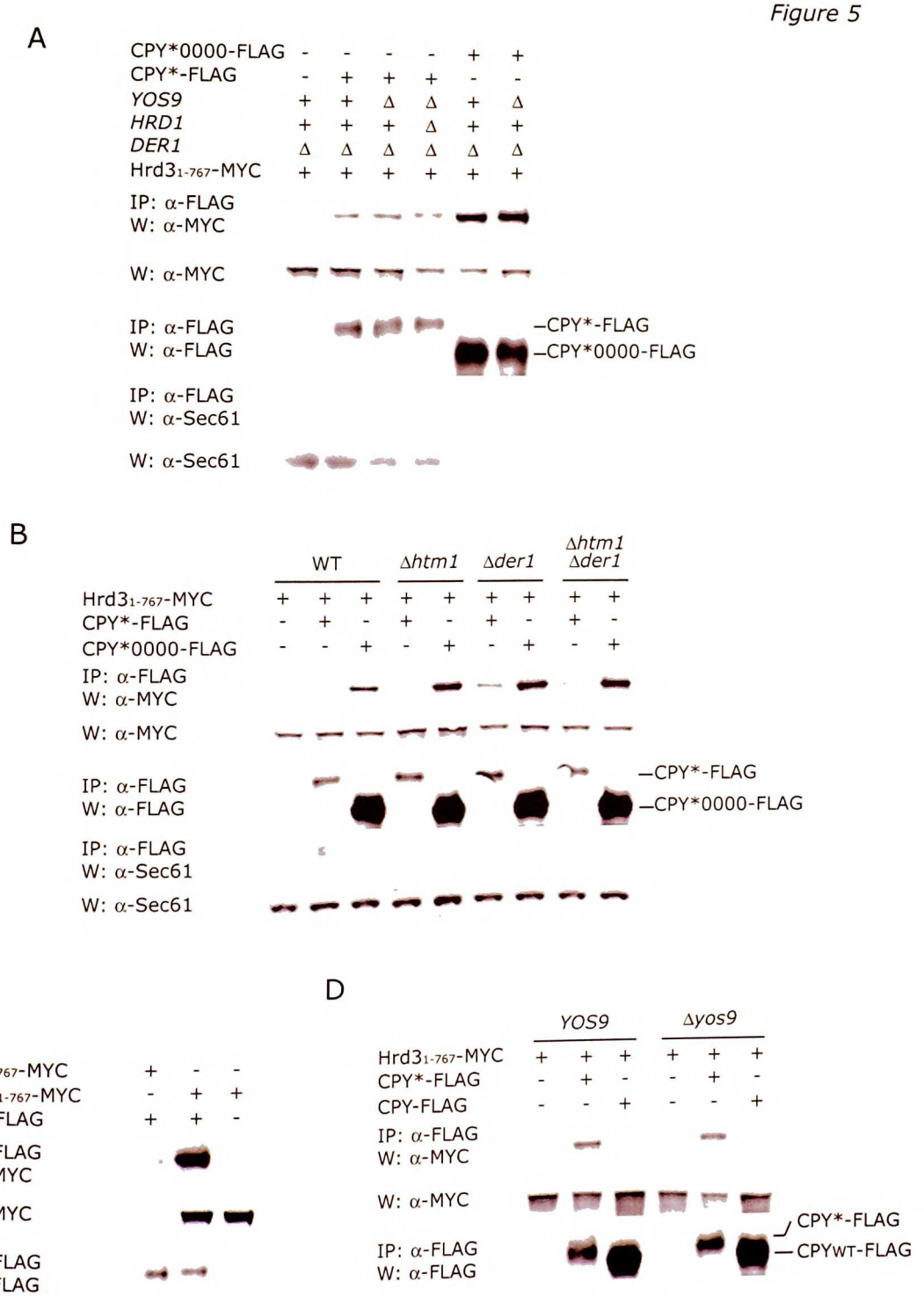
A
CPY*0000-FLAG - - - - + +
CPY*-FLAG - + + + - -
YOS9 + + Δ Δ + Δ
HRD1 + + + Δ + +
DER1 Δ Δ Δ Δ Δ Δ
Hrd3₁₋₇₆₇-MYC + + + + + +
IP: α-FLAG
W: α-MYC
W: α-MYC
IP: α-FLAG
W: α-FLAG
—CPY*-FLAG
—CPY*0000-FLAG
IP: α-FLAG
W: α-Sec61
W: α-Sec61
B
WT
Δhtm1
Δder1
Δhtm1 Δder1
Hrd3₁₋₇₆₇-MYC + + + + + + + +
CPY*-FLAG - + - + - + - +
CPY*0000-FLAG - - + - + - + - +
IP: α-FLAG
W: α-MYC
W: α-MYC
IP: α-FLAG
W: α-FLAG
—CPY*-FLAG
—CPY*0000-FLAG
IP: α-FLAG
W: α-Sec61
W: α-Sec61
C
Hrd3₁₋₇₆₇-MYC + - -
↑Hrd3₁₋₇₆₇-MYC - + +
CPY*-FLAG + + -
IP: α-FLAG
W: α-MYC
W: α-MYC
IP: α-FLAG
W: α-FLAG
D
YOS9
Δyos9
Hrd3₁₋₇₆₇-MYC + + + + + +
CPY*-FLAG - + - - + -
CPY-FLAG - - + - - +
IP: α-FLAG
W: α-MYC
W: α-MYC
CPY*-FLAG
IP: α-FLAG
W: α-FLAG
—CPYWT-FLAG

Usa1-MYC
CPY*-FLA
CPY*000
IP: α-FLA
W: α-MYC
W: α-MYC
IP: α-FLA
W: α-FLA
IP: α-FLA
W: α-Sec
W: α-Sec

Figure 6

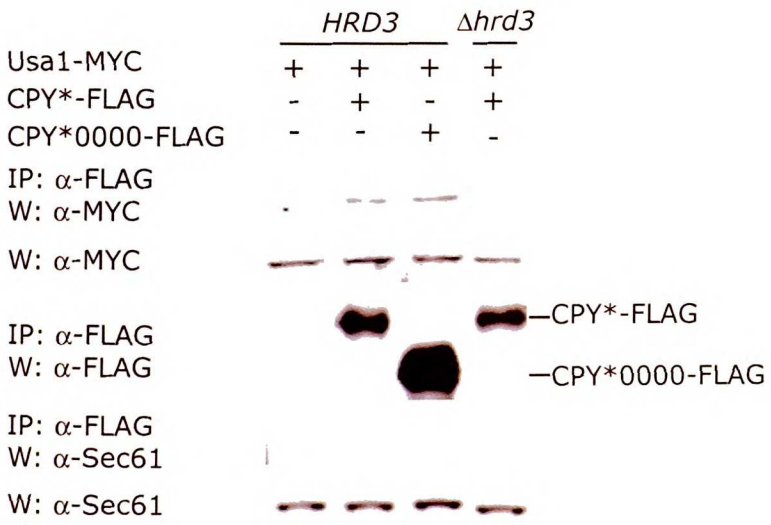
HRD3
Δhrd3
Usa1-MYC
CPY*-FLAG
CPY*0000-FLAG
+ + + +
- + - +
- - + -
IP: α-FLAG
W: α-MYC
W: α-MYC
IP: α-FLAG
W: α-FLAG
—CPY*-FLAG
—CPY*0000-FLAG
IP: α-FLAG
W: α-Sec61
W: α-Sec61

A
% Remaining
100
80
60
40
20
0
0
C
Δhrd3
Δhrd3

Figure 7

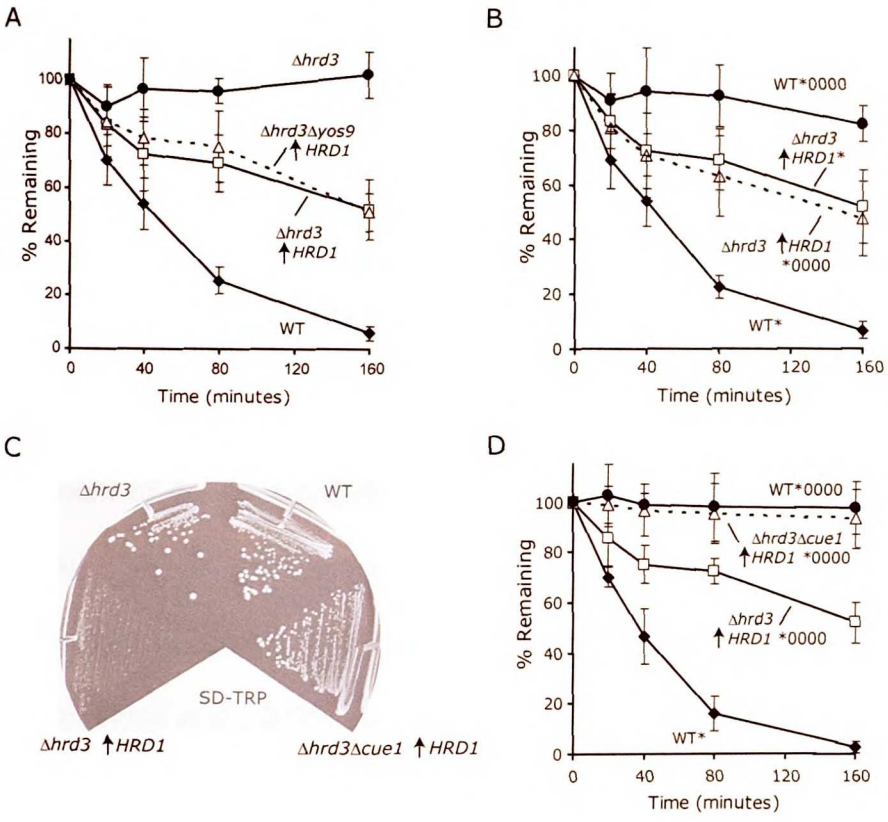
A
Δhrd3
Δhrd3Δyos9
↑HRD1
Δhrd3
↑HRD1
WT
% Remaining
Time (minutes)
B
WT*0000
Δhrd3
↑HRD1*
Δhrd3 ↑HRD1
*0000
WT*
% Remaining
Time (minutes)
C
Δhrd3
WT
SD-TRP
Δhrd3 ↑HRD1
Δhrd3Δcue1 ↑HRD1
D
WT*0000
Δhrd3Δcue1
↑HRD1 *0000
Δhrd3
↑HRD1 *0000
WT*
% Remaining
Time (minutes)

Supplemen

Plasmid C

Plasmids p

as previous

The

variants w

constructe

by PCR a

upstream

codon).

(Sikorski

(Bhamidi

gift from

the glyc

SexAI an

T

CPY*-F

with a

Next, C

basepai

(in the

fusion

Supplemental Experimental Procedures

Plasmid Construction

Plasmids pRS425-YOS9-FLAG3, and pRS425-R200AYOS9-FLAG3 were constructed as previously described (Bhamidipati et al., 2005)

The CEN/ARS plasmids expressing CPY* from its native promoter and its variants were generated in the following manner: pRS316-BIPss-CPY*-HA3 was constructed as described (Bhamidipati et al., 2005). pRS316-CPYwt-HA3 was generated by PCR amplification of the PRC1 gene plus its endogenous promoter (~500 base pairs upstream of the start codon) and terminator (~300 base pairs downstream of the stop codon). The PCR fragment was subcloned into the *KpnI* and *EcoRI* sites of pRS316 (Sikorski and Hieter, 1989). The HA3 tag was introduced as described previously (Bhamidipati et al., 2005). pRS316-CPY*abcd-HA (pES150, (Spear and Ng, 2005) was a gift from Davis Ng (National University of Singapore). The region of pES150 containing the glycosylation site mutations was subcloned into pRS316-BIPss-CPY*-HA3 using *SexAI* and *AflII* to yield pRS316-BIPss-CPY*0000-HA3.

The 3xFLAG tag variants of CPY* were assembled as follows: p416-BIPss-CPY*-FLAG3 was made by first introducing annealed oligos bearing 3xFLAG sequence with a stop codon into the *XmaI/ClaI* sites of p416 MET25 (Mumberg et al., 1994). Next, CPY* was amplified from pRS-BIPss-316CPY*-HA3 with approximately 500 basepairs of its promoter and subcloned into the *SacI/XmaI* sites of p416-MET25-FLAG3 (in the process eliminating the MET25 promoter) resulting in an in-frame C-terminal fusion with the 3xFLAG tag. p416-CPY*0000-FLAG3 was constructed by subcloning

the *SacI/Msc*

FLAG3 was

pRS316-CPY

FLAG3.

Strains

The *YOS9*-

of *YOS9* i

Kluyverom

replacemen

transforme

al., 2005)

detection

resistance

methods

T

Y3656

ura3Δ0

resistan

(Winze

pFA6-

Schuld

ERV2

the *SacI/MscI* fragment from pES150 into p416-BIPss-CPY*-FLAG3. p416-CPYwt-FLAG3 was generated by PCR amplification of the PRC1 gene and its promoter from pRS316-CPYwt-HA3 and subcloning it into the *SacI/XmaI* sites in p416-BIPss-CPY*-FLAG3.

Strains

The *YOS9*-FLAG3 genomic strain was generated by first replacing the endogenous copy of *YOS9* in BY4741 (S288C, MATa *his3Δ1 leu2Δ0 met15Δ0 ura3Δ0*), with the *Kluyveromyces lactis* prototrophic marker *URA3*, using standard PCR-based gene replacement methods (Delneri et al., 1999). The resulting strain, *Δyos9::URA3,* was then transformed with the *XmaI/SacI* fragment from pRS425-YOS9-FLAG3 (Bhamidipati et al., 2005). Following recovery, transformants were selected on 5FOA. To facilitate detection of the Yos9-FLAG locus in subsequent crosses, we transformed in a kanamycin resistance cassette ~500 basepairs downstream of the *YOS9* stop codon using standard methods (Longtine et al., 1998)

The parent strains of *Δcue1*, *Δyos9*, *Δder1*, *Δhrd3*, and *Δhrd1* are BY4741 or Y3656 (Mat α can1Δ::MFA1pr-His3-MFalpha1pr-Leu2 *his3Δ1 leu2Δ0 met15Δ0* u*ra3Δ0 lys2Δ0*). Deletions made in the BY4741 background using the kanamycin resistance cassette were generated by the *Saccharomyces cerevisae* deletion consortium (Winzeler et al., 1999a). Deletions in the Y3656 background were generated using the pFA6-NAT-MX3 cassette using standard methods (Goldstein and McCusker, 1999; Schuldiner et al., 2005). *Δerv29* strains were made by replacing the endogenous copy of *ERV29* with the *Candida glabrata HIS3* prototrophic marker using standard methods in

the specified

Western blot

Figur

trp1-1 ura3

Candida gl

plasmid. T

kar2-51 (C

(University

UB

HRD3-MY

cassette f

amino ac

MYC13::

the genor

T

al., 200

pRH808

Δhrd3::

the *Can*

1999) i

PCR-b

691 to

the specified genetic backgrounds (Sakumoto et al., 1999). They were checked by Western blotting using anti-CPY for increased levels of the ER form of CPY.

Figure 1D *KAR2* and *kar2-1* strains were made in the W303 (MAT a *leu2-3,112 trp1-1 ura3-1 can1-100 ade2-1 his3-11,15*) background. Kar2p was deleted with the *Candida glabrata HIS3* prototrophic marker while the strain was covered by a *KAR2* plasmid. The *KAR2* plasmid was chased out and replaced by pMR713 *KAR2* or pMR713 *kar2-51* (CEN4, LEU2) (Kabani et al., 2003) which were a gift from Jeff Brodsky (University of Pittsburgh).

UBX2-TAP::HIS3 was generated as described (Ghaemmaghami et al., 2003). The *HRD3-MYC13* strains were made by tagging the genomic *HRD3* with the 13MYC cassette from pFA6a-13MYC-HIS3MX6 in the indicated genetic backgrounds after amino acid positions 390, 767 or the stop codon (Longtine et al., 1998). *USA1-MYC13::HIS3* was analogously made by inserting the 13MYC before the stop codon of the genomic *USA1*

The plasmid overexpressing *HRD1* from the *TDH3* promoter (pRH808, (Bays et al., 2001a) was a gift from Randy Hampton (University of California, San Diego). pRH808 was cut with *HincII* and recombined into the *HRD1* genomic locus of BY4741, *Δhrd3::kan* and *Δhrd3::kanΔyos9::nat* strains. *TRP1* was first deleted in BY4741 with the *Candida glabrata HIS3* prototrophic marker using standard methods (Sakumoto et al., 1999) in order to allow for selection of recombinants on SD-TRP selective media.

The over-expressing Yos9-FLAG and $Hrd3_{1-767}$-MYC strains were made by using PCR-based gene insertion methods to knock in the *TDH3* promoter (687 base pairs from -691 to -4) with a pFA6a-NATMX6/KANMX6-based vector (Longtine et al., 1998) into

Yos9-FLAG

indicated.

Strai

by crossing

(Guthrie an

checked by

available u

Yos9-FLAG and $Hrd3_{1-767}$-MYC strains. The strains were subsequently were mated as indicated.

Strains with multiple deletions or genomically integrated proteins tags were made by crossing opposite mating types using standard yeast techniques except where noted (Guthrie and Fink, 1991). All strains altered by genomic deletions or protein tags were checked by colony PCR. The primer sequences used for gene deletions/taggings are available upon request.

Figure S
Western
FLAG,
timepoi

Supplementary Figure S1

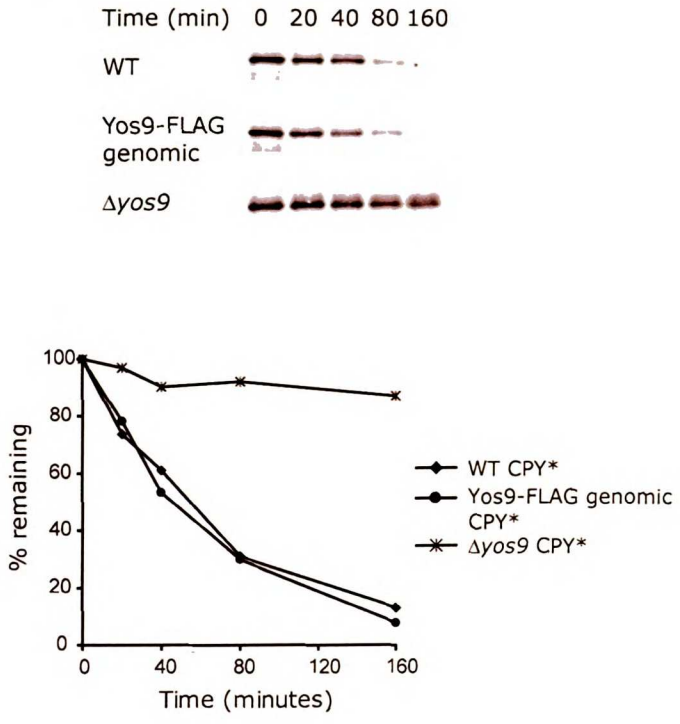

Figure S1. Yos9-FLAG genomic is functional for ERAD-L

Western blots and quantification of CPY* degradation in isogenic (◆) wild-type, (●) Yos9-FLAG, (✱) Δyos9::*MET15* (Bhamidipati et al., 2005) backgrounds at the specified timepoints after addition of cycloheximide.

Protei

Figure S2

Yos9-FL

mass spe

Proteins

Prospect

their pre

Protein Identified	# of Peptides Identified	% Coverage
Cdc48	35	51
Hrd3	25	31
Usa1	19	29
Kar2	11 6	23 10
Yos9	9 7 17	21 16 30
Ubx2	5	8
Hrd1	12	21
Emp47	7	17

Figure S2. Mass Spectrometry Statistics

Yos9-FLAG associated proteins were separated by SDS-PAGE, excised, trypsinized and mass spectra were acquired on a Bruker Reflex III MALDI-TOF mass spectrometer. Proteins were identified by searching NCBInr database using the MS-Fit program on Protein Prospector (Jimenez et. al., 1998). The multiple statistics for Kar2p and Yos9p arise from their presence in multiple, contiguous gel slices.

Boston Public Library

Figure S3. Yos9p associates with Hrd1p

HRD1-TAP::HIS3MX6 cells were transformed with either empty vector, or pRS425-Yos9-FLAG and immunoprecipitated with anti-FLAG as described in Figure 1D.

UCSD LIBRARIES

Figure
Yos9-F
PAGE
antibo

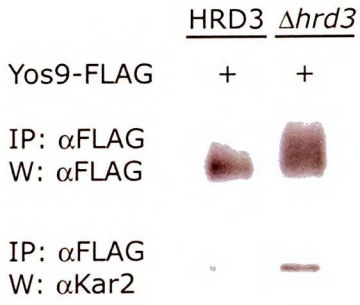

Figure S4. Yos9p/Kar2p association is independent of Hrd3p
Yos9-FLAG cells were immunoprecipitated as in 1A except that the SDS-PAGE gel was followed by Western blot analysis with the indicated antibodies.

UNIVERSITY OF CALIFORNIA
BERKELEY

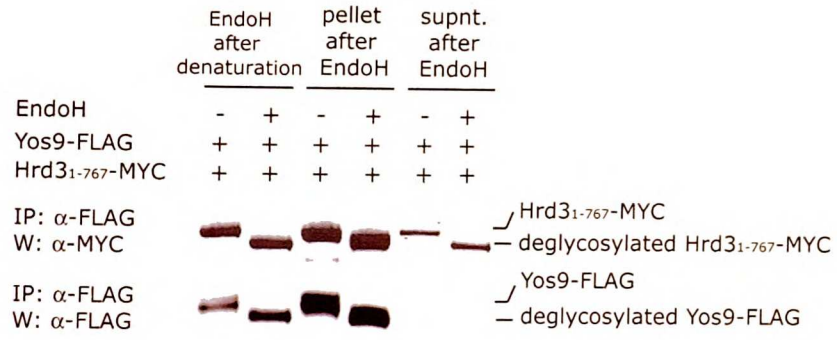

Figure S5. Deglycosylated Yos9p interacts with deglycosylated Hrd3p
A strain overexpressing Yos9p-FLAG and Hrd3$_{1-767}$-MYC was subjected to immunoprecipitation with anti-FLAG resin as described in Figure 1D. Following IP washes, immune-complexes were split in two. One was denatured by boiling in SDS loading buffer before being subjected to deglycosylation by EndoH while the other was subjected to native deglycosylation on the resin. Following treatment, the resin was spun out and the supernatant removed. The resin was then washed before the immunocomplexes were eluted by boiling in SDS loading buffer. The native deglycoslyation samples contain ~4x as many IP equivalents as the denatured samples.

Figure S
Δder1Δ
R200A
CPY* (
with an

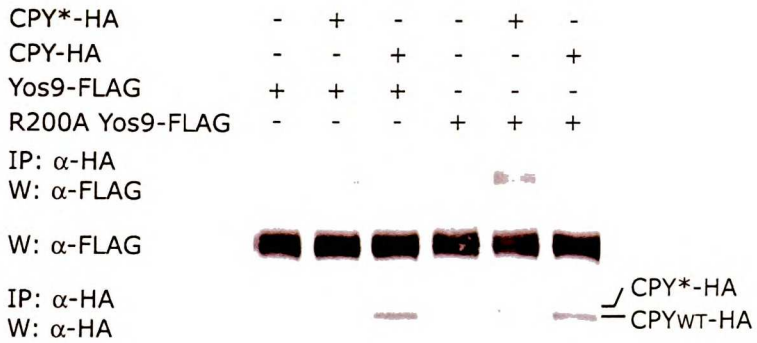

Figure S6. Yos9p and R200A Yos9p interact with CPY* but not CPY wild type
Δ*der1*Δ*erv29*Δ*yos9* cells were transformed with pRS425-Yos9-FLAG or pRS425-R200AYos9-FLAG, together with an empty vector or a vector expressing either CPY* or CPY wildtype, as indicated. Spheroplasting and immunoprecipitation with anti-HA were performed as in Figure 4.

Boston
Public
Library

Figure
Weste
degra

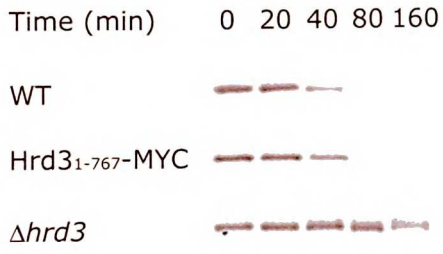

Figure S7. Hrd3$_{1-767}$-MYC is functional for CPY* degradation
Western blots from a cyloheximide chase degradation assay showing the degradation of CPY* in isogenic wild type, Hrd3$_{1-767}$-MYC and Δ*hrd3* strains.

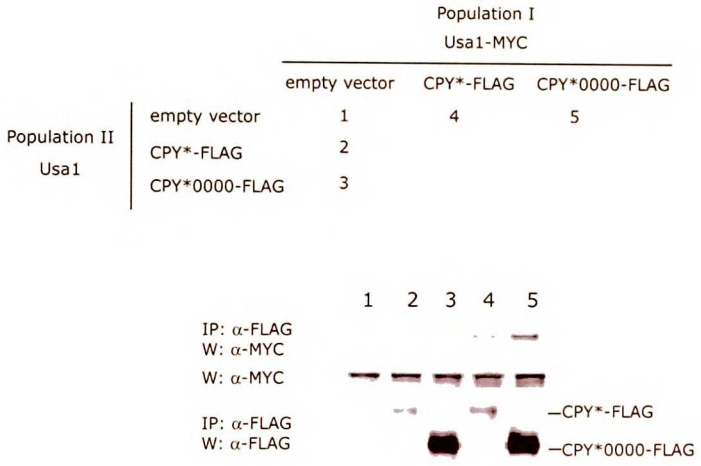

Figure S8. Usa1p is in a multiprotein complex containing misfolded carboxypeptidase Y prior to cell lysis

Wild type or Usa1-MYC expressing strains were transformed with empty vector, CPY*, or CPY*0000. Prior to lysis the indicated combinations of two populations (I and II) were mixed together. This was followed by bead beating and immunoprecipitation with anti-FLAG as described in Figure 1D.

UCSF LIBRARY

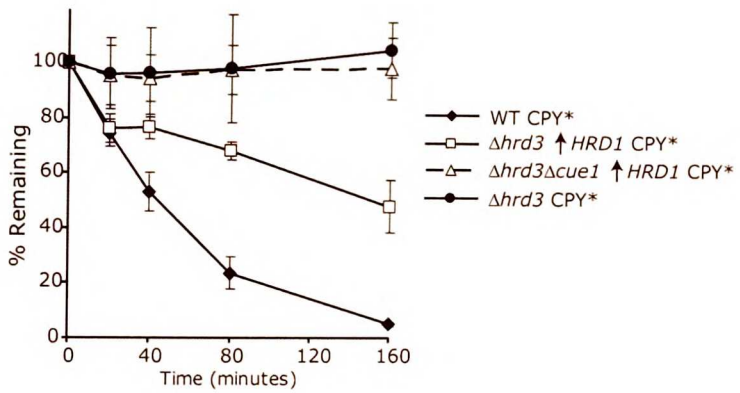

Figure S9: Degradation of CPY* when Hrd1p is overexpressed in a Δ*hrd3* background is suppressed by Δ*cue1*

Degradation of CPY* in (♦) wild type (WT), (□) Δ*hrd3* ↑*HRD1* CPY*, (△) Δ*hrd3*Δ*cue1* ↑*HRD1*, (●) Δ*hrd3* CPY* cells was monitored as in Figure 7A.

UCSF LIBRARY

CHAPTER 6

Summary

At

mechanis

studies ha

appreciati

More fun

requirem

demonst

decades-

complet

to be th

synthet

standin

but als

elonga

within

under

divers

ques

Elo

pres

cata

At the time this work was begun, relatively little was known about the molecular mechanism that catalyzes the production of VLCFAs in the cell. While previous genetic studies have implicated several components in this process, there has been virtually no appreciation at the biochemical level of what activity any of the components might have. More fundamentally, in the absence of such biochemical evidence, the minimal requirements for catalyzing the elongation cycle remained obscure. The convincing demonstration of Phs1p's ability to act as the elongation dehydratase marked the end of a decades-long search for this activity and at the same time raised the possibility that a complete reconstitution of the elongation cycle was within reach. This was indeed shown to be the case upon reintroduction of components purified from ER membranes into synthetic liposomes. This technical achievement not only marks the end of a long-standing debate in the field pertaining to the nature of the elongase condensing activity but also paves the way for a detailed understanding of the molecular mechanism used to elongate fatty acids in the cell. Finally, the identification of the molecular ruler embedded within the newly-defined condensing enzyme family offers a tangible starting point for understanding the mechanistic and structural determinants of VLCFA chain-length diversification across species.

Future work will be necessary to address the details of the catalytic cycle. This question seems particularly relevant in the context of the condensation reaction, as the Elo family of proteins bears no obvious homology to known condensing enzymes. The presence of a highly conserved HxxHH motif within this family of enzymes suggest that catalysis might be facilitated by the presence of an iron cluster. The amounts of purified

Fen1p/Su

protein-a

as future

quantitie

to the m

the bioi

chemist

within

feature

the VI

region

lumin

None

cytos

end c

bilay

prec

lum

lack

and

elo

Fen1p/Sur4p from the yeast expression system are too low to allow for detection of any protein-associated metal ions. However, a spectroscopic analysis of these proteins as well as future mechanistic and structural studies will be facilitated by expression of larger quantities of these proteins from an improved expression source. A related issue pertains to the mechanism of the dehydratase reaction catalyzed by Phs1p, a formidable task given the bioinformatically-opaque sequence requirements for catalyzing the sort of acid-base chemistry typically associated with this chemical reaction.

The presence of a short defined region capable of acting as a molecular ruler within the Elo family poses some interesting questions. What are the exact structural features of this region that are important for defining length? Is the repetitive nature of the VLCFA substrates in some ways reflected in a repetitive structural feature of this region? While most transmembrane prediction algorithms place this region within the last luminal loop, a more detailed characterization of the topology seems in order. Nonetheless, it is tempting to speculate that the predicted cytosolic (or just inside the cytosolic leaflet of the ER membrane) disposition of the HxxHH region engages the CoA end of an acyl-CoA precursor while the hydrocarbon chain penetrates through thelipid bilayer (perhaps guided by some of the transmembrane segments). In this model, precursors beyond a certain length are expected to depend on accommodation from the luminal ruler region for further elongation. It is interesting to note that Trypanosomes lack a traditional FAS system and instead rely on their Elo homologs for synthesis of C14 and C18 starting with a C4 precursor. It will be interesting to see if this property to elongate shorter precursors can be transplanted into the yeast homologs which normally

lack the

acceptin

and a br

condens

be used

VLCFA

elonga

large r

fact th

and co

comp

elong

intere

lack the ability to do so. More broadly, higher organisms have Elo homologs dedicated to accepting VLCFA absent from yeast such as those with multiple degrees of unsaturation and a branched hydrocarbon chain. What are the sequence determinants embedded in the condensing enzymes that dictate these forms of structural diversity? Can this information be used to engineer Elo proteins with unique specificities for production of novel VLCFAs with commercial or therapeutic potential?

Lastly, the observation that all the activities necessary for a complete round of the elongation cycle are able to co-immunoprecipitate suggests that they are organized in a large multi-enzyme complex. The size of this complex remains to be determined but the fact that Phs1p is able to interact with itself suggests that the complex may be very large and contain multiple copies of each activity. The three-dimensional structure of such a complex may address the fundamental issue regarding the processive nature of the elongation reaction which given the absence of an obvious ACP equivalent might be very interesting indeed.

Bancroft Library

APPENDIX A

References

Adams,
the treat
Ahner,
me, wh
Aubour
Jambac
two-ye
adreno
Baek,
A., Gi
Factor
HIF-1
Baud,
Roch
impa
Bays
Hrd1
degr
Bay
Hrd
deg

Adams, J. (2002). Preclinical and clinical evaluation of proteasome inhibitor PS-341 for the treatment of cancer. Curr Opin Chem Biol *6*, 493-500.

Ahner, A., and Brodsky, J. L. (2004). Checkpoints in ER-associated degradation: excuse me, which way to the proteasome? Trends Cell Biol *14*, 474-478.

Aubourg, P., Adamsbaum, C., Lavallard-Rousseau, M. C., Rocchiccioli, F., Cartier, N., Jambaque, I., Jakobezak, C., Lemaitre, A., Boureau, F., Wolf, C., and et al. (1993). A two-year trial of oleic and erucic acids ("Lorenzo's oil") as treatment for adrenomyeloneuropathy. N Engl J Med *329*, 745-752.

Baek, J. H., Mahon, P. C., Oh, J., Kelly, B., Krishnamachary, B., Pearson, M., Chan, D. A., Giaccia, A. J., and Semenza, G. L. (2005). OS-9 Interacts with Hypoxia-Inducible Factor 1alpha and Prolyl Hydroxylases to Promote Oxygen-Dependent Degradation of HIF-1alpha. Mol Cell *17*, 503-512.

Baud, S., Bellec, Y., Miquel, M., Bellini, C., Caboche, M., Lepiniec, L., Faure, J. D., and Rochat, C. (2004). gurke and pasticcino3 mutants affected in embryo development are impaired in acetyl-CoA carboxylase. EMBO Rep *5*, 515-520.

Bays, N. W., Gardner, R. G., Seelig, L. P., Joazeiro, C. A., and Hampton, R. Y. (2001a). Hrd1p/Der3p is a membrane-anchored ubiquitin ligase required for ER-associated degradation. Nat Cell Biol *3*, 24-29.

Bays, N. W., Gardner, R. G., Seelig, L. P., Joazeiro, C. A., and Hampton, R. Y. (2001b). Hrd1p/Der3p is a membrane-anchored ubiquitin ligase required for ER-associated degradation. Nat Cell Biol *3*, 24-29.

UNIVERSITY OF CALIFORNIA
BERKELEY

Beaudoin
Saccharo
encodes
Beaudoi
and Nap
acid bio
Belden
protein
Bellec
Pastic
differ
Belsh
cond
489.
Bern
enzy
CoA
Ber
pro
Bi
Be
el

Beaudoin, F., Gable, K., Sayanova, O., Dunn, T., and Napier, J. A. (2002). A Saccharomyces cerevisiae gene required for heterologous fatty acid elongase activity encodes a microsomal beta-keto-reductase. J Biol Chem *277*, 11481-11488.

Beaudoin, F., Michaelson, L. V., Hey, S. J., Lewis, M. J., Shewry, P. R., Sayanova, O., and Napier, J. A. (2000). Heterologous reconstitution in yeast of the polyunsaturated fatty acid biosynthetic pathway. Proc Natl Acad Sci U S A *97*, 6421-6426.

Belden, W. J., and Barlowe, C. (2001). Role of Erv29p in collecting soluble secretory proteins into ER-derived transport vesicles. Science *294*, 1528-1531.

Bellec, Y., Harrar, Y., Butaeye, C., Darnet, S., Bellini, C., and Faure, J. D. (2002). Pasticcino2 is a protein tyrosine phosphatase-like involved in cell proliferation and differentiation in Arabidopsis. Plant J *32*, 713-722.

Belshaw, P. J., Walsh, C. T., and Stachelhaus, T. (1999). Aminoacyl-CoAs as probes of condensation domain selectivity in nonribosomal peptide synthesis. Science *284*, 486-489.

Bernert, J. T., Jr., and Sprecher, H. (1979a). Solubilization and partial purification of an enzyme involved in rat liver microsomal fatty acid chain elongation: beta-hydroxyacyl-CoA dehydrase. J Biol Chem *254*, 11584-11590.

Bernert, J. T., Jr., and Sprecher, H. (1979b). The isolation of acyl-CoA derivatives as products of partial reactions in the microsomal chain elongation of fatty acids. Biochim Biophys Acta *573*, 436-442.

Bessoule, J. J., Lessire, R., and Cassagne, C. (1989). Partial purification of the acyl-CoA elongase of Allium porrum leaves. Arch Biochem Biophys *268*, 475-484.

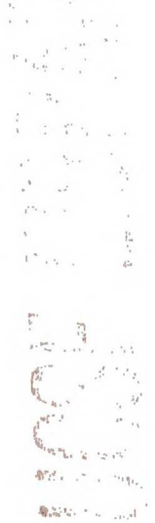

Bhamidipati, A., Denic, V., Quan, E. M., and Weissman, J. S. (2005). Exploration of the topological requirements of ERAD identifies Yos9p as a lectin sensor of misfolded glycoproteins in the ER lumen. Mol Cell *19*, 741-751.

Biederer, T., Volkwein, C., and Sommer, T. (1997). Role of Cue1p in ubiquitination and degradation at the ER surface. Science *278*, 1806-1809.

Bley, T., Gaillard, C., Bilzer, T., Braund, K. G., Faissler, D., Steffen, F., Cizinauskas, S., Neumann, J., Vogtli, T., Equey, R., and Jaggy, A. (2002). Genetic aspects of Labrador Retriever myopathy. Res Vet Sci *73*, 231-236.

Blobel, G., and Dobberstein, B. (1975). Transfer to proteins across membranes. II. Reconstitution of functional rough microsomes from heterologous components. J Cell Biol *67*, 852-862.

Bonifacino, J. S., Suzuki, C. K., and Klausner, R. D. (1990). A peptide sequence confers retention and rapid degradation in the endoplasmic reticulum. Science *247*, 79-82.

Brachmann, C. B., Davies, A., Cost, G. J., Caputo, E., Li, J., Hieter, P., and Boeke, J. D. (1998). Designer deletion strains derived from Saccharomyces cerevisiae S288C: a useful set of strains and plasmids for PCR-mediated gene disruption and other applications. Yeast *14*, 115-132.

Brodsky, J. L., Hamamoto, S., Feldheim, D., and Schekman, R. (1993). Reconstitution of protein translocation from solubilized yeast membranes reveals topologically distinct roles for BiP and cytosolic Hsc70. J Cell Biol *120*, 95-102.

Buschhorn, B. A., Kostova, Z., Medicherla, B., and Wolf, D. H. (2004). A genome-wide screen identifies Yos9p as essential for ER-associated degradation of glycoproteins. FEBS Lett *577*, 422-426.

UNIVERSITY OF CALIFORNIA

Carvalh
define c
Casagra
and Plo
intact u
Casagr
and Pl
intact
Cinti,
elong
Cook
beta-
origi
Cou
(20
pro
Cra
lun
Jo
D
A
s

Carvalho, P., Rapoport, T. A., and Goder, V. (2006). Distinct ubiquitin-ligase complexes define convergent pathways for degradaiton of ER proteins. Cell *submitted.*

Casagrande, R., Stern, P., Diehn, M., Shamu, C., Osario, M., Zuniga, M., Brown, P. O., and Ploegh, H. (2000a). Degradation of proteins from the ER of S. cerevisiae requires an intact unfolded protein response pathway. Mol Cell *5*, 729-735.

Casagrande, R., Stern, P., Diehn, M., Shamu, C., Osario, M., Zuniga, M., Brown, P. O., and Ploegh, H. (2000b). Degradation of proteins from the ER of S. cerevisiae requires an intact unfolded protein response pathway. Mol Cell *5*, 729-735.

Cinti, D. L., Cook, L., Nagi, M. N., and Suneja, S. K. (1992). The fatty acid chain elongation system of mammalian endoplasmic reticulum. Prog Lipid Res *31*, 1-51.

Cook, L., Nagi, M. N., Suneja, S. K., Hand, A. R., and Cinti, D. L. (1992). Evidence that beta-hydroxyacyl-CoA dehydrase purified from rat liver microsomes is of peroxisomal origin. Biochem J *287 (Pt 1)*, 91-100.

Coursol, S., Fan, L. M., Le Stunff, H., Spiegel, S., Gilroy, S., and Assmann, S. M. (2003). Sphingolipid signalling in Arabidopsis guard cells involves heterotrimeric G proteins. Nature *423*, 651-654.

Craven, R. A., Egerton, M., and Stirling, C. J. (1996). A novel Hsp70 of the yeast ER lumen is required for the efficient translocation of a number of protein precursors. Embo Journal *15*, 2640-2650.

Dawkins, J. L., Hulme, D. J., Brahmbhatt, S. B., Auer-Grumbach, M., and Nicholson, G. A. (2001). Mutations in SPTLC1, encoding serine palmitoyltransferase, long chain base subunit-1, cause hereditary sensory neuropathy type I. Nat Genet *27*, 309-312.

Deak, P.
a ubiqui
Chem 2
Delneri
hypoth
constru
Denic
select
Denic
Targ
Dick
cere
Die
P.
co
J
D
J
b

Deak, P. M., and Wolf, D. H. (2001). Membrane topology and function of Der3/Hrd1p as a ubiquitin-protein ligase (E3) involved in endoplasmic reticulum degradation. J Biol Chem *276*, 10663-10669.

Delneri, D., Gardner, D. C., Bruschi, C. V., and Oliver, S. G. (1999). Disruption of seven hypothetical aryl alcohol dehydrogenase genes from Saccharomyces cerevisiae and construction of a multiple knock-out strain. Yeast *15*, 1681-1689.

Denic, V., Quan, E. M., and Weissman, J. S. (2006). A luminal surveillance complex that selects misfolded glycoproteins for ER-associated degradation. Cell *126*, 349-359.

Denic, V., Quan, E., Weissman, J. S. (2006). A Luminal Surveillance Complex for Targeting Misfolded Glycoprotein for ER-Associated Degradation. Cell.

Dickson, R. C., and Lester, R. L. (2002). Sphingolipid functions in Saccharomyces cerevisiae. Biochim Biophys Acta *1583*, 13-25.

Dietrich, C. R., Perera, M. A., M, D. Y.-N., Meeley, R. B., Nikolau, B. J., and Schnable, P. S. (2005). Characterization of two GL8 paralogs reveals that the 3-ketoacyl reductase component of fatty acid elongase is essential for maize (Zea mays L.) development. Plant J *42*, 844-861.

Dittrich, F., Zajonc, D., Huhne, K., Hoja, U., Ekici, A., Greiner, E., Klein, H., Hofmann, J., Bessoule, J. J., Sperling, P., and Schweizer, E. (1998). Fatty acid elongation in yeast--biochemical characteristics of the enzyme system and isolation of elongation-defective mutants. Eur J Biochem *252*, 477-485.

Domergue, F., Chevalier, S., Creach, A., Cassagne, C., and Lessire, R. (2000). Purification of the acyl-CoA elongase complex from developing rapeseed and

characterization of the 3-ketoacyl-CoA synthase and the 3-hydroxyacyl-CoA dehydratase. Lipids *35*, 487-494.

Drumm, M. L., Wilkinson, D. J., Smit, L. S., Worrell, R. T., Strong, T. V., Frizzell, R. A., Dawson, D. C., and Collins, F. S. (1991). Chloride conductance expressed by delta F508 and other mutant CFTRs in Xenopus oocytes. Science *254*, 1797-1799.

Dunn, T. M., Lynch, D. V., Michaelson, L. V., and Napier, J. A. (2004). A post-genomic approach to understanding sphingolipid metabolism in Arabidopsis thaliana. Ann Bot (Lond) *93*, 483-497.

Eilers, M., and Schatz, G. (1986). Binding of a specific ligand inhibits import of a purified precursor protein into mitochondria. Nature *322*, 228-232.

Faure, J. D., Vittorioso, P., Santoni, V., Fraisier, V., Prinsen, E., Barlier, I., Van Onckelen, H., Caboche, M., and Bellini, C. (1998). The PASTICCINO genes of Arabidopsis thaliana are involved in the control of cell division and differentiation. Development *125*, 909-918.

Fehling, E., Lessire, R., Cassagne, C., and Mukherjee, K. D. (1992). Solubilization and partial purification of constituents of acyl-CoA elongase from Lunaria annua. Biochim Biophys Acta *1126*, 88-94.

Ferri, R., and Chance, P. F. (2005). Lorenzo's oil: advances in the treatment of neurometabolic disorders. Arch Neurol *62*, 1045-1046.

Fewell, S. W., Travers, K. J., Weissman, J. S., and Brodsky, J. L. (2001). The action of molecular chaperones in the early secretory pathway. Annu Rev Genet *35*, 149-191.

Fiebig, A., Mayfield, J. A., Miley, N. L., Chau, S., Fischer, R. L., and Preuss, D. (2000). Alterations in CER6, a gene identical to CUT1, differentially affect long-chain lipid content on the surface of pollen and stems. Plant Cell *12*, 2001-2008.

Fiebiger, E., Story, C., Ploegh, H. L., and Tortorella, D. (2002). Visualization of the ER-to-cytosol dislocation reaction of a type I membrane protein. Embo J *21*, 1041-1053.

Flower, A. M., Doebele, R. C., and Silhavy, T. J. (1994). PrlA and PrlG suppressors reduce the requirement for signal sequence recognition. J Bacteriol *176*, 5607-5614.

Friedlander, R., Jarosch, E., Urban, J., Volkwein, C., and Sommer, T. (2000a). A regulatory link between ER-associated protein degradation and the unfolded-protein response. Nat Cell Biol *2*, 379-384.

Friedlander, R., Jarosch, E., Urban, J., Volkwein, C., and Sommer, T. (2000b). A regulatory link between ER-associated protein degradation and the unfolded-protein response. Nat Cell Biol *2*, 379-384.

Friedmann, E., Salzberg, Y., Weinberger, A., Shaltiel, S., and Gerst, J. E. (2002). YOS9, the putative yeast homolog of a gene amplified in osteosarcomas, is involved in the endoplasmic reticulum (ER)-Golgi transport of GPI-anchored proteins. J Biol Chem *277*, 35274-35281.

Futerman, A. H., and Hannun, Y. A. (2004). The complex life of simple sphingolipids. EMBO Rep *5*, 777-782.

Gable, K., Garton, S., Napier, J. A., and Dunn, T. M. (2004). Functional characterization of the Arabidopsis thaliana orthologue of Tsc13p, the enoyl reductase of the yeast microsomal fatty acid elongating system. J Exp Bot *55*, 543-545.

Gardner, R. G., Shearer, A. G., and Hampton, R. Y. (2001). In vivo action of the HRD ubiquitin ligase complex: mechanisms of endoplasmic reticulum quality control and sterol regulation. Mol Cell Biol *21*, 4276-4291.

Gardner, R. G., Swarbrick, G. M., Bays, N. W., Cronin, S. R., Wilhovsky, S., Seelig, L., Kim, C., and Hampton, R. Y. (2000a). Endoplasmic reticulum degradation requires lumen to cytosol signaling. Transmembrane control of Hrd1p by Hrd3p. J Cell Biol *151*, 69-82.

Gardner, R. G., Swarbrick, G. M., Bays, N. W., Cronin, S. R., Wilhovsky, S., Seelig, L., Kim, C., and Hampton, R. Y. (2000b). Endoplasmic reticulum degradation requires lumen to cytosol signaling. Transmembrane control of Hrd1p by Hrd3p. J Cell Biol *151*, 69-82.

Gauss, R., Sommer, T., and Jarosch, E. (2006). The Hrd1p ligase complex forms a linchpin between ER-lumenal substrate selection and Cdc48p recruitment. Embo J *advanced online publication.*

Ghaemmaghami, S., Huh, W. K., Bower, K., Howson, R. W., Belle, A., Dephoure, N., O'Shea, E. K., and Weissman, J. S. (2003). Global analysis of protein expression in yeast. Nature *425*, 737-741.

Ghosh, P., Dahms, N. M., and Kornfeld, S. (2003). Mannose 6-phosphate receptors: new twists in the tale. Nat Rev Mol Cell Biol *4*, 202-212.

Gill, I., and Valivety, R. (1997). Polyunsaturated fatty acids, Part 1: Occurrence, biological activities and applications. Trends Biotechnol *15*, 401-409.

Goldstein, A. L., and McCusker, J. H. (1999). Three new dominant drug resistance cassettes for gene disruption in Saccharomyces cerevisiae. Yeast *15*, 1541-1553.

Golovko, M. Y., and Murphy, E. J. (2004). An improved method for tissue long-chain acyl-CoA extraction and analysis. J Lipid Res *45*, 1777-1782.

Gorlich, D., and Rapoport, T. A. (1993). Protein translocation into proteoliposomes reconstituted from purified components of the endoplasmic reticulum membrane. Cell *75*, 615-630.

Grayson, C., and Molday, R. S. (2005). Dominant negative mechanism underlies autosomal dominant Stargardt-like macular dystrophy linked to mutations in ELOVL4. J Biol Chem *280*, 32521-32530.

Guillas, I., Kirchman, P. A., Chuard, R., Pfefferli, M., Jiang, J. C., Jazwinski, S. M., and Conzelmann, A. (2001). C26-CoA-dependent ceramide synthesis of Saccharomyces cerevisiae is operated by Lag1p and Lac1p. Embo J *20*, 2655-2665.

Guthrie, C., and Fink, G. (1991). Guide to Yeast Genetics and Molecular Biology. Methods in Enzymology *194*, 933.

Haberer, G., Erschadi, S., and Torres-Ruiz, R. A. (2002). The Arabidopsis gene PEPINO/PASTICCINO2 is required for proliferation control of meristematic and non-meristematic cells and encodes a putative anti-phosphatase. Dev Genes Evol *212*, 542-550.

Han, G., Gable, K., Kohlwein, S. D., Beaudoin, F., Napier, J. A., and Dunn, T. M. (2002). The Saccharomyces cerevisiae YBR159w gene encodes the 3-ketoreductase of the microsomal fatty acid elongase. J Biol Chem *277*, 35440-35449.

Han, J., Luhs, W., Sonntag, K., Zahringer, U., Borchardt, D. S., Wolter, F. P., Heinz, E., and Frentzen, M. (2001). Functional characterization of beta-ketoacyl-CoA synthase genes from Brassica napus L. Plant Mol Biol *46*, 229-239.

Hanc

resid

II/ma

Harr

proli

Hele

291

Hill

mis

172

Hir

B.,

en

Hi

as

H

sc

Y

H

c

Hancock, M. K., Haskins, D. J., Sun, G., and Dahms, N. M. (2002). Identification of residues essential for carbohydrate recognition by the insulin-like growth factor II/mannose 6-phosphate receptor. J Biol Chem *277*, 11255-11264.

Harrar, Y., Bellec, Y., Bellini, C., and Faure, J. D. (2003). Hormonal control of cell proliferation requires PASTICCINO genes. Plant Physiol *132*, 1217-1227.

Helenius, A., and Aebi, M. (2001). Intracellular functions of N-linked glycans. Science *291*, 2364-2369.

Hiller, M. M., Finger, A., Schweiger, M., and Wolf, D. H. (1996). ER degradation of a misfolded luminal protein by the cytosolic ubiquitin-proteasome pathway. Science *273*, 1725-1728.

Hirao, K., Natsuka, Y., Tamura, T., Wada, I., Morito, D., Natsuka, S., Romero, P., Sleno, B., Tremblay, L. O., Herscovics, A., *et al.* (2006). EDEM3, a soluble EDEM homolog, enhances glycoprotein ERAD and mannose trimming. J Biol Chem.

Hirsch, C., Jarosch, E., Sommer, T., and Wolf, D. H. (2004). Endoplasmic reticulum-associated protein degradation--one model fits all? Biochim Biophys Acta *1695*, 215-223.

Hitt, R., and Wolf, D. H. (2004a). Der1p, a protein required for degradation of malfolded soluble proteins of the endoplasmic reticulum: topology and Der1-like proteins. FEMS Yeast Res *4*, 721-729.

Hitt, R., and Wolf, D. H. (2004b). DER7, encoding alpha-glucosidase I is essential for degradation of malfolded glycoproteins of the endoplasmic reticulum. FEMS Yeast Res *4*, 815-820.

Hopfield, J. J. (1974). Kinetic proofreading: a new mechanism for reducing errors in biosynthetic processes requiring high specificity. Proc Natl Acad Sci U S A *71*, 4135-4139.

Horvath, A., Sutterlin, C., Manning-Krieg, U., Movva, N. R., and Riezman, H. (1994). Ceramide synthesis enhances transport of GPI-anchored proteins to the Golgi apparatus in yeast. Embo J *13*, 3687-3695.

Hosokawa, N., Wada, I., Hasegawa, K., Yorihuzi, T., Tremblay, L. O., Herscovics, A., and Nagata, K. (2001). A novel ER alpha-mannosidase-like protein accelerates ER-associated degradation. EMBO Rep *2*, 415-422.

Huh, W. K., Falvo, J. V., Gerke, L. C., Carroll, A. S., Howson, R. W., Weissman, J. S., and O'Shea, E. K. (2003). Global analysis of protein localization in budding yeast. Nature *425*, 686-691.

Huyer, G., Piluek, W. F., Fansler, Z., Kreft, S. G., Hochstrasser, M., Brodsky, J. L., and Michaelis, S. (2004). Distinct machinery is required in Saccharomyces cerevisiae for the endoplasmic reticulum-associated degradation of a multispanning membrane protein and a soluble luminal protein. J Biol Chem *279*, 38369-38378.

Jakob, C. A., Bodmer, D., Spirig, U., Battig, P., Marcil, A., Dignard, D., Bergeron, J. J., Thomas, D. Y., and Aebi, M. (2001). Htm1p, a mannosidase-like protein, is involved in glycoprotein degradation in yeast. EMBO Rep *2*, 423-430.

Jakob, C. A., Burda, P., Roth, J., and Aebi, M. (1998). Degradation of misfolded endoplasmic reticulum glycoproteins in Saccharomyces cerevisiae is determined by a specific oligosaccharide structure. J Cell Biol *142*, 1223-1233.

Jakob
mam
Jaros
T. (2
ATP
Jenn
acid
Jen
(19
pro
Jin
Pr
16
Jo
sl
J
i

Jakobsson, A., Westerberg, R., and Jacobsson, A. (2006). Fatty acid elongases in mammals: Their regulation and roles in metabolism. Prog Lipid Res.

Jarosch, E., Taxis, C., Volkwein, C., Bordallo, J., Finley, D., Wolf, D. H., and Sommer, T. (2002). Protein dislocation from the ER requires polyubiquitination and the AAA-ATPase Cdc48. Nat Cell Biol *4*, 134-139.

Jenni, S., Leibundgut, M., Maier, T., and Ban, N. (2006). Architecture of a fungal fatty acid synthase at 5 A resolution. Science *311*, 1263-1267.

Jensen, T. J., Loo, M. A., Pind, S., Williams, D. B., Goldberg, A. L., and Riordan, J. R. (1995). Multiple proteolytic systems, including the proteasome, contribute to CFTR processing. Cell *83*, 129-135.

Jimenez, C. R., Huang, L., Qiu, Y., and Burlingame, A. L. (1998). In-Gel Digestion of Proteins for MALDI-MS Fingerprint Mapping. Current Protocols in Protein Science *16.4.1-16.4.5.*

Johnson, A. E., and Haigh, N. G. (2000). The ER translocon and retrotranslocation: is the shift into reverse manual or automatic? Cell *102*, 709-712.

Johnston, J. A., Johnson, E. S., Waller, P. R., and Varshavsky, A. (1995). Methotrexate inhibits proteolysis of dihydrofolate reductase by the N-end rule pathway. J Biol Chem *270*, 8172-8178.

Kabani, M., Beckerich, J. M., and Gaillardin, C. (2000). Sls1p stimulates the Sec63p-mediated activation of Kar2p in a conformation dependent manner in the yeast endoplasmic reticulum. Mol Cell Biol *20*, 6923-6934.

Kabani, M., Kelley, S. S., Morrow, M. W., Montgomery, D. L., Sivendran, R., Rose, M. D., Gierasch, L. M., and Brodsky, J. L. (2003). Dependence of endoplasmic reticulum-

associated degradation on the peptide binding domain and concentration of BiP. Mol Biol Cell *14*, 3437-3448.

Kemp, S., Valianpour, F., Denis, S., Ofman, R., Sanders, R. J., Mooyer, P., Barth, P. G., and Wanders, R. J. (2005). Elongation of very long-chain fatty acids is enhanced in X-linked adrenoleukodystrophy. Mol Genet Metab *84*, 144-151.

Kim, S., Fyrst, H., and Saba, J. (2000). Accumulation of phosphorylated sphingoid long chain bases results in cell growth inhibition in Saccharomyces cerevisiae. Genetics *156*, 1519-1529.

Kim, W., Spear, E. D., and Ng, D. T. (2005). Yos9p detects and targets misfolded glycoproteins for ER-associated degradation. Mol Cell *19*, 753-764.

Kniazeva, M., Crawford, Q. T., Seiber, M., Wang, C. Y., and Han, M. (2004). Monomethyl branched-chain fatty acids play an essential role in Caenorhabditis elegans development. PLoS Biol *2*, E257.

Knoll, A., Bessoule, J. J., Sargueil, F., and Cassagne, C. (1999). Dehydration of 3-hydroxyacyl-CoA in brain very-long-chain fatty acid synthesis. Neurochem Int *34*, 255-267.

Knop, M., Finger, A., Braun, T., Hellmuth, K., and Wolf, D. H. (1996a). Der1, a novel protein specifically required for endoplasmic reticulum degradation in yeast. Embo J *15*, 753-763.

Knop, M., Hauser, N., and Wolf, D. H. (1996b). N-Glycosylation affects endoplasmic reticulum degradation of a mutated derivative of carboxypeptidase yscY in yeast. Yeast *12*, 1229-1238.

Kobayashi, S. D., and Nagiec, M. M. (2003). Ceramide/long-chain base phosphate rheostat in Saccharomyces cerevisiae: regulation of ceramide synthesis by Elo3p and Cka2p. Eukaryot Cell *2*, 284-294.

Kohlwein, S. D., Eder, S., Oh, C. S., Martin, C. E., Gable, K., Bacikova, D., and Dunn, T. (2001). Tsc13p is required for fatty acid elongation and localizes to a novel structure at the nuclear-vacuolar interface in Saccharomyces cerevisiae. Mol Cell Biol *21*, 109-125.

Kostova, Z., and Wolf, D. H. (2005). Importance of carbohydrate positioning in the recognition of mutated CPY for ER-associated degradation. J Cell Sci *118*, 1485-1492.

Kumar, A., Agarwal, S., Heyman, J. A., Matson, S., Heidtman, M., Piccirillo, S., Umansky, L., Drawid, A., Jansen, R., Liu, Y., *et al.* (2002). Subcellular localization of the yeast proteome. Genes Dev *16*, 707-719.

Kunst, L., and Samuels, A. L. (2003). Biosynthesis and secretion of plant cuticular wax. Prog Lipid Res *42*, 51-80.

Larson, T. R., and Graham, I. A. (2001). Technical Advance: a novel technique for the sensitive quantification of acyl CoA esters from plant tissues. Plant J *25*, 115-125.

Lechelt-Kunze, C., Meissner, R. C., Drewes, M., and Tietjen, K. (2003). Flufenacet herbicide treatment phenocopies the fiddlehead mutant in Arabidopsis thaliana. Pest Manag Sci *59*, 847-856.

Lee, C., Schwartz, M. P., Prakash, S., Iwakura, M., and Matouschek, A. (2001). ATP-dependent proteases degrade their substrates by processively unraveling them from the degradation signal. Mol Cell *7*, 627-637.

Leonard, A. E., Pereira, S. L., Sprecher, H., and Huang, Y. S. (2004). Elongation of long-chain fatty acids. Prog Lipid Res *43*, 36-54.

Stanford Libraries

Lessire, R., Chevalier, S., Lucet-Levannier, K., Lellouche, J. P., Mioskowski, C., and Cassagne, C. (1999). Study of the 3-hydroxy eicosanoyl-coenzyme A dehydratase and (E)-2,3 enoyl-coenzyme A reductase involved in acyl-coenzyme A elongation in etiolated leek seedlings. Plant Physiol *119*, 1009-1016.

Lester, R. L., and Dickson, R. C. (2001). High-performance liquid chromatography analysis of molecular species of sphingolipid-related long chain bases and long chain base phosphates in Saccharomyces cerevisiae after derivatization with 6-aminoquinolyl-N-hydroxysuccinimidyl carbamate. Anal Biochem *298*, 283-292.

Li, D., Gonzalez, O., Bachinski, L. L., and Roberts, R. (2000). Human protein tyrosine phosphatase-like gene: expression profile, genomic structure, and mutation analysis in families with ARVD. Gene *256*, 237-243.

Lilley, B. N., and Ploegh, H. L. (2004). A membrane protein required for dislocation of misfolded proteins from the ER. Nature *429*, 834-840.

Lilley, B. N., and Ploegh, H. L. (2005). Multiprotein complexes that link dislocation, ubiquitination, and extraction of misfolded proteins from the endoplasmic reticulum membrane. Proc Natl Acad Sci U S A *102*, 14296-14301.

Litovchick, L., Friedmann, E., and Shaltiel, S. (2002). A selective interaction between OS-9 and the carboxyl-terminal tail of meprin beta. J Biol Chem *277*, 34413-34423.

Liu, Y., Choudhury, P., Cabral, C. M., and Sifers, R. N. (1999). Oligosaccharide modification in the early secretory pathway directs the selection of a misfolded glycoprotein for degradation by the proteasome. J Biol Chem *274*, 5861-5867.

UNIVERSITY OF CALIFORNIA
LIBRARY

Lolle, S. J., Cheung, A. Y., and Sussex, I. M. (1992). Fiddlehead: an Arabidopsis mutant constitutively expressing an organ fusion program that involves interactions between epidermal cells. Dev Biol *152*, 383-392.

Longtine, M. S., McKenzie, A., 3rd, Demarini, D. J., Shah, N. G., Wach, A., Brachat, A., Philippsen, P., and Pringle, J. R. (1998). Additional modules for versatile and economical PCR-based gene deletion and modification in Saccharomyces cerevisiae. Yeast *14*, 953-961.

Maier, T., Jenni, S., and Ban, N. (2006). Architecture of mammalian fatty acid synthase at 4.5 A resolution. Science *311*, 1258-1262.

Mao, C., Wadleigh, M., Jenkins, G. M., Hannun, Y. A., and Obeid, L. M. (1997). Identification and characterization of Saccharomyces cerevisiae dihydrosphingosine-1-phosphate phosphatase. J Biol Chem *272*, 28690-28694.

Matlack, K. E., Mothes, W., and Rapoport, T. A. (1998). Protein translocation: tunnel vision. Cell *92*, 381-390.

Matouschek, A., Azem, A., Ratliff, K., Glick, B. S., Schmid, K., and Schatz, G. (1997). Active unfolding of precursor proteins during mitochondrial protein import. Embo J *16*, 6727-6736.

Matsuoka, K., and Schekman, R. (2000). The use of liposomes to study COPII- and COPI-coated vesicle formation and membrane protein sorting. Methods *20*, 417-428.

Mayor, S., and Riezman, H. (2004). Sorting GPI-anchored proteins. Nat Rev Mol Cell Biol *5*, 110-120.

Meusser, B., Hirsch, C., Jarosch, E., and Sommer, T. (2005). ERAD: the long road to destruction. Nat Cell Biol *7*, 766-772.

UNIVERSITY OF CALIFORNIA
SAN DIEGO

Millar, A. A., Clemens, S., Zachgo, S., Giblin, E. M., Taylor, D. C., and Kunst, L. (1999). CUT1, an Arabidopsis gene required for cuticular wax biosynthesis and pollen fertility, encodes a very-long-chain fatty acid condensing enzyme. Plant Cell *11*, 825-838.

Millar, A. A., and Kunst, L. (1997). Very-long-chain fatty acid biosynthesis is controlled through the expression and specificity of the condensing enzyme. Plant J *12*, 121-131.

Mnaimneh, S., Davierwala, A. P., Haynes, J., Moffat, J., Peng, W. T., Zhang, W., Yang, X., Pootoolal, J., Chua, G., Lopez, A., *et al.* (2004). Exploration of essential gene functions via titratable promoter alleles. Cell *118*, 31-44.

Molinari, M., Calanca, V., Galli, C., Lucca, P., and Paganetti, P. (2003). Role of EDEM in the release of misfolded glycoproteins from the calnexin cycle. Science *299*, 1397-1400.

Moon, Y. A., and Horton, J. D. (2003). Identification of two mammalian reductases involved in the two-carbon fatty acyl elongation cascade. J Biol Chem *278*, 7335-7343.

Moser, H. W., Moser, A. B., Smith, K. D., Bergin, A., Borel, J., Shankroff, J., Stine, O. C., Merette, C., Ott, J., Krivit, W., and et al. (1992). Adrenoleukodystrophy: phenotypic variability and implications for therapy. J Inherit Metab Dis *15*, 645-664.

Mumberg, D., Muller, R., and Funk, M. (1994). Regulatable promoters of Saccharomyces cerevisiae: comparison of transcriptional activity and their use for heterologous expression. Nucleic Acids Res *22*, 5767-5768.

Munro, S. (2001). The MRH domain suggests a shared ancestry for the mannose 6-phosphate receptors and other N-glycan-recognising proteins. Curr Biol *11*, R499-501.

Pasadena City College

Nakatsukasa, K., Nishikawa, S., Hosokawa, N., Nagata, K., and Endo, T. (2001). Mnl1p, an alpha -mannosidase-like protein in yeast Saccharomyces cerevisiae, is required for endoplasmic reticulum-associated degradation of glycoproteins. J Biol Chem *276*, 8635-8638.

Neuber, O., Jarosch, E., Volkwein, C., Walter, J., and Sommer, T. (2005). Ubx2 links the Cdc48 complex to ER-associated protein degradation. Nat Cell Biol *7*, 993-998.

Nicchitta, C. V., and Blobel, G. (1990). Assembly of translocation-competent proteoliposomes from detergent-solubilized rough microsomes. Cell *60*, 259-269.

Nicchitta, C. V., and Blobel, G. (1993). Lumenal proteins of the mammalian endoplasmic reticulum are required to complete protein translocation. Cell *73*, 989-998.

Nicchitta, C. V., Migliaccio, G., and Blobel, G. (1991). Biochemical fractionation and assembly of the membrane components that mediate nascent chain targeting and translocation. Cell *65*, 587-598.

Nishikawa, S., Brodsky, J. L., and Nakatsukasa, K. (2005). Roles of molecular chaperones in endoplasmic reticulum (ER) quality control and ER-associated degradation (ERAD). J Biochem (Tokyo) *137*, 551-555.

Nishikawa, S. I., Fewell, S. W., Kato, Y., Brodsky, J. L., and Endo, T. (2001). Molecular chaperones in the yeast endoplasmic reticulum maintain the solubility of proteins for retrotranslocation and degradation. J Cell Biol *153*, 1061-1070.

Nugteren, D. H. (1965). The enzymic chain elongation of fatty acids by rat-liver microsomes. Biochim Biophys Acta *106*, 280-290.

Oda, Y., Hosokawa, N., Wada, I., and Nagata, K. (2003). EDEM as an acceptor of terminally misfolded glycoproteins released from calnexin. Science *299*, 1394-1397.

BERKELEY LIBRARIES

Oda, Y., Okada, T., Yoshida, H., Kaufman, R. J., Nagata, K., and Mori, K. (2006). Derlin-2 and Derlin-3 are regulated by the mammalian unfolded protein response and are required for ER-associated degradation. J Cell Biol *172*, 383-393.

Oh, C. S., Toke, D. A., Mandala, S., and Martin, C. E. (1997). ELO2 and ELO3, homologues of the Saccharomyces cerevisiae ELO1 gene, function in fatty acid elongation and are required for sphingolipid formation. J Biol Chem *272*, 17376-17384.

Olson, L. J., Zhang, J., Lee, Y. C., Dahms, N. M., and Kim, J. J. (1999). Structural basis for recognition of phosphorylated high mannose oligosaccharides by the cation-dependent mannose 6-phosphate receptor. J Biol Chem *274*, 29889-29896.

Osei, P., Suneja, S. K., Laguna, J. C., Nagi, M. N., Cook, L., Prasad, M. R., and Cinti, D. L. (1989). Topography of rat hepatic microsomal enzymatic components of the fatty acid chain elongation system. J Biol Chem *264*, 6844-6849.

Paciorek, T., Zazimalova, E., Ruthardt, N., Petrasek, J., Stierhof, Y. D., Kleine-Vehn, J., Morris, D. A., Emans, N., Jurgens, G., Geldner, N., and Friml, J. (2005). Auxin inhibits endocytosis and promotes its own efflux from cells. Nature *435*, 1251-1256.

Paul, S., Gable, K., Beaudoin, F., Cahoon, E., Jaworski, J., Napier, J. A., and Dunn, T. M. (2006). Members of the Arabidopsis FAE1-like 3-Ketoacyl-CoA Synthase Gene Family Substitute for the Elop Proteins of Saccharomyces cerevisiae. J Biol Chem *281*, 9018-9029.

Pele, M., Tiret, L., Kessler, J. L., Blot, S., and Panthier, J. J. (2005). SINE exonic insertion in the PTPLA gene leads to multiple splicing defects and segregates with the autosomal recessive centronuclear myopathy in dogs. Hum Mol Genet *14*, 1417-1427.

Pelham, H. R., Hardwick, K. G., and Lewis, M. J. (1988). Sorting of soluble ER proteins in yeast. Embo J *7*, 1757-1762.

Plemper, R. K., Bordallo, J., Deak, P. M., Taxis, C., Hitt, R., and Wolf, D. H. (1999a). Genetic interactions of Hrd3p and Der3p/Hrd1p with Sec61p suggest a retro-translocation complex mediating protein transport for ER degradation. J Cell Sci *112 (Pt 22)*, 4123-4134.

Plemper, R. K., Deak, P. M., Otto, R. T., and Wolf, D. H. (1999b). Re-entering the translocon from the lumenal side of the endoplasmic reticulum. Studies on mutated carboxypeptidase yscY species. Febs Letters *443*, 241-245.

Pruitt, R. E., Vielle-Calzada, J. P., Ploense, S. E., Grossniklaus, U., and Lolle, S. J. (2000). FIDDLEHEAD, a gene required to suppress epidermal cell interactions in Arabidopsis, encodes a putative lipid biosynthetic enzyme. Proc Natl Acad Sci U S A *97*, 1311-1316.

Puyaubert, J., Garbay, B., Costaglioli, P., Dieryck, W., Roscoe, T. J., Renard, M., Cassagne, C., and Lessire, R. (2001). Acyl-CoA elongase expression during seed development in Brassica napus. Biochim Biophys Acta *1533*, 141-152.

Puyaubert, J., Garcia, C., Chevalier, S., and Lessire, R. (2005). Acyl-CoA elongase, a key enzyme in the development of high-erucic acid rapeseed? Eur J Lipid Sci Technol *107*, 263-267.

Rajendran, L., and Simons, K. (2005). Lipid rafts and membrane dynamics. J Cell Sci *118*, 1099-1102.

UNIVERSITY OF CALIFORNIA
BERKELEY
LIBRARIES

Richly, H., Rape, M., Braun, S., Rumpf, S., Hoege, C., and Jentsch, S. (2005). A series of ubiquitin binding factors connects CDC48/p97 to substrate multiubiquitylation and proteasomal targeting. Cell *120*, 73-84.

Romisch, K. (2005). Endoplasmic reticulum-associated degradation. Annu Rev Cell Dev Biol *21*, 435-456.

Rossler, H., Rieck, C., Delong, T., Hoja, U., and Schweizer, E. (2003). Functional differentiation and selective inactivation of multiple Saccharomyces cerevisiae genes involved in very-long-chain fatty acid synthesis. Mol Genet Genomics *269*, 290-298.

Saba, J. D., Nara, F., Bielawska, A., Garrett, S., and Hannun, Y. A. (1997). The BST1 gene of Saccharomyces cerevisiae is the sphingosine-1-phosphate lyase. J Biol Chem *272*, 26087-26090.

Sakumoto, N., Mukai, Y., Uchida, K., Kouchi, T., Kuwajima, J., Nakagawa, Y., Sugioka, S., Yamamoto, E., Furuyama, T., Mizubuchi, H., *et al.* (1999). A series of protein phosphatase gene disruptants in Saccharomyces cerevisiae. Yeast *15*, 1669-1679.

Sayeed, A., and Ng, D. T. (2005). Search and destroy: ER quality control and ER-associated protein degradation. Crit Rev Biochem Mol Biol *40*, 75-91.

Schindelman, G., Morikami, A., Jung, J., Baskin, T. I., Carpita, N. C., Derbyshire, P., McCann, M. C., and Benfey, P. N. (2001). COBRA encodes a putative GPI-anchored protein, which is polarly localized and necessary for oriented cell expansion in Arabidopsis. Genes Dev *15*, 1115-1127.

Schneiter, R., Hitomi, M., Ivessa, A. S., Fasch, E. V., Kohlwein, S. D., and Tartakoff, A. M. (1996). A yeast acetyl coenzyme A carboxylase mutant links very-long-chain fatty

UNIVERSITY OF CALIFORNIA
SAN DIEGO

acid synthesis to the structure and function of the nuclear membrane-pore complex. Mol Cell Biol *16*, 7161-7172.

Schneiter, R., and Kohlwein, S. D. (1997). Organelle structure, function, and inheritance in yeast: a role for fatty acid synthesis? Cell *88*, 431-434.

Schuberth, C., and Buchberger, A. (2005). Membrane-bound Ubx2 recruits Cdc48 to ubiquitin ligases and their substrates to ensure efficient ER-associated protein degradation. Nat Cell Biol *7*, 999-1006.

Schuldiner, M., Collins, S. R., Thompson, N. J., Denic, V., Bhamidipati, A., Punna, T., Ihmels, J., Andrews, B., Boone, C., Greenblatt, J. F., *et al.* (2005). Exploration of the function and organization of the yeast early secretory pathway through an epistatic miniarray profile. Cell *123*, 507-519.

Schweizer, E., and Hofmann, J. (2004). Microbial type I fatty acid synthases (FAS): major players in a network of cellular FAS systems. Microbiol Mol Biol Rev *68*, 501-517.

Sekijima, Y., Wiseman, R. L., Matteson, J., Hammarstrom, P., Miller, S. R., Sawkar, A. R., Balch, W. E., and Kelly, J. W. (2005). The biological and chemical basis for tissue-selective amyloid disease. Cell *121*, 73-85.

Shanklin, J., Whittle, E., and Fox, B. G. (1994). Eight histidine residues are catalytically essential in a membrane-associated iron enzyme, stearoyl-CoA desaturase, and are conserved in alkane hydroxylase and xylene monooxygenase. Biochemistry *33*, 12787-12794.

Sieber, P., Schorderet, M., Ryser, U., Buchala, A., Kolattukudy, P., Metraux, J. P., and Nawrath, C. (2000). Transgenic Arabidopsis plants expressing a fungal cutinase show

UCSB LIBRARY
Research Archive

alterations in the structure and properties of the cuticle and postgenital organ fusions. Plant Cell *12*, 721-738.

Sikorski, R. S., and Hieter, P. (1989). A system of shuttle vectors and yeast host strains designed for efficient manipulation of DNA in Saccharomyces cerevisiae. Genetics *122*, 19-27.

Simons, K., and Toomre, D. (2000). Lipid rafts and signal transduction. Nat Rev Mol Cell Biol *1*, 31-39.

Sims, K. J., Spassieva, S. D., Voit, E. O., and Obeid, L. M. (2004). Yeast sphingolipid metabolism: clues and connections. Biochem Cell Biol *82*, 45-61.

Smith, S., Witkowski, A., and Joshi, A. K. (2003). Structural and functional organization of the animal fatty acid synthase. Prog Lipid Res *42*, 289-317.

Spear, E. D., and Ng, D. T. (2005). Single, context-specific glycans can target misfolded glycoproteins for ER-associated degradation. J Cell Biol *169*, 73-82.

Spiro, R. G. (2004). Role of N-linked polymannose oligosaccharides in targeting glycoproteins for endoplasmic reticulum-associated degradation. Cell Mol Life Sci *61*, 1025-1041.

Su, Y. A., Hutter, C. M., Trent, J. M., and Meltzer, P. S. (1996). Complete sequence analysis of a gene (OS-9) ubiquitously expressed in human tissues and amplified in sarcomas. Mol Carcinog *15*, 270-275.

Swanson, R., Locher, M., and Hochstrasser, M. (2001). A conserved ubiquitin ligase of the nuclear envelope/endoplasmic reticulum that functions in both ER-associated and Matalpha2 repressor degradation. Genes Dev *15*, 2660-2674.

UNIVERSITY OF CALIFORNIA
BERKELEY

Szathmary, R., Bielmann, R., Nita-Lazar, M., Burda, P., and Jakob, C. A. (2005). Yos9 protein is essential for degradation of misfolded glycoproteins and may function as lectin in ERAD. Mol Cell *19*, 765-775.

Taxis, C., Hitt, R., Park, S. H., Deak, P. M., Kostova, Z., and Wolf, D. H. (2003). Use of modular substrates demonstrates mechanistic diversity and reveals differences in chaperone requirement of ERAD. J Biol Chem *278*, 35903-35913.

Tirosh, B., Furman, M. H., Tortorella, D., and Ploegh, H. L. (2003). Protein unfolding is not a prerequisite for endoplasmic reticulum-to-cytosol dislocation. J Biol Chem *278*, 6664-6672.

Toke, D. A., and Martin, C. E. (1996). Isolation and characterization of a gene affecting fatty acid elongation in Saccharomyces cerevisiae. J Biol Chem *271*, 18413-18422.

Travers, K. J., Patil, C. K., Wodicka, L., Lockhart, D. J., Weissman, J. S., and Walter, P. (2000). Functional and genomic analyses reveal an essential coordination between the unfolded protein response and ER-associated degradation. Cell *101*, 249-258.

Trotter, P. J. (2001). The genetics of fatty acid metabolism in Saccharomyces cerevisiae. Annu Rev Nutr *21*, 97-119.

Tsai, B., Ye, Y., and Rapoport, T. A. (2002). Retro-translocation of proteins from the endoplasmic reticulum into the cytosol. Nat Rev Mol Cell Biol *3*, 246-255.

Tsuji, S., Ohno, T., Miyatake, T., Suzuki, A., and Yamakawa, T. (1984). Fatty acid elongation activity in fibroblasts from patients with adrenoleukodystrophy (ALD). J Biochem (Tokyo) *96*, 1241-1247.

Tsuji, S., Sano, T., Ariga, T., and Miyatake, T. (1981). Increased synthesis of hexacosanoic acid (C23:0) by cultured skin fibroblasts from patients with

UNIVERSITY OF CALIFORNIA
BERKELEY

adrenoleukodystrophy (ALD) and adrenomyeloneuropathy (AMN). J Biochem (Tokyo) *90*, 1233-1236.

Tvrdik, P., Westerberg, R., Silve, S., Asadi, A., Jakobsson, A., Cannon, B., Loison, G., and Jacobsson, A. (2000). Role of a new mammalian gene family in the biosynthesis of very long chain fatty acids and sphingolipids. J Cell Biol *149*, 707-718.

Uwanogho, D. A., Hardcastle, Z., Balogh, P., Mirza, G., Thornburg, K. L., Ragoussis, J., and Sharpe, P. T. (1999). Molecular cloning, chromosomal mapping, and developmental expression of a novel protein tyrosine phosphatase-like gene. Genomics *62*, 406-416.

Vashist, S., Kim, W., Belden, W. J., Spear, E. D., Barlowe, C., and Ng, D. T. (2001). Distinct retrieval and retention mechanisms are required for the quality control of endoplasmic reticulum protein folding. J Cell Biol *155*, 355-368.

Vashist, S., and Ng, D. T. (2004). Misfolded proteins are sorted by a sequential checkpoint mechanism of ER quality control. J Cell Biol *165*, 41-52.

Wakil, S. J., Stoops, J. K., and Joshi, V. C. (1983). Fatty acid synthesis and its regulation. Annu Rev Biochem *52*, 537-579.

Wanders, R. J. (2004). Metabolic and molecular basis of peroxisomal disorders: a review. Am J Med Genet A *126*, 355-375.

Ward, C. L., Omura, S., and Kopito, R. R. (1995). Degradation of CFTR by the ubiquitin-proteasome pathway. Cell *83*, 121-127.

White, S. W., Zheng, J., Zhang, Y. M., and Rock (2005). The structural biology of type II fatty acid biosynthesis. Annu Rev Biochem *74*, 791-831.

Winzeler, E. A., Shoemaker, D. D., Astromoff, A., Liang, H., Anderson, K., Andre, B., Bangham, R., Benito, R., Boeke, J. D., Bussey, H., *et al.* (1999a). Functional

UNIVERSITY OF CALIFORNIA
SAN DIEGO
LIBRARY

characterization of the S. cerevisiae genome by gene deletion and parallel analysis. Science *285*, 901-906.

Winzeler, E. A., Shoemaker, D. D., Astromoff, A., Liang, H., Anderson, K., Andre, B., Bangham, R., Benito, R., Boeke, J. D., Bussey, H., *et al.* (1999b). Functional characterization of the S. cerevisiae genome by gene deletion and parallel analysis. Science *285*, 901-906.

Wu, Y., Swulius, M. T., Moremen, K. W., and Sifers, R. N. (2003). Elucidation of the molecular logic by which misfolded alpha 1-antitrypsin is preferentially selected for degradation. Proc Natl Acad Sci U S A *100*, 8229-8234.

Yan, D., Wong, D., Zheng, K., Thiselton, D., Fujita, R., Sieving, P. A., Bhattacharya, S. S., Yang-Feng, T. L., Richards, J. E., and Swaroop, A. (1994). Dinucleotide repeat polymorphism at the DXS977 locus. Hum Mol Genet *3*, 1030.

Ye, Y., Meyer, H. H., and Rapoport, T. A. (2001). The AAA ATPase Cdc48/p97 and its partners transport proteins from the ER into the cytosol. Nature *414*, 652-656.

Ye, Y., Shibata, Y., Kikkert, M., van Voorden, S., Wiertz, E., and Rapoport, T. A. (2005). Inaugural Article: Recruitment of the p97 ATPase and ubiquitin ligases to the site of retrotranslocation at the endoplasmic reticulum membrane. Proc Natl Acad Sci U S A *102*, 14132-14138.

Ye, Y., Shibata, Y., Yun, C., Ron, D., and Rapoport, T. A. (2004). A membrane protein complex mediates retro-translocation from the ER lumen into the cytosol. Nature *429*, 841-847.

Yephremov, A., Wisman, E., Huijser, P., Huijser, C., Wellesen, K., and Saedler, H. (1999). Characterization of the FIDDLEHEAD gene of Arabidopsis reveals a link

UCSF LIBRARY

between adhesion response and cell differentiation in the epidermis. Plant Cell *11*, 2187-2201.

Yoshida, Y., Chiba, T., Tokunaga, F., Kawasaki, H., Iwai, K., Suzuki, T., Ito, Y., Matsuoka, K., Yoshida, M., Tanaka, K., and Tai, T. (2002). E3 ubiquitin ligase that recognizes sugar chains. Nature *418*, 438-442.

Zhang, X., Skrzypek, M. S., Lester, R. L., and Dickson, R. C. (2001). Elevation of endogenous sphingolipid long-chain base phosphates kills Saccharomyces cerevisiae cells. Curr Genet *40*, 221-233.

Zheng, H., Rowland, O., and Kunst, L. (2005). Disruptions of the Arabidopsis Enoyl-CoA reductase gene reveal an essential role for very-long-chain fatty acid synthesis in cell expansion during plant morphogenesis. Plant Cell *17*, 1467-1481.

5227R

52271

UCSF LIBRARY